NEUTRALIZATION OF RED MUD USING CO_2 SEQUESTRATION AND THEIR UTILIZATIONS

A Thesis Submitted
In partial fulfillment of the requirements for the degree of

DOCTOR OF PHILOSOPHY
IN
CHEMISTRY

BY
RAMESH CHANDRA SAHU

Under the guidance of
Prof. (Dr.) R.K. Patel and Prof. (Dr.) B.C. Ray

DEPARTMENT OF CHEMISTRY
NATIONAL INSTITUTE OF TECHNOLOGY
ROURKELA–769008, ORISSA, INDIA

January, 2011

Dedicated to my parents
&
to the everlasting memory of
my departed
grandfather
Late Dharanidhar Sahu
& grandmother
Late Bijuli Sahu

NATIONAL INSTITUTE OF TECHNOLOGY
ROURKELA

CERTIFICATE

This is to certify that the thesis entitled, **"Neutralization of red mud using CO_2 sequestration and their utilizations"** being submitted by **Sri Ramesh Chandra Sahu** to the National Institute of Technology, Rourkela, India, for the award of the degree of **Doctor of Philosophy** in Chemistry, is a record of bonafide research work carried out by him under our supervision. In our opinion, the work fulfills part of the requirements for which it is being submitted.

The work incorporated in this thesis has not been submitted elsewhere earlier, in part or in full, for the award of any other degree or diploma of this or any other Institute or University.

Prof. (Dr.) R.K. Patel, Supervisor
Department of Chemistry,
National Institute of Technology,
Rourkela-769008, Orissa, India

Prof. (Dr.) B.C. Ray, Co-Supervisor
Dept. of Metallurgical and Materials Engg.,
National Institute of Technology,
Rourkela-769008, Orissa, India

ACKNOWLEDGEMENTS

I would like to express my sincere gratitude to my supervisors Prof. R.K. Patel, Department of Chemistry, NIT Rourkela and Prof. B.C. Ray, Department of Metallurgical and Materials Engineering, NIT Rourkela, for their continuous guidance, whole hearted support and encouragement throughout this study.

I am grateful to Prof. S.K. Sarangi, former Director, and Prof. P.C. Panda, Director, NIT Rourkela, for their inspiration and encouragement throughout the research work.

I acknowledge National Institute of Technology, Rourkela for constant support to carry out the present investigations. I also acknowledge CSIR (Council of Scientific and Industrial Research), and MHRD (Ministry of Human Resource Development), Government of India, New Delhi, for providing financial support during my research work. I would like to thank B.W. Harry (DGM, R&D, NALCO, Damanjodi, India), for encouragement and providing fresh dried red mud.

I am thankful to Prof. K.M. Purohit and Prof. G. Hota, Dept. of Chemistry, Prof. S. Mishra, Prof. T.K. Sen, Dept. of Chemical Engineering for their helpful discussions and suggestions. I would like to thank Prof. M. Kumar, Prof. G.S. Agarwal, Rajesh Pattanaik, Uday Sahu, Bhanja, Kishor Tanty, Hembram, Dept. of MME, G. Behera, Ceramic Engineering, for their constant encouragement and laboratory facilities. I am also grateful to Hemanta and all other members of Library, NIT Rourkela for permitting me to carry out reference work. My hearty thank to all my friends, Upendra, Islam, Ganesh, Anil, Satish, Sarat, PhD research scholars for their cooperation and encouragement.

I thank to all other faculty members, laboratory colleagues and the supporting staff members of the Dept. of Chemistry, Dept. of MME, NIT Rourkela, for their help and cooperation, at various phases of the experimental work. I would also like to warmly acknowledge all those who directly or indirectly supported the research work.

Finally, I would like to express a special tribute of gratitude to my parents, brothers, and other family members for their encouragement and moral support throughout the research work.

NIT Rourkela **(Ramesh Chandra Sahu)**

Roll No. 507CY002, PhD

ABSTRACT

Red mud is a highly caustic waste product of alumina industry. More than 70 million tons of red mud has been generated worldwide per annum. It pollutes the industry area due to its alkaline nature. Its storage and maintenance is costly and causes great problem to the industries. Moreover, CO_2 is a global warming gas generated from fossil fuel power plant. Each 500 MW coal power plant emits about 3 million tons of CO_2 per year which may cause serious disruption to the global climate change.

A laboratory study was conducted to investigate the ability of neutralization of red mud (RM) using carbon dioxide gas sequestration cycle at ambient conditions. The neutralized red mud (NRM) was characterized by XRD, SEM, EDX, FT-IR, CHNS, TG-DSC and auto titration method. X-ray diffraction pattern of NRM was revealed that the intensity of gibbsite was increased prominently and formed ilmenite due to dissolution of minerals. EDX analysis was showed that the %(w/w) of Na, C, O, Si were higher in the carbonated filtrate as compared to the RM and NRM. The permanently sequestered CO_2 %(w/w) per 10 g of red mud were ~26.33, ~58.01, ~55.37, and ~54.42 in NRM and first, second, third cycles of carbonated filtrate, respectively. Amount of CO_2 removed for cycle 1, 2, 3 of carbonated filtrate and NRM were 3.54, 2.28, 0.63, 0.57 g CO_2/100 g of red mud, respectively, as determined by CHNS analyzer at 1150°C. So, total calculated CO_2 removal was 7.02 g/100 g of red mud. The pH of red mud was decreased from ~11.8 to ~8.45 and alkalinity was decreased from ~10,789 to ~178 mg/L. The acid neutralizing capacity of NRM was ~0.23 mol H^+/kg of red mud. The specific advantages of these cyclic processes are that, large amount of CO_2 can be captured as compared to single step. Subsequently, this study has shown the effective neutralization of red mud.

Furthermore, the fine iron oxide was extracted from CO_2–NRM by using biodegradable surfactant and heat treatment. In fact, it is an enrichment process of Fe in red mud. The micro morphological studies of recovered fine iron oxide showed 71.71% of Fe. Therefore, larger amount of fine iron oxide can be utilized in the iron industry.

Furthermore, a laboratory study was conducted to investigate the ability of activated CO_2-neutralized red mud (ANRM) for the removal of arsenate from the aqueous solutions. The mechanisms involved in adsorption of arsenate ions on ANRM were characterized by using XRD, FT-IR, UV–vis, SEM/EDX, and chemical methods. The percentage removal was found to increase gradually with decrease of pH and maximum removal was achieved at pH ~4. Adsorption kinetic studies revealed that the adsorption process followed pseudo-second-order kinetics and equilibrates within 24 h. This study has shown that ANRM is highly effective new adsorbent for arsenate removal. Therefore, it is a low-cost environment-friendly material.

Therefore, neutralization of red mud using CO_2 sequestration is a nature-bio-inspired absorption method. Today's most urgent need for CO_2 emission reductions can be possible by using low-cost CO_2 sequestration technology.

Keywords: Alumina industry; Global warming; Red mud; CO_2; Carbonation; Neutralization; Sequestration; Caustic; Arsenate; Kinetics; Isotherms; Utilizations; Fine iron oxides; Biodegradable surfactant.

Contents

*****

LIST OF FIGURES

*****

LIST OF TABLES

*****

Abbreviations

AAS	Atomic Absorption Spectrometer
ANC	Acid Neutralizing Capacity
ANRM	Activated Neutralized Red Mud
BET	Brunauer–Emmett–Teller
CCD	Close Cycle Disposal
CCS	Carbon Dioxide Capture and Storage
CHNS	Carbon Hydrogen Nitrogen Sulpher Elemental Analyzer
CNRM	CO_2-Neutralized Red Mud
DSC	Differential Scanning Calorimetry
EDX	Energy Dispersive X-Ray
FT-IR	Fourier Transform Infrared
GHGs	Greenhouse Gases
IPCC	Intergovernmental Panel on Climate Change
MCCD	Modified Close Cycle Disposal
NRM	CO_2-Neutralized Red Mud
RM	Red Mud
SEM	Scanning Electron Microscope
TGA	Thermo Gravimetric Analysis
UV-vis	Ultra Violet-visible
XRD	X-Ray Diffraction

*****

Chapter 1

Introduction

1.1. Background

The increase of anthropogenic CO_2 concentration in the atmosphere is creating global challenging problem for future generation. The climate change and global warming can be reduced through utilization of greenhouse gases [**1**]. CO_2 is a greenhouse gas that makes the largest contribution from human activities. It is released into the atmosphere by the combustion of fossil fuels such as coal, oil or natural gas, and renewable fuels like biomass. CO_2 is an abundant, inexpensive, nontoxic biorenewable, and economical resource. It is an attractive raw material for incorporation into important industrial processes [**2**]. Its use is considered as "green chemistry" which subsequently reduces global warming.

The utilization of renewable resources is a prerequisite for a sustainable society. One easily available carbon resource is CO_2. It is also an attractive environment-

friendly chemical reagent. However, few industrial processes utilize CO_2 as a raw material. Because CO_2 is the most oxidized state of carbon, the biggest obstacle for establishing industrial processes based on CO_2 as a raw material, due to its low energy level and high stability. In other words, a large energy input is required to transform CO_2 to other form [**3**].

Presently used materials for CO_2 sequestrations are soil [**4**], steel slags [**5**], fly ash [**6**], amine solutions, zeolites, porous membranes, metal-organic frameworks (MOFs) [**7**], and deep geological strata [**8,9**], oceanic sink [**10**], microorganisms [**11**]. Capture and storage of CO_2 in a safer and permanent way is known as CO_2 sequestration.

Red mud (RM) is the caustic waste material of bauxite ore processing for alumina extraction. The Bayer process is commonly used for digestion of bauxite ore in a solution of conc. NaOH at temperatures between 150 to 230°C under pressure. During the digestion process, aluminum reacts with NaOH to form soluble sodium aluminate leaving red mud slurry [**12**]. Red mud slurry is highly alkaline having pH > 13, due to presence of NaOH and Na_2CO_3 (1–6%, w/w), these are expressed in terms of Na_2O [**13**,**14**]. The main constituents of red mud (% w/w) are: Fe_2O_3 (30–60%), Al_2O_3 (10–20%), SiO_2 (3–50%), Na_2O (2–10%), CaO (2–8%), and TiO_2 (trace–10%) [**15**]. The amount of red mud generated, per ton of alumina extraction, varies greatly depending on the type of bauxite ore used, from 0.3 tons for high-grade bauxite to 2.5 tons for very low-grade [**12**,**15**].

The main problems of storing red mud slurry are as follows:

- Costly maintenance of large red mud pond areas.
- Risk of caustic for all living organisms.
- Leakage of alkaline compounds into the ground water.
- Overflow of materials cause harmful effects on the surrounding environment.
- Dusting of dry surfaces interfere with nearby rehabilitation on plant life [**16**,**17**].

Various methods have been used for neutralization of red mud by adding liquid carbon dioxide [**16**,**18**], saline brines or seawater [**19**], Ca and Mg-rich brines, soluble Ca and Mg salts, acidic water from mine tailing, fly ash, carbon dioxide gas [**20**,**21**]. According to the standard environmental permissible level when the red mud pH < 9.0 is known as neutralized red mud (NRM). The NRM is utilized for environmental benefits. These processes are costly, so, hardly any industry takes the major to neutralize the red mud. From literature it was cleared that neutralization by using CO_2 showed pH reversion to unaccepted environmental levels as additional alkaline material leaches from the mud.

Utilization of industrial wastes as a resource to solve the problem of another wastes provide economic benefit. The use of CO_2 from the atmosphere or from industrial emissions is another potentially significant source of acid for neutralization of red mud. Since each 500 MW coal power plant emits about 3 million tons of CO_2 per year which may cause serious disruption to the global climate [**6**]. Red mud is an alkaline waste of alumina industry which can be used as a resource to capture and storage of anthropogenic CO_2, mainly from near source fossil fuel power plants [**22**]. Neutralization of aqueous caustic red mud solution takes place by the following carbonation reactions of CO_2 (Mechanism of neutralization):

$$CO_2\,(aq) + OH^-\,(aq) \leftrightarrow HCO_3^-\,(aq) \quad (1.1)$$

$$HCO_3^-\,(aq) \leftrightarrow H^+\,(aq) + CO_3^{2-}\,(aq) \quad (1.2)$$

$$NaAl(OH)_4\,(aq) + CO_2\,(aq) \leftrightarrow NaAl(OH)_2CO_3\,(s) + H_2O \quad (1.3)$$

$$3Ca(OH)_2{\cdot}2Al(OH)_3\,(s) + 3CO_2\,(aq) \leftrightarrow 3CaCO_3\,(s) + 2Al(OH)_3\,(s) + 3H_2O \quad (1.4)$$

$$Na_6[AlSiO_4]_6{\cdot}2NaOH + 2CO_2\,(aq) \leftrightarrow Na_6[AlSiO_4]_6 + 2NaHCO_3 \quad (1.5)$$

Furthermore, NRM can be used as low-cost environment-friendly adsorbent for removal of poisonous metal ions from water. Millions of people worldwide are exposed

to arsenic contaminated water as their only source of drinking water, due to natural and man-made sources. Arsenic can be easily solubilized in ground waters depending on pH, redox conditions, temperature, and solution composition. Arsenic contaminated water is one of the most challenging global environmental problems today [**23**]. Long-term exposure to arsenic contaminated water causes various types of cancers. Therefore, World Health Organization (WHO) has recommended the standard concentration of arsenic in drinking water is 10 μg L^{-1} [**24**]. But the typical arsenic concentration in arsenic contaminated water used for human consumption is about 100–300 μg L^{-1} [**25**].

Various methods for arsenate removal have been investigated for the rising demand of standard drinking water. Thus, there is a growing interest for development of low-cost materials and methods to remove arsenic from drinking water or industrial effluents before it may cause significant contamination. Although many different methods such as precipitation, coprecipitation of aluminum and iron hydroxides [**26**,**27**], adsorbing colloid flotation, ion-exchange, ultrafiltration, and reverse osmosis has been used for arsenic removal [**28**], but the process based on adsorption methods are promising, due to high concentration removal efficiency. Many types of adsorbents have been used: goethite [**29**], iron oxide minerals [**30**], zerovalent iron [**31**], soil [**32**,**33**], high surface area iron oxide based sorbent [**34**], activated red mud[**35**], Bauxsol and activated Bauxsol [**13**,**36**], are mostly used in arsenic adsorption, due to strong affinity of iron toward arsenic. Arsenic is mostly present in the form of arsenate [As(V)] and arsenite [As(III)] in natural water. Both As(V) and As(III) sorbs more efficiently to iron oxides [**30**].

Previous research has observed strong adsorption of arsenic to seawater neutralized RM (Bauxsol), further activated by acid treatment or combined acid and heat treatment method [**13**,**36**]. The results showed that combination of acid and heat treatment has greater removal efficiency.

The storage and maintenance of red mud is a challenging environmental problem in the alumina industry area due to its alkaline nature, which is a risk for living organisms [**17**,**18**,**37**,**38**]. Furthermore, arsenate adsorption mainly takes place in acidic medium [**13**,**39**]. But, its neutralization through a cost-effective process is highly needed for sustainable development of alumina industry. Therefore, its neutralization using CO_2 sequestration can solve some problem of global warming and these wastes can be used as resources for the alumina industry.

1.2. Motivation

Every waste is a resource if we give science and technology to them. CO_2 sequestration is a robust technique to reduce the global warming and climate change. However, high cost and high energy requirements are the main problems to control the global warming. Therefore, utilization of industrial waste is a novel resource as rapid industrialization for global economic competition. So, neutralization of caustic red mud using CO_2 sequestration and their utilizations for environmental benefits can enhance the socio-ecological-economical value of alumina industries.

For these reasons, it was thought appropriate to choose this topic. This would constitute a source of information for future research work in this field, and for large-scale utilization of these wastes as resources.

1.3. Objectives

Red mud causes global environmental problem near the alumina industry area and its further utilization is hindered, due to its caustic nature. However, worldwide > 70 million tons of red mud has been generated per annum. But, till now there is no successful technology has developed for large-scale utilization of red mud in commercial scale or industrial scale. Global warming and climate change are the most challenging environmental problems of today and future generation, mainly due to increase of anthropogenic CO_2 concentration in the atmosphere and industrial revolution. A survey of past literature reveals that many neutralization methods of red mud have been used, but they are not cost-effective for alumina industries which are far away from seashore. Furthermore, the amount of permanent capture of CO_2 and neutralization of red mud using CO_2 gas up to environmental accepted level has not been reported due to rebound pH. Hence an attempt has been made in the present study to neutralize the red mud using CO_2 sequestration and their utilizations. Similarly, utilization of activated CO_2–neutralized red mud for the removal of arsenate from aqueous solutions has not been reported as revealed from literature studies. Furthermore, large-scale utilization of red mud for extraction of fine iron oxide has not been reported previously.

The main objectives of the present research work carried out in this thesis are the following:

1. To neutralize the caustic red mud using CO_2 sequestration cycle at ambient temperature (24–27°C) and pressure (1 atm) by simple absorption method.
2. To find out the permanent capture of CO_2 by reuse of caustic red mud as a low-cost absorbent.
3. To estimate cost of CO_2 sequestration cycle during neutralization of red mud.
4. To utilize the activated CO_2–neutralized red mud (ANRM) for removal of arsenate from aqueous solutions by batch experiments.

5. To characterize the materials using XRD, SEM, EDX, BET, FT-IR, TG-DSC, solid UV-vis, AAS, CHNS, and chemical methods.

6. To utilize CO_2 and red mud for "extraction of fine iron from red mud", *Indian Patent Filed*, 884/KOL/2009A.

*****

Chapter 2

Literature Review

The knowledge of related literatures of the past studies is very much essential for any research for the formulation of the sound methodology which acts as the guiding force during the development of research. New areas of research can be inferred from literature. The review of literature related to the present research is organized and presented as follows:

2.1. Bayer process of alumina industry

The Bayer process is an economical method of producing aluminum oxide from bauxite ore using concentrated NaOH solution (caustic soda) at high temperature and pressure. The Bayer process was invented and patented in 1887 by the Austrian chemist Karl Bayer. Working in Saint Petersburg, Russia to develop a method for supplying alumina to the textile industry (it was used as a mordant in dyeing cotton), and Bayer discovered in 1887 that the aluminum hydroxide that precipitated from alkaline solution

was crystalline and could easily filtered and washed [**40**]. The NaOH selectively dissolves Al_2O_3 from bauxite ore [**41**]. This produces a sodium-aluminum solution from which pure alumina tri-hydrate, $Al(OH)_3$ precipitated, which is then calcined to produce Al_2O_3, from which metal is recovered.

A few year earlier, Henry Louis Le Chatelier in France develop a method for making alumina by heating bauxite in sodium carbonate, Na_2CO_3, at 1200 °C, leaching the sodium aluminate formed with water, then precipitating $Al(OH)_3$ by CO_2, which was then filtered and dried. This process was abandoned in favour of the Bayer process. The Bayer process is capable of producing huge quantities of high-purity aluminum hydroxide and aluminum oxides at relatively low-cost. This fact created opportunities early on for marketing profitable Bayer plant products outside the aluminum industry. A breakthrough in the quest for a cost-effective production process for aluminum occurred in 1886 [**42**]. The process began to get importance in metallurgy together with the invention of the electrolytic aluminum process invented in 1886. The cyanidation process was also invented in 1887. The Bayer process is the birth of the modern field of hydrometallurgy. Today, the process is virtually unchanged and it produces nearly all the world's alumina supply as an intermediate in aluminum production.

The Bayer process is the principal industrial method of refining bauxite to produce alumina. Bauxite is the most important ore of aluminum. It contains only 30–54% alumina, Al_2O_3; the rest is a mixture of silica, various iron oxides, and titanium dioxide, and also zinc, phosphorous, nickel and vanadium, etc. are found in trace amounts. The alumina must be purified before it can be refined to aluminum metal.

A Bayer process plant is principally a device for heating and cooling a large re-circulating stream of caustic soda solution. Bauxite is added at the high temperature point, red mud is separated at an intermediate temperature, and alumina is precipitated at the low temperature point in the cycle. Bauxite usually consists of two forms of alumina- a monohydrate form Boehmite ($Al_2O_3.H_2O$), and a tri-hydrate form Gibbsite

($Al_2O_3.3H_2O$). Boehmite requires elevated temperatures (above 200°C) to dissolve readily in 10% NaOH solution. The tri-hydrate grade bauxite is mainly Gibbsite which dissolves readily in 10% NaOH solution at temperatures below 150°C [**40**].

Alumina is produced by Bayer's process through the continuous four stages **[41]**:

1. Digestion of Bauxite: selective dissolution of alumina from bauxite ore

- **Grinding:** Bauxite ore is finely grinded by ball mill to size < 20 mm to allow better solid–liquid contact during digestion. Then recycled caustic soda solution is added to produce pump-able slurry, and lime is introduced for phosphate control and mud conditioning.

- **Desilication:** The silica component of the bauxite is chemically attacked by caustic soda, causing alumina and soda losses by combining to form solid desilication products. To desilicate the slurry prior to digestion, it is heated and held at atmospheric pressure in the pre-treatment tanks. Most desilication products pass out with the mud waste as sodium-aluminum silicate compounds.

- **Digestion:** The bauxite slurry is pumped by high pressure pumps through agitated, vertical digester vessels operating in series. Mixed with steam and caustic solution, this dissolves the alumina content of the bauxite selectively and forms a concentrated sodium alumina solution leaving un-dissolved impurities. Reaction conditions to extract the monohydrate alumina are about 250°C and a pressure of about 3500kPa, achieved by steam generated at 5000 kPa in coal-fired boilers. However for trihydrate alumina temperature of digestion is < 150°C.

The chemical reactions are:

$$2NaOH + Al_2O_3.3H_2O \rightarrow 2NaAlO_2 + 4H_2O \quad (2.1)$$

$$2NaOH + Al_2O_3.H_2O \rightarrow 2NaAlO_2 + 2H_2O \quad (2.2)$$

After digestion about 30% of the bauxite mass remains in suspension as thin red mud slurry of silicates, and oxides of iron and titanium. The mud-laden liquor leaving the digestion vessel is flash-cooled to atmospheric boiling point by flowing through a series of flash vessels which operates at successively at lower pressures.

2. Clarification of the liquor stream: settling out un-dissolved impurities

- **Settlers:** Most red mud waste solids are settled from the liquor stream in single deck settling tanks. Flocculants are added to the settler feed stream to improve the rate of mud settling and achieve good clarity in the overflow liquor.

- **Washers:** The mud is washed with fresh water in counter-current washing process to remove the soda and alumina content in the mud before being pumped to large disposal dams. Slaked lime is added to dilute caustic liquor in the washing process to remove Na_2CO_3, which forms by reaction with compounds in bauxite, and also from the atmospheric CO_2 which reduces the effectiveness of liquor to dissolve alumina. Lime regenerates caustic soda, allowing the insoluble calcium carbonate (precipitated) to be removed with the waste red mud [**41,42**].

$$Na_2CO_3 + Ca(OH)_2 \rightarrow CaCO_3 \downarrow + 2NaOH \quad (2.3)$$

- **Filters:** Settlers overflow liquor containing traces of fine mud is filtered in Kelly-type constant pressure filters using polypropylene filter cloth.

3. Precipitation of alumina tri-hydrate:

- **Crystallization:** Dissolved alumina is recovered from the liquor by precipitation of crystals. Alumina precipitates as the tri-hydrate ($Al_2O_3.3H_2O$) in a reaction, which is the reverse of the digestion of tri-hydrate:

  $$2NaAlO_2 + 4H_2O \rightarrow Al_2O_3.3H_2O + 2NaOH \quad (2.4)$$

  The cooled pregnant liquor flows to rows of precipitation tanks which are seeded with previously precipitated crystalline tri-hydrate alumina, usually of an intermediate or fine particle size to assist crystal growth. As correct particle size is important to smelter operations, so sizing is carefully controlled. The finished mix of crystal sizes is settled from the liquor stream and separated into three size ranges "gravity" classification tanks.

  Spent caustic liquor essentially free from solid overflows from the tertiary classifiers and is returned through an evaporation stage where it is re-concentrated, heated and recycled to dissolve more alumina in the digesters. Fresh caustic soda is added to the stream to make up for process losses [**41,42**].

4. Calcination of alumina: High temperature drying of alumina

Slurry of $Al_2O_3.3H_2O$ from the primary thickeners is pumped to hydrate storage tanks and washed on horizontal-table vacuum filters to remove process liquor. The resulting filter cake is fed to a series of calcining units and the feed material is calcined at 1100°C by circulating fluidized bed calciner or rotary kilns to remove both free moisture and chemically combined water.

$$2Al(OH)_3 + \text{heat} \rightarrow Al_2O_3 + 3H_2O \quad (2.5)$$

The circulating fluidized bed calciner is more energy efficient than the rotary kilns. Finally, produces 90% sandy alumina particle of size +45 μm. Rotary or satellite coolers are used to cool the calcined alumina from the rotary kilns. Fluidised-bed coolers further reduce alumina temperature to less than 90°C before it is discharged into conveyer belts, which carry it into storage buildings.

Alumina (aluminum oxide, Al_2O_3) is a fine white material. It is the main component of bauxite. The largest manufacturers in the world of alumina are Alcoa, Alcan, Ruscal, NALCO, Queensland Alumina Limited (QAL), etc.

The residue also contains alumina which is undissoved during the alumina extraction from bauxite. The other components of bauxite Fe_2O_3, SiO_2,TiO_2, etc. do not dissolve in the basic medium, however some SiO_2 dissolve as silicate $Si(OH)_6^{2-}$ and are filtered from the solution as solid impurities (clarification). For various reasons, most alumina producers add lime at some point in the process and the lime forms a number of compounds that end up with the bauxite residue. The solid impurities are called red mud. The red mud causes disposal problem, due to its caustic nature.

A large amount of the alumina so produced is then subsequently smelted in the Hall-Heroult process in order to produce aluminum. Metallic aluminum is very reactive with atmospheric oxygen, and a thin passive layer of alumina quickly forms on any exposed aluminum surface. This layer protects the metal from further oxidation. The thickness and properties of this oxide layer can be enhanced using a process called anodizing. A number of alloys, such as aluminum bronzes, magnalum, are prepared to enhance corrosion resistance [**41,42**]. One metal whose growth in the past century has been unsurpassed is aluminum. Its strength and light weight guarantees its demand, especially in transportation where fuel efficiency is paramount.

Annual world production of alumina is approximately 45 million tons, over 90% of which is used in the manufacture of aluminum metal. Al_2O_3 is a refractory material,

due to its high melting point. The major uses of aluminum oxides are in refractory, ceramics, polishing and abrasive applications.

Aluminum oxide is an electrical insulator, but has a relatively high thermal conductivity. The most commonly occurring crystalline alumina is α-Al_2O_3 called corundum. Its hardness makes it suitable for use as an abrasive and as a component in cutting tools [**41**].

2.1.1. Origin of red mud

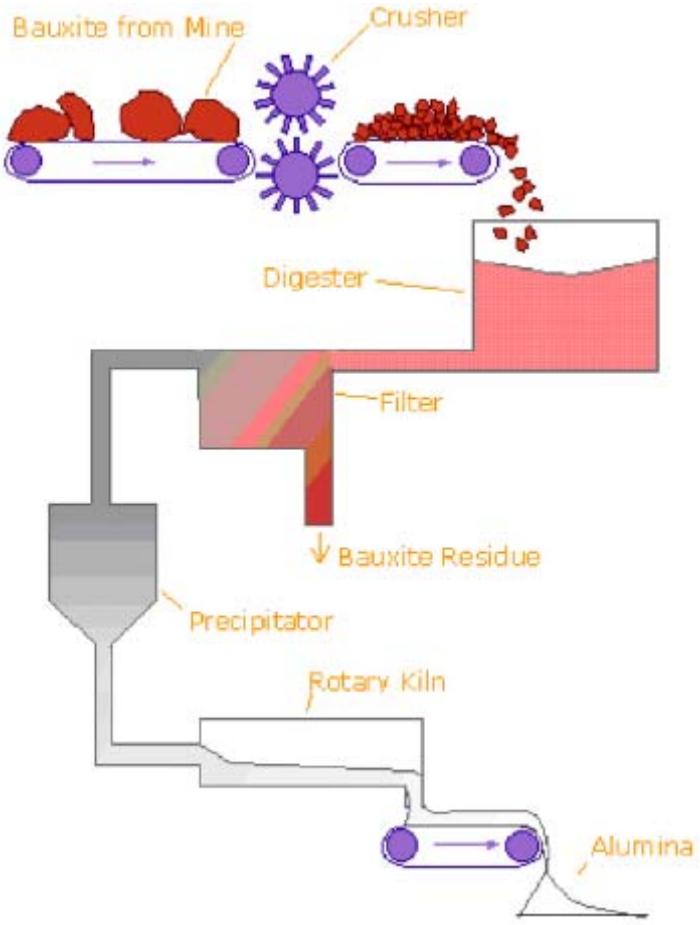

Fig. 2.1. Production process of alumina and red mud (bauxite residue) in the Bayer process [**43**].

Bauxite residue (also known as "red mud") is a by-product of the Bayer Process (Fig. 2.1). It looks red in color (Fig. 2.2a), due to presence of iron oxides. The amount of residue generated, per ton of alumina produced varies greatly depending on the type of bauxite used, from 0.3 tons for high-grade bauxite to 2.5 tons for very low grade. The chemical and physical properties of red mud depends primary on the bauxite used and, to a lesser extent, the manner in which it is processed. Red mud is the main solid waste product of alumina industry. The worldwide annual production of red mud is 70 million tons. Its disposal remains an issue of great importance with environmental implications [**44**].

The following data gives some idea about the worldwide chemical composition of red mud found from different bauxites.

Table 2.1: Average chemical composition (wt%) of red mud in worldwide [**43,44**].

Fe_2O_3	30-60%
Al_2O_3	10-20%
SiO_2	3-50%
Na_2O	2-10%
CaO	2-8%
TiO_2	Trace-10%

Table 2.2: Chemical composition (wt%) of red mud in different alumina industry worldwide [**45,46**].

Country		Major chemical composition, wt%				
		Fe_2O_3	**Al_2O_3**	**TiO_2**	**SiO_2**	**Na_2O**
India	MALCO	45.17	27.00	5.12	5.70	3.64
	HINDALCO	35.46	23.00	17.20	5.00	4.85
	BALCO	33.80	15.58	22.50	6.84	5.20
	NALCO	52.39	14.73	3.30	8.44	4.00-
Hungary		38.45	15.20	4.60	10.15	8.12
Jamaica		50.9	14.20	6.87	3.40	3.18
Surinam		24.81	19.00	12.15	11.90	9.29
USA	ALCOA Mobile	30.40	16.20	10.11	11.14	2
	Arkansas	55.6	12.15	4.5	4.5	1.5-5.0
	Sherwon	50.54	11.13	Traces	2.56	9.00
FRG Baudart		38.75	20.00	5.5	13.00	8.16
Taiwan		41.30	20.21	2.90	17.93	3.8
Australia		40.50	27.70	3.50	19.90	1-2

Depending on the quality of the bauxite, the quantity of red mud generated varies from 55–65% of the bauxite processed. Generally red mud is dumped near the plant site in the red mud ponds. But, in some countries like France, England, Germany, Japan the red mud has been discharged into the sea, where availability of land for dumping is less and sea is nearby. Furthermore, the red mud utilization in laboratory scale has been increasing in worldwide as the technology is changing day by day. A lot of research and developmental activities are going on throughout the world to find effective utilization of red mud, which involves various product developments [**45**].

Table 2.3: The approximate amount of red mud generation in India [**47**].

Generation of red mud in India by 2010, (lakh tons/annum)		
Company	**2008-09**	**Additional generations by 2010**
NALCO	20.33	6.50
HINDALCO	16.54	4.55
BALCO	2.97	
MALCO	0.95	
VEDANTA	3.66	18.20
UTKAL		19.50
RAYKAL		18.20
ADITYA		18.20
JSW		18.20
Total	~44.45	~103.35
Grand Total = 44.45 + 103.35 = ~147.8		

India is the 4th largest deposit of bauxite in the world. Whereas, more than 50% of bauxite deposit of India is present in the state of Orissa. The measure constituents of red mud are the oxides of Fe, Al, Si, Ti, Na and Ca along with a large number of minor constituents. The alumina, silica and soda account for about 40% of the total red mud and rest are mostly in the form of iron and titanium oxides. The chemical compositions of Indian red mud are given in Table 2.4. Loss on Ignition (LOI) is the loss of volatile gases (e.g. H_2O, CO_2) from the material when treated at specific temperature.

Table 2.4: Chemical composition (wt%) of Indian red mud [**47**].

Composition	**East cost bauxite (high Fe & low Ti)**	**Central India bauxite (low Fe & high Ti)**
Al_2O_3	18-20	18-20
Fe_2O_3	50-55	35-37
TiO_2	4-5	18-20
SiO_2	5-6	7-9
Na_2O	4.5-6	5-6
CaO	0.1-0.6	1-2
LOI(Loss On Ignition)	11-12	10-12

2.1.1.1. Disposal methods

Generally two types of red mud disposal methods (dry and wet disposal) have been followed by alumina industries. Red mud disposal in alumina industries areas causes seepage of alkaline liquid into ground water, which might contaminate industrial, domestic, and agricultural water supplies; spillage from damaged pipelines or from retaining-dyke failure, reduction in the availability of arable land, requirement of huge area (about 2 million square kilometer per annum), dust pollution in arid regions, aesthetic impacts, etc. are the other problems of alumina industry **[48]**. With the growing concern of the environmental protection as well as land conservation, a systematic effort has been made to modify and improve upon the methods of disposal. The details of the red mud disposal practices at the Indian alumina plants are as given in Table 2.5.

Table 2.5: Red mud disposal practices at the Indian alumina plants **[48].**

Name of the plant	**Red mud (t/t) of alumina**	**Dumping process**
INDAL,Muri	1.35-1.45	This refinery adopted the close cycle (wet slurry disposal) system (CCD). The disposal ponds have not been provided with any liner.
NALCO, Damonjodi	1.2	A modified CCD method is used for wet disposal. Subjected to six stages counter current washing by pond returned water (0.5g/Na_2O) and condensate from the evaporators. The washed red mud repulped and sent to disposal sites. The bottom and the sites of the pond are covered by impervious and semi pervious clay with base filters (Fig. 2.2b).
Vedanta, Lanjigarh	1.3	Wet disposal
BALCO, Korba	1.3	Residue after setting, counter current washing in four stages and filtered. The filtered cake is repulped with the pond returned water and dumped in the pond. Uses MCCD system of wet disposal. The dykes of the currently used pond have stone masonry and well protected polythene liner and clay layer.
HINDALCO, Renukoot	1.4	Traditional CCD method of impoundment was used. In late 1979 dry disposal method was implemented. After five stages counter current washing the solid is filtered (70% solids) and disposed off into the pond.
INDAL, Belgaum	1.16	The plant switched over to dry disposal mode from wet slurry disposal mode in 1985. The mud after clarification process through six stage counter current washing and after filtration (65% solids), it is disposed by dumpers at the pond site. The dry portion of the pond is covered with a 15 cm black cotton soil for promoting green vegetation.

2.1.1.2. Advantages and disadvantages

Advantages of wet disposal:

- Lower capital cost (if land is cheap).
- No cost towards thickening/filtration of slurry.
- No dust problem due to presence of liquor.

Disadvantages of wet disposal:

- Large area required for disposal.
- Environmental hazards associated with caustic leachate contaminating ground water and surface water.
- High capital required during closing and rehabilitation and difficulty in closing ponds.
- High soda and alumina loss with adhering moisture with mud.

Advantages of dry disposal:

- Land requirement for storage is minimized.
- The soluble soda and alumina losses are reduced.
- Due to reduced hydraulic head ground water contamination is reduced.
- Surface water contamination can be reduced by reducing the catchment area and returning runoff water to plant.
- Because disposal into sea or river streams is not favoured for aquatic/marine flora and fauna. Only very few alumina plants of world are still practicing the sea disposal in a planned manner because of scarcity of land **[47,49].**

Disadvantages of dry disposal:

- Not ideally suitable for area with high precipitation (rainfall).
- Dust control requires sprinkling of dust suppressant.
- Requires additional filtration stage to reduce moisture **[47].**

(a)

(b)

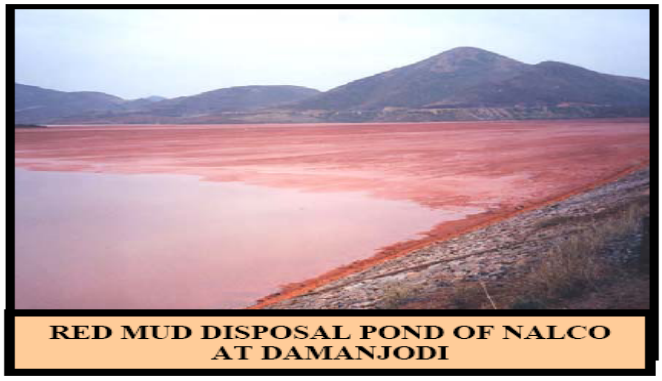

Fig. 2.2: (a) Red mud, (b) Red mud pond of NALCO **[50].**

2.1.2. Environmental pollution

Alumina refinery is a mineral-based chemical plant involving refining of crushed bauxite ore. Alumina plant operation includes various physical operations like crushing, grinding, conveying, loading, transporting, etc., which generate fine particles. It can cause serious health hazards on inhalation, depending upon its size, shape, constituents and duration of exposure. Out of these parameters, concentration of respirable fraction of airborne dust (0.5 to 5.0 micron size) and its free silica content have been reported to cause lung fibrosis as well as occupational disorders. Expose to dust causes lung-related diseases called pneumoconiosis. Silicosis is the most common form of pneumoconiosis, which is caused due to exposure of free silica [**51**]. Furthermore, the captive power plant (coal based) is also responsible for air and dust pollution. Noise pollution is found

in industrial and mining area. Plantation and afforestation around the conveyer belt can effectively reduce the noise and air pollution.

Water pollution: Leakage and overflow of alkaline slurry from red mud ponds into the water bodies and river are causing cattle deaths and crop loss. Villagers are mostly affected due to the discharge of effluent from the effluent treatment plant (ETP). The domestic animals as well as human beings exposed to such polluted water are severely affected with various types of skin diseases due to high alkaline pH of the water.

Ground water pollution near the refinery area is due to leakage from fly ash pond and red mud pond (Fig. 2.2b). During heavy rain the ponds overflow and their toxic materials spilled into the nearer stream and river [**51**]. Moreover, coal-power plant releases large amount of CO_2 into the atmosphere which causes air pollution.

2.2. Neutralization methods

Untreated red mud is highly caustic (the pH usually >13.0), due to the presence of the residual NaOH during bauxite digestion and the formation of some Na_2CO_3. This high alkalinity is environmentally hazardous, and therefore red mud needs to be neutralized before it can be used. It also needs to be neutralized if it is to be stored safely or regenerated. Sodium hydroxide (NaOH) is known as caustic soda. It is a caustic metallic base. Caustic soda forms a strong alkaline solution when dissolved in a solvent such as water. NaOH is completely ionic, containing Na^+ and OH^- ions. The OH^- ion makes NaOH a strong base which reacts with acids to form H_2O and the corresponding salts. For example,

$$NaOH\ (aq) + HCl\ (aq) \rightarrow NaCl\ (aq) + H_2O\ (l) \qquad (2.6)$$

This neutralization reaction is represented by simple ionic equation:

$$OH^-(aq) + H_3O^+(aq) \rightarrow 2H_2O \quad (2.7)$$

The cost of red mud management can be reduced by their utilization; usually it requires at least partial/complete neutralization of the caustic component of the red mud in a cost-effective method. Thus, it is desirable to neutralize the red mud in such a way that it is no longer highly caustic [**52**]. Several methods of neutralization for red mud have been reported previously e.g. with the addition of gypsum or acid, or using either Ca- and Mg-rich brines, infiltration of rain water, sea water neutralization, adding waste acids like H_2SO_4, heat treatment with strong acids, etc. But none are in widespread use due to limitations in the neutralization methods.

2.2.1. Using Mg- and Ca- or brine, Polycationic salts ($FeCl_3$, $MgCl_2$, $CaCl_2$):

Baldwin et al., [**53**] investigated the neutralization of highly alkaline waste materials using different cationic salts. In this method hydroxide alkaline waste and by-products were neutralized from pH 14 to 5.3 using aluminum polycation salts. After that the waste materials is suitable for disposal or reuse. The alkaline material is treated with sufficient amount of water and with one or more polycationic salts in the dry form taken from a group of salts containing tri-valent aluminum, tri-valent iron, di-valnt calcium, di-valent magnesium, di-valent manganese, divalent zinc. The materials react to form a soluble salt and an insoluble hydroxide precipitate with water. Similarly, $CaSO_4.2H_2O$ (gypsum) is added to reduce the alkaline pH. The addition of salts may be dry or made up of brine or dilute salt solution, which reduces the hydroxide alkalinity in red mud materials causing the pH to drop immediately upon proper mixing.

Kotai et al., [**54**] studied the neutralization of the alkaline materials using iron (III) sulfate or its mixture with aluminum sulfate. This was used as a solid phase sulfatizing agent to destroy sodium aluminum silicates in red mud within 2 h at 200–500 °C. These solid phase sulfatizing agents transform solid aluminum silicates and basic sodium-compounds into water-soluble sodium sulfate without SO_2 or SO_3 evolution. Subsequently, by means of an aqueous leaching of the sulfatized red mud a

raw material with high iron and low sodium content is obtained for blast furnace technologies. But, these methods are not economically feasible for industrial use.

2.2.2. Using waste acids (H_2SO_4, HCl)

Neutralization using gypsum, strong acid or similar additive can produce safer storage of red mud. However the processes are usually costly and the resulting neutralized red mud has almost no value for reuse. It should be stored in small area so that storage area must ultimately be rehabilitated.

2.2.3. Using fly ash, liquid CO_2, and CO_2

Neutralization can be possible by utilizing fly ash solid waste of power plant and mixing with other low-cost acidic gas and low purity salt solutions, ground water, rain water. These methods are not cost-effective for management of red mud pond. Some researchers studied the neutralization of red mud using liquid CO_2, and CO_2. But due to some drawbacks of rebound pH, these processes could not feasible. Moreover, over flow of caustic water from red mud pond during rainy season create problems near the rehabilitation. [**16,18,20–22**].

2.2.4. Using sea water

The use of seawater can be very effective for plants that are nearer to the coast and the process can be made more efficient if the site is an arid or semi-arid area where evaporative concentrated seawater is available. The addition of seawater to red mud helps pumping of slurry and also conserves fresh water. However, large amount of seawater will be required (typically between 12–18 times the volume of red mud) to be neutralized. But the discharge water will be required large pond to allow the solids to settle down. These limitations add substantially to the cost of the neutralization process [**19,55**].

The cost of the red mud management can be reduced if it is turned into a useable product. This logic has been applied by an Australian company, Virotec, to the treatment and disposal of red mud. Virotec scientists looked at the problem of neutralization of red mud and if possible turned into a usable product. To neutralize red mud and turn it into saleable product, only suitable neutralization procedures that involve the conversion of basicity (mainly NaOH) and soluble alkalinity (mainly $NaHCO_3$) into alkalinity are mainly considered. Owing to this idea they mixed the red mud with seawater**.**

Seawater or Ca- and Mg-rich brines (e.g. salt lake brines) are added to caustic red mud. As a result the pH of the mixture is reduced, which causes precipitation of hydroxide, carbonate or hydroxyl carbonate minerals. The neutralizing effects of the Ca^{2+} and Mg^{2+} ions is initially large but decreases rapidly as complete neutralization is approached. Neutralization is considered to be complete when the liquid that can be separated from the treated red mud has a pH < 9.0 and a total alkalinity < 200 mg L^{-1} (as calcium carbonate equivalent alkalinity) such water can be safely discharged to the marine environment **[40].**

The mechanism of neutralization using sea water:

The red mud is actively mixed with the sea water for a period of around 30 minutes to enable the reactions to take place. Seawater is added until the liquid phase of the precipitates can be decanted and reduced in alkalinity from pH 9.5 to 9.0. To meet marine discharge standards the liquid is treated with acid to bring the pH to below 9.0. This would normally require 0.05 liters of concentrated H_2SO_4 per 1000 liters of red mud after treating with sea water. Alternatively, the liquid fraction can be solar evaporated to salts, with the remainder retained as slurry or dried for further use **[40]**.

The effect of degrees of neutralization:

If red mud is completely neutralized by sea water, it required 15-20 times the volume of red mud. This requires extensive and expensive pumping, furthermore it produces inert red mud, but it is completely worthless. However, Virotec has found that slightly less than complete neutralization can be achieved with less sea water. For example, if untreated red mud has pH ~13.5 and an alkalinity ~20,000 mg/L, whereas the addition of ~ 5 volumes of average sea water will reduce the pH to between 9.0 to 9.5 and the alkalinity to about 300 mg/L.

To increase the efficiency of the process, Virotec scientists were used 1.5 times higher saline sea water as compared to ocean average. Subsequently, the process was more efficient and required only 3.5 litres per 1000 litres of red mud, as compared to 6 litres of average salinity sea water.

Neutralization for commercial gain:

Initial treatment of red mud with sea water is the first step in the conversion of red mud into a useful and saleable product. Since the neutralized red mud will reduce the storage and management costs.

It can be used as a raw material for commercial reagents with acid neutralizing capacities in excess of 15 moles of acid/kg. Partly neutralized red mud has a very high trace metal trapping capacity. It also has a high capacity to trap and bind hazardous metal ions from water, and is an excellent flocculent. Commercial reagents based on these characteristics have wide spread applications in the sewage treatment industries [**17,19,40,56**].

2.3. Utilizations of red mud

The storage of large amounts of red mud in landfills generally creates not only serious environmental problem for the local population because of its high level of alkalinity (usually near pH 12–13), but also economic problems for its maintenance. The use of

these minerals deposits as a secondary raw material for a variety of applications would produce economic benefits and solve a great environmental problem.

Difficulties of red mud utilization:

1. **Soda content**
    - Leachable soda around 1-2%.
    - Bound soda around 3-6% in the form of sodium aluminum silicate.
    - High amount of soda act as a preliminary barrier for its use as a raw material for industrial application such as cement and clinker production, steel industry, constructional bricks, blocks, etc.
2. **Composition variability**
    - Chemical and mineralogical composition of red mud generated depends on the nature of bauxite and processing parameters.

Hence the utilization of red mud cannot be uniform since it is constituent dependent **[47]**.

The feasible reuse of red mud for any application should have following criteria:

- **Volume:** The application should have high volume usage.
- **Performance:** It should be a low-cost substitute for other material and its performance should be the same.
- **Cost:** It should be cost-effective.
- **Risk:** There should be no environmental risk associated with its use as health and safety **[47]**.

Different Utilizations of red mud:

- Removal of toxic heavy metals from water such as fluoride **[57],** Cr(VI) **[58],** arsenic [**36,56]**, vanadate and molybdate **[59],** copper **[60],** phosphate **[61,62],** Ni^{2+} **[63].**
- Used as coagulant, adsorbent and catalyst [**64–66].**
- Additives for production of cements [**64, 67–69**].

- Used as soil conditioner/fertilizer, revegetation [**70**].
- Preparation of ceramic materials, tiles, glass ceramics [**71**].
- Constructional bricks as building material, road bed material [**72**], synthesis of inorganic polymeric materials [**73**].
- Development of red mud building block, brick, hollow bricks, using an admixture of red mud, blast furnace slag and fly ash.
- Development of fiber reinforced red mud composite doors.
- Acid mine drainage remediation.
- Red oxide and primer is produced using an admixture of red mud.
- Recovery of metals iron, alumina, zirconia, titanium, etc. from red mud, and production of Ferro-titanium **[47,49,64**,**74**].

Because of the high alkalinity, the red mud is usually not suitable for cement production, metal extraction, and pig iron production, etc. However, red mud contains appreciable amount of iron oxide (25–60%) depending upon the origin of bauxite ore and chemical treatment process. Various attempts have been made by previous researchers to recover iron**,** Al_2O_3, TiO_2, etc. from it. But till now no economically feasible technology has been developed due to some drawbacks [**45,49**].

Genc-Fuhrman et al., [**36,56**] investigated the removal of arsenic by using sea water neutralized red mud (Bauxsol). The arsenate removal capacity of Bauxsol is significantly increased with the increase of reactive surface area of the sorbent. The acid and heat treated Bauxsol (activated Bauxsol) was the most effective because the heat treatment allowed the Bauxsol to develop more porosity. Moreover, the arsenic removal capacity was suppressed in the presence of multimetal ions in the solution. The surface is attractive to several anions other than arsenate, and the selectivity of the activated Bauxsol surface on a molar basis is: arsenate > phosphate > silicate > sulfate > bicarbonate > chloride.

Zhang et al., [**75**] studied the effect of coexisting ions on the adsorption of arsenate. Ca^{2+}, HCO_3^-, and NO_3^- always exist in natural water. Ca^{2+} significantly enhanced the adsorption capacity of red mud. Ca^{2+} can link the modified red mud (MRM) particle with arsenate, forming a metal-arsenate complex or a metal–H_2O–arsenate complex. HCO_3^- decreased the arsenate removal efficiency. This may be due to the competition between HCO_3^- and $HAsO_4^{2-}$ for positively charged adsorption sites. NO_3^- had no effect on adsorption of arsenate because it did not compete with $HAsO_4^{2-}$.

Kumar et al., **[49]** also studied on utilization of red mud for recovery of iron and other metals using red mud of NALCO, Bhubaneswar, which contains about 50–60% of Fe_2O_3. The recovery process involves alkaline roasting of red mud in presence of carbon at 750–800 °C, leaching of aluminum values for aluminum recovery and separating the iron values from the residues as magnetic fraction and titania as the non-magnetic fraction.

Furthermore, red mud and ferrous slag are two very large volume waste materials that are accumulated at the industrial areas. Their strength can be accelerated by adding small amounts (2%) of CaO or Portland cement. The high strength of these new materials renders them applicable in the construction of roads and airfield runways, industrial and municipal dumps, building foundations, in tile and brick production, etc. [**76**].

Common practices of waste management in these industries are through recycling and recovering the metal values and dumping. Due to the presence of toxic elements in some of the solid wastes cause environmental degradation. Non-ferrous metals besides gold, silver and platinum are somewhat toxic to living organism. Aluminum industries are non-ferrous metallurgical industries. It is important that all the metallurgical industries not only take care of the process of manufacture but also safe disposal of the pollutants generated in the form of solids, liquids or gaseous wastes.

Metallurgical industries generate vast quantities of solid waste such as slag, fly ash, red mud, sludge, etc. **[48]**.

2.4. CO_2 sequestration and utilizations

2.4.1. Increase of [CO_2] in the atmosphere

More than 80% of the world's energy is coming from fossil fuel [**77**]. Anthropogenic CO_2 emission caused by fossil-fuel burning is a primary reason for rapid global warming and climate change. Increasing atmospheric CO_2 concentration is creating a catastrophic risk for earth's climate system. However, our civilization depends mostly on the energy gained by burning fossil-fuels. Yet fossil fuel emissions increased by 29% between 2000 to 2008, this is due to increased economies, from the production and international trade of goods and services, and from the use of coal as a fuel source. Between 1959 and 2008, 43% of each year's CO_2 emissions remained in the atmosphere on average; the rest was absorbed by carbon sinks on lands and in the oceans. But the CO_2 concentration in the atmosphere has increased due to decrease of CO_2 sink. This is mainly due to deforestation and increase of acidity of ocean. Therefore, the potential utilization of CO_2 as an abundant and inexpensive chemical resource is of widespread interest for stabilization of atmospheric CO_2 concentration. At present, the utilization of technologies for CO_2, such as CO_2 capture and storage, separation, sequestration, CO_2 chemical conversion, mineral carbonation, utilization of alkaline wastes, geological sequestration, are promising options to reduce the risk of future devastating effects [**78–80**].

Over the last 200 years a number of greenhouse gases (e.g., CO_2, CH_4, N_2O, H_2O vapors, chlorofluorocarbons (CFCs)) concentrations have been increasing in the atmosphere. These gases absorb solar infrared energy radiation reflected from the earth, which results in an increase in the temperature of the troposphere. At the present time, the most important greenhouse gas is CO_2 (contribute ~80% of the total impact), but

other greenhouse gases (GHGs) also play crucial role. The continued burning of fossil fuels has and will continue to increase the [CO_2] in the atmosphere. It is quite clear from the pioneering CO_2 measurements of Keeling and Whorf at Wawaii and the ice core measurement that the CO_2 is increasing. The preindustrial CO_2 concentration levels were 280 ppmv and have increased to the level of 370 ppmv by 2007 [**81**]. For each 4 gigatons (Gt) of fossil carbon burned, the atmosphere's CO_2 concentration rises about 1 ppm; including deforestation. We now emit about 8 Gt of carbon per year [**82**]. Worldwide, the 5.4 billion tons of coal burned each year generate roughly a third of the world's carbon dioxide emissions. But coal's low cost compared to other energy sources makes it irresistible to nations with plentiful deposits [**83**].

CO_2 is mainly responsible for increase of global average temperatures since the mid-20^{th} century [**79**]. To save the earth from Climate Change, world should maintain the concentration of greenhouse gases (GHGs) that would prevent dangerous anthropogenic interference with the climate system [**84**].

Chemical compositions of air:

Air is a mixture of gases which make up the Earth's atmosphere. The composition, physical, and chemical properties of air are very similar everywhere. It is useful to think of the air which we encounter every day as being a locally-produced mixture of three types of ingredients, standard dry air, water vapor (humidity, ~0-5%), and other constituents depends on local conditions.

Standard dry air is mainly composed of three gases: N_2 (~78%), O_2 (~21%), and Ar (~1%). These three gases make up 99.96% of dry air. All three can be economically recovered as industrial gas products. Standard dry air also contains small amount of CO_2 (0.038%), very small amount of Ne, He, Kr, H_2, Xe. Local additions to the composition of air can be very site-specific. They depend on the immediate surroundings, including wind direction, time of day, season of the year. Non-standard

components may be present due to natural processes (biological or geological) or human activities (industrial, transportation, agricultural).

CO_2 is considered to be a standard component of air, although the concentration of the CO_2 in air will vary somewhat by location, and by season of the year. Therefore, any standard value for the concentration of CO_2 in air is approximation. So, 385 ppmv ± 5 ppmv is a reasonable value. Worldwide, the average concentration of CO_2 in Earth's atmosphere is rising at a rate of about 2 ppmv per year.

CO_2 is continually produced and removed from the atmosphere by a multitude of natural mechanism. CO_2 dissolves in water (including rain) and carried into rivers, lakes, and oceans, and it is removed by photosynthesis. It is again returned to atmosphere by oxidation of dead organic matter and by animal respiration [**85**].

2.4.2. Chemistry of Inorganic CO_2:

Properties of CO_2:

CO_2 is a colorless, odorless, acidic gas. It is a necessary raw material for most plants, which remove CO_2 from air using the process of photosynthesis and release oxygen (O_2). CO_2 is formed by combustion and by biological processes. These include decomposition of organic materials, fermentation and digestion [**81**].

(i). Physical Properties of CO_2:

CO_2 is a gas at normal temperature and pressure. The physical state of the CO_2 varies with respect to the temperature and pressure as shown in Figure 2.3. At low temperature CO_2 is solid; on warming, if the pressure is below 5.1 bar, the solid will sublimate directly into the vapour state. CO_2 may be turned from a vapour into liquid by compressing it to the corresponding liquefaction pressure by removing the heat produced.

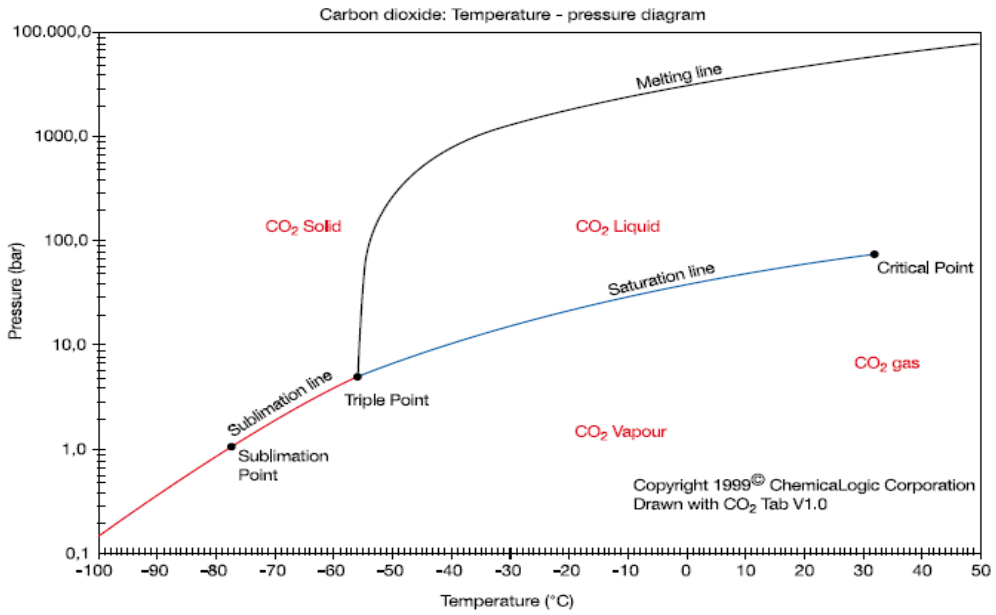

Fig. 2.3: Phase diagram of CO_2 [**84**].

At temperature higher than 31.1°C (if pressure > 73.9 bar, the pressure at critical point), CO_2 is said to be supercritical state where it behave as a gas, as a result under high pressure, the density of the gas can be very high, which approaching or even exceeding the density of liquid water. This is an important aspect of CO_2's behavior and is helpful for its storage.

Heat is released or absorbed in each of the phase changes across the solid-gas, solid-liquid and liquid-gas boundaries. However, the phase changes from the supercritical condition to liquid or from supercritical to gas do not require or release heat. This property is useful for the design of CO_2 compression facilities [**84**]. It will form "dry ice" at -78.5°C [**85**]. Some physical properties of CO_2 are given in Table 2.6.

Table 2.6: Some physical properties of CO_2 [**84**].

Properties	**Value**
Molecular weight	44.01
Critical temperature	31.1°C
Critical pressure	73.9 bar
Critical density	467 kg m^{-3}
Triple point temperature	–56.5°C
Triple point pressure	5.18 bar
Boiling (sublimation) point (1.013 bar)	–78.5°C
Gas phase	
Gas density (1.013 bar at boiling point)	2.814 kg m^{-3}
Gas density (@ STP)	1.976 kg m^{-3}
Solubility in water (@ STP)	1.716 vol vol^{-1}
Liquid phase	
Vapour pressure (at 20°C)	58.5 bar
Liquid density (at –20°C and 19.7 bar)	1032 kg m^{-3}
Solid phase	
Density of CO_2 snow at freezing point	1562 kg m^{-3}
Latent heat of vapourisation (1.013 bar at sublimation point)	571.1 kJ kg^{-1}

Where STP stands for Standard Temperature and Pressure, which is 0°C and 1.013 bar.

(ii). Chemical Properties of CO_2:

CO_2 in aqueous solution forms carbonic acid, which is too unstable. The solubility of CO_2 in water decreases with increasing temperature and increases with increasing pressure.

Carbon dioxide is a stable compound ($\Delta G°_f$ = –394.4 kJ mol^{-1}) whose reaction with Lewis bases are of large important in biology, geology and industrial applications. The thermodynamics of the carbonate system in natural waters is governed by the following equilibria [**84,86**]:

$$CO_2\,(g) + n\,H_2O \leftrightarrow CO_2\,(aq) \quad (2.8)$$

$$CO_2\,(aq) + H_2O \leftrightarrow H_2CO_3\,(aq) \quad (2.9)$$

$$H_2CO_3\,(aq) \leftrightarrow H^+\,(aq) + HCO_3^-\,(aq) \quad (2.10)$$

$$HCO_3^-\,(aq) \leftrightarrow H^+\,(aq) + CO_3^{2-}\,(aq) \quad (2.11)$$

Addition of CO_2 to water initially leads to an increase in the amount of dissolved CO_2. The dissolved CO_2 reacts with water to form carbonic acid (H_2CO_3). Carbonic acid dissociates to form bicarbonate ions (HCO_3^-), which can further dissociate into carbonate ions (CO_3^{2-}).

Table 2.7: Thermodynamics data for CO_2 and a few related carbon-containing compounds [**84**].

Compound	**Heat of formation ΔH_f° (kJ mol^{-1})**	**Gibbs free energy of formation ΔG_f° (kJ mol^{-1})**	**Standard molar entropy S_f° (J mol^{-1} K^{-1})**
$CO_2\,(g)$	–393.51	–394.4	213.78
$CO_2\,(aq)$	–413.26		119.36
$CO_3^{2-}\,(aq)$	–675.23		–50.0
$HCO_3^-\,(aq)$	–689.93	–603.3	98.4
$H_2O\,(l)$	–285.83		69.95

The net effect of dissolving anthropogenic CO_2 in water is the removal of carbonate ions and production of bicarbonate ions, with a lowering in pH. CO_2

dissolves in sea water so the pH of sea water is 7.8–8.1 at 25°C. These values are strongly depending on carbonate/bicarbonate buffering [**84**]. Even though CO_2 has very poor solubility in water, the pH drops to 2.84 at 71 bar and 40 °C. Further at higher pressure, there is very little change [**87**].

2.4.3. Utilizations of CO_2:

Carbon dioxide recovered from flue stacks or the atmosphere can be sequestered in oceans or spent gas and oil wells in an effort to mitigate increase of concentration of atmospheric CO_2. Alternatively, recovered CO_2 can be used for producing chemicals, fuels, and other useful products.

There are several motivations for producing chemicals from CO_2 wherever possible.

1. CO_2 is generally considered as a green chemical, environmentally friendly, relatively nontoxic solvent, nonflammable, and naturally abundant.
2. CO_2 has been suggested as a sustainable replacement for organic solvents in a number of chemical processes.
3. The production of chemicals from CO_2 could have a small but significant positive impact on the global carbon balance.
4. CO_2 possesses a number of characteristics that suggest the use of CO_2 could provide both environmental and economic benefit **[88].**

Various Utilizations of CO_2:

- **Multi-Industry uses:** CO_2 in solid and in liquid form is used for refrigeration and cooling. It is used as an inert gas in chemical processes, in the storage of carbon powder and in fire extinguishers.

- **Metal industry:** CO_2 is used in the manufacture of casting molds to enhance their hardness.
- **Manufacture and construction uses:** CO_2 is used on a large scale as a shield gas in welding, where the gas protects the weld puddle against oxidation by the surrounding air. A mixture of argon and CO_2 is commonly used today to achieve a higher welding rate and reduce the need for post weld treatment.
- **Chemicals, pharmaceuticals and petroleum industry uses:** Large quantities of CO_2 are used as a raw material in the chemical process industry, especially for the methanol and urea production.

- **Large quantities of CO_2 are used in oil wells for enhance oil recovery** and also maintain pressure within a formation. When CO_2 is pumped into an oil well, it is partially dissolved into the oil, causing it less viscous, allowing the oil to be extracted more easily from the bedrock. As a result more oil can be extracted using this process [**85**]. Furthermore, enhanced oil recovery has been identified as a method of sequestering CO_2, recovered from power plants **[89].**

- **Rubber and plastics industry uses:** Flash is removed from rubber objects by tumbling them with crushed dry ice in a rotating drum.
- **Food and beverages:** Liquid or solid CO_2 is used for quick freezing, surface freezing of food products such as poultry, meats, vegetables and fruits.CO_2 gas is used to carbonate soft drinks, beers, and wine and to prevent fungal and bacterial growth.
- **Health care uses:** CO_2 is used as an additive to oxygen for medical use as a respiration stimulant.
- **Environmental uses:** Used as a propellant in aerosol cans. It is used to neutralize alkaline water.
- **Miscellaneous uses:** Liquid CO_2 solvent has been used in some dry cleaning equipment as an alternative for conventional solvents [**85**].

- **Production of Organic Chemicals** such as CO, CH_4, CH_3OH, polymers, plastics, and polyurethanes, etc. Generally they are costly method and eliminate hazardous chemical intermediates as well as toxic wastes. Methanol production is an example of the synthesis of liquid fuels from CO_2 and hydrogen. Transition-metal complexes, especially of copper and zinc, as well as simple salts such as lithium hydroxide monohydrate and soda-lime (mixture of sodium and calcium hydroxides) are well known for their assistance in the stoichiometric transformation of CO_2 to carbonate salts. Mixtures of glycol and amines (glycol-amine) and coordination complexes of polyamines have been reported to bind CO_2 reversibly through the formation of carbamates. In contrast, reductive conversion of CO_2 into useful products of industrial significance such as formaldehyde, formic acid, methanol, or oxalic acid has proven more challenging to achieve selectively [**90**].

- **Production of fuels using CO_2** such as liquid carbon-based fuels, gasoline, and methanol. But all these conversion processes involve energy losses, the total CO_2 generated during fuel synthesis tends to exceed the CO_2 converted, which once used up is also emitted [**84**].

Capture of CO_2 in biomass: Biomass fuels also fall into the category of fuels generated from CO_2. Atmospheric inorganic CO_2 is converted into energetic organic compounds like starch with the help of photosynthesis, solar energy and H_2O. Currently, cellulose biofuels and algal biodiesels are prominent biological approaches to sequester and convert CO_2. But use of micro-algai has lower efficiency in overall, which could become an economically feasible option after further improvement [**84,91**].

Current status:

Chemicals: Approximately 110 MT (megatons) of CO_2 are currently used for chemical synthesis annually. The chemicals has been synthesized include urea, salicylic acid,

cyclic carbonates, and polycarbonates. Out of these chemicals, urea has been synthesized in largest amount. Furthermore, there are a number of reactions in which CO_2 is reduced during chemical transformation. For example, insertion of CO_2 into organic amines to afford carbamic acids, and also that may be converted into organic carbamates.

Furthermore, CO_2 is a highly stable, inert gas, and also present in highly oxidized state. So CO_2 needs efficient catalyst and additional energy for its reduction [**84**]. Recently, efficient heterogeneous catalysts have been developed for CO_2 hydrogenation for methanol. Based on this technology pilot-scale plants study have been demonstrated. However, the thermodynamics for methanol production from H_2 and CO_2 are not as favorable as that for production of methanol from H_2 and CO.

Supercritical CO_2 as a reaction medium:

The nontoxic nature of CO_2 has a number of advantages. So its use greatly reduces future liability costs. The use of CO_2 as the hydrophobic phase produces contamination that is both benign and readily reversible. Examples include liquid-liquid extraction between organic and aqueous phases as well as emulsion polymerization of water soluble monomers. Also the use of CO_2 in enhanced oil recovery to use as a foaming agent or as the solvent in dry cleaning [**88**]. Furthermore, supercritical CO_2 has been injected into a saline water or brine aquifers in compressible porous medium [**92**].

CO_2 fixation by inorganic materials:

The reaction of $CaCO_3$ and CO_2 in water to form $Ca(HCO_3)_2$ is responsible for the fixation of large amounts of CO_2 in the oceans. However, it is kinetically slow. Similarly, CO_2 can also be fixed by naturally occurring minerals as shown in Eqs. 2.12 and 2.13.

$2Mg_2SiO_4 + 2H_2O + CO_2 \rightarrow H_4Mg_3Si_2O_9 + MgCO_3$ (2.12)
(Olivine) (Serpentine)

$3KAlSi_3O_8 + H_2O + CO_2 \rightarrow KH_2Al_3Si_3O_{12} + K_2CO_3 + 6SiO_2$ (2.13)
(Orthoclase) (Muscovite)

The reactions are thermodynamically favorable and slow. Therefore, they could be enhanced kinetically before they could contribute significantly to adjust the carbon balance. Furthermore, this would generally require mining and processing of large amounts of materials to store relatively little CO_2. Currently, large quantities of $CaCO_3$ are converted into CaO and CO_2 (which is released into the atmosphere) in cement manufacture. If a natural ore could be substituted for CaO, a significant release of CO_2 into the atmosphere could be avoided [**88**].

Furthermore, the $Mg(OH)_2$ reclaimed from wet lime/limestone flue gas desulfurization system is also used for the sequestration of CO_2. It has great potential as a scrubbing sorbent for separation of CO_2. However, wet magnesium-enhanced lime process is used more effectively in coal-fired power plant to remove sulfur dioxide (SO_2) from the flue gases [**93**]. Similarly, the solid alkaline waste cement kiln dust is also used for CO_2 sequestration [**94**].

2.4.4. Sources of CO_2:

CO_2 can be recovered from stationary sources in various industrial processes. The concentration of CO_2 in gas stream % (v/v): coal power plant (12-15), natural gas (3-10), cement production (20%), refineries (3-13%), iron and steel industry (15%), biomass fermentation (100%), ammonia process (100%), ethylene oxide (100%), etc. [**84**].

Much of CO_2 used commercially is recovered from synthetic fertilizer and hydrogen plants, using either a chemical or physical solvent scrubbing system.

- Other industrial sources of CO_2 include the fermentation of sugar (dextrose) used to produce ethyl alcohol:

$$C_6H_{12}O_6 \rightarrow 2C_2H_5OH + 2CO_2 \quad (2.14)$$

- Industrial CO_2 is also produced from lime kilns, such as those used in the production of Na_2CO_3 and in the Kraft wood pulping process. This involves the heating (calcining) of a raw material such as limestone:

$$CaCO_3 \rightarrow CaO + CO_2 \quad (2.15)$$

The CO_2 recovered for other commercial uses is purified, liquefied, delivered, stored mostly as a liquid, typically at 20 bar and –18°C [**95**]. It is commercially available as high pressure cylinder gas. A large proportion of all CO_2 recovered is used at the point of production to make further chemicals of commercial importance, chiefly urea and methanol, rubber, and pesticides.

- Large quantities of CO_2 are produced by lime kilns, which burn lime stone (primarily $CaCO_3$) to produce CaO (lime, used to make cement); and in the production of magnesium from dolomite ($CaCO_3.MgCO_3$). The most common industries from which produce commercially large amount of CO_2 are NH_3 or H_2 production from natural gas, coal or other hydrocarbon raw materials. Similarly ethanol and beer plants are the main sources to recover CO_2.

- CO_2 plays a major role as a component of the carbon cycle in which carbon is exchanged between the atmosphere, the terrestrial biosphere (which includes freshwaters and soil), the oceans, and sediments (including fossil fuels).

- Recovery of CO_2 has not been commercially feasible from its low concentration sources like air, and stack gases from simple combustion (heaters, boilers, furnaces) **[85]**.

- The power and industry sectors are dominant global CO_2 emitters, accounting for about 60% of total CO_2 emissions. Coal is currently the dominant fuel in the power sector, accounting for 38% (highest %) of electricity generated in 2000. Coal is projected to remain the dominant fuel (about 36%) for power generation till 2020.

- The residential and transport sectors, contribute around 30% of global CO_2 emissions, and also produce a large number of point source emissions. However, the emission volumes from the individual sources in these sectors tend to be small in comparison to those from the power and industry sectors, and are much more widely distributed, or even mobile rather than stationary [**84**].

2.4.5. Effects of Global Warming and Climate Change:

Increased atmospheric CO_2 concentration affects global climate not only directly through its radiative effect (i.e., trapping long wave IR radiation), but also indirectly through its physiological effect (i.e., reducing transpiration of land plants). The radiative effect of CO_2 causes mean surface air temperature over land to increase by 2.86 ± 0.02 K, whereas the physiological effects of CO_2 on land plants alone causes air temperature over land to increase by 0.42 ± 0.02 K. Combining these two effects cause a land surface warming of 3.33 ± 0.03 K. Plant stomata open less widely under elevated CO_2 concentrations which reduce plant transpiration. Decrease in transpiration triggering changes in atmospheric water vapor and clouds, and affecting surface radiative fluxes. Thus, it changes the temperature and the water cycle. This driver of climate change, referred to as CO_2-physiological forcing [**86**].

Ocean process:

The release of fossil fuel CO_2 to the atmosphere by human activity has been implicated as the predominant cause of recent global climate change. The ocean plays a crucial role in mitigating the effects of this perturbation to the climate system, sequestrating 20 to 35% of anthropogenic CO_2 emissions. Anthropogenic CO_2 concentration in the ocean is the total dissolved inorganic carbon concentration which changes due to biological activity and air–sea disequilibrium [**97**].

Most of the investigated scenarios show warming of atmosphere as well as oxygen depletion, acidification and elevated CO_2 concentrations in the ocean. Specifically, deep-ocean carbon storage leads to extreme acidification and CO_2 concentrations in the deep ocean, then less sequestration state. Geological storage by offshore sediments may be more effective. But there may be leakage of 1% or less per thousand years from an underground stored reservoir [**98**].

Global climate and the atmospheric partial pressure of carbon dioxide are correlated over recent glacial cycles, with lower CO_2 partial pressure during ice ages, but the causes of the CO_2 partial pressure changes are unknown [**99**].The oceans are thought to take up about 40% of the CO_2 produces from the burning of the fossil fuels. The increase in the concentration of CO_2 in the atmosphere will increase its flux across the air–sea interface. Ocean acidification in response to rising atmospheric CO_2 partial pressures is widely expected to reduce calcification by marine organisms. One consequence of increasing P_{CO2} in seawater is the formation of carbonic acid (H_2CO_3), which causes acidification. Carbonic acid combines with carbonate ions (CO_3^{2-}) and water molecules to form bicarbonate ions (HCO_3^-), reducing [CO_3^{2-}] and the ocean's saturation state with respect to calcite, the form of calcium carbonate ($CaCO_3$) produced by coccolithophores [**100**]. This oceanic sink will result in a decrease in the pH of ocean water from the present level of 8.0 to 7.4. This decrease in the pH is expected to cause large change in the carbonate system ($CaCO_3$ particles) in the oceans [**81,101,102**]. Acid-base imbalances can lead to dissolution of exoskeletal components

such as calcarious shells, metabolic suppression (a condition expected to related growth and reproduction), reduced activity, loss of consciousness due to disruption of oxygen transport metabolisms, and also cause death of aquatic organisms **[103].**

In oceans, phytoplankton account for approximately half the production of organic matter on Earth. Phytoplankton strongly influences climate processes and biogeochemical cycles, particularly the carbon cycle. Furthermore, the total chlorophyll pigment concentration of phytoplankton has been destroying due to increase of sea surface temperatures [**104**].

Photosynthesis:

The continuing rise in atmospheric CO_2 concentration causes stomatal pores in leaves to close and thus globally affects CO_2 influx into plants, water use efficiency and leaf heat stress. Guard cells form adjustable stomatal pores in the plant epidermis that allow CO_2 influx for photosynthesis in exchange for transpirational water loss from plants to the atmosphere [**105,106**]. The research has shown that global change factors such as elevated CO_2 concentrations and N pollution affect plant productivity, as a result plant community changes differently. Hence plant community shifts can act as a feedback effect that alters the whole ecosystem response to elevated CO_2 concentrations [**107**].

At the present time, most scientists agree that the atmospheric concentrations of greenhouse gases are increasing, and that will increase the average global temperature. Some of the expected effects of the global warming are the following [**81**]:

- Ocean circulation disrupted, disrupting and having unknown effects on world climate.
- Rising of sea level leads to flooding of low-lying lands, and deaths and disease from flood and evacuation.
- Drought and desertification increases.

- Agricultural yield decreases **[108]** and that can lead to food shortages.
- Water shortages in already water-scarce areas.
- Starvation, malnutrition, and increased deaths due to food and crop shortages.
- More extreme weather and an increased frequency of severe and catastrophic storms.
- Spread of diseases in humans and animals increase.
- Increase of deaths from heat waves and change of ecosystem.
- Loss of animal and plant habitats leads to species extinctions.
- Low and irregular rainfall, and also increase of acidic rainfall [**109**].

The fastest greenhouse gas (GHG) emissions contributors are the electricity generation, transport, cement, waste, and residential sectors. Climate change is one of the world's biggest challenging problems. It also affects the life of aquatic flora and fauna, and social life and economic growth. Finding solutions has become a matter of necessity as people, and communities suffer the consequences of our planet heating up. The carbon emissions can be reduced by using renewable energy, solar energy, and green technology.

2.4.6. Different technological mitigation approaches:

Even with huge improvements in efficiency and phenomenal rates of growth in nuclear, solar, wind, and biomass energy sources, the world will still rely heavily on coal, especially the five countries that hold 75% of world reserves: the United State, Russia, China, India, and Australia. As a technological strategy, carbon sequestration can be applied to coal-fired power plants and also point sources including biomass combustion. Carbon sequestration also refers to enhanced biological uptake through reforestation or fertilization of marine phytoplankton [**110**].

Amine scrubbing has been used for 80 years (since 1930) and is a robust technique for large scale capture of CO_2 from coal-fired power plants. Amine scrubbing systems provide 90% removal. This roughly uses 30% of the energy from the coal

combustion in the first place, and may raise the generating cost of electricity from coal by 50%. Further development of this technology (process and solvent improvements) will provide more efficient systems to reduce energy cost, large single absorbers, heat exchangers, and compressors to reduce capital cost, as well as more robust solvents to reduce makeup costs and secondary environmental impact [**110,111**].

United State could reduce greenhouse gas emissions from the electricity sector by at least 10% by shutting down inefficient coal-fired plants and ramping up gas-powered generators. Burning natural gas to generate electricity emits roughly half as much carbon dioxide as coal. Natural gas could also be deployed to fuel fleet vehicles, buses and long-haul trucks in the transport sector. Natural gas drives down use of coal to minimal levels by 2035, largely because of the high carbon price on coal. For this further detail research and development programs on natural gas and coal replacement will be needed [**112**].

"The environmental risks are manageable but challenging". Although natural gas can enable the shift toward low-carbon energy, ultimately other solutions will be needed. Thus research and development programmes should continue for renewable sources, nuclear energy. Moreover carbon capture and storage systems can be applied to both coal- and natural gas–fired electric generation. "Gas really is a bridge, but the bridge has to go somewhere" [**112**].

In recent years, a number of studies have investigated the options for disposing the CO_2:

- Capturing at power stations
- Chemical conversion
- Terrestrial sequestration

Geological sequestration, which includes (i) use in enhanced oil recovery **[110]**, (ii) injection into deep-sea basalt (iii) unmined coal beds, (iv) depleted oil and gas reservoirs, (v) deep salt deposits, and (vi) deep ocean [**81**]. Geological sequestration

also in porous sedimentary rocks **[110,113]**, and mineral sequestration using CaO and MgO sorbent [**114,115**]. The chemical reaction of CO_2 with deep-sea basalt to produce stable and nontoxic carbonates of calcium, magnesium and iron infilling minerals [**116**]. The chemical reactions can take place, and that immobilize the CO_2 in the form of minerals. Which reactions take place and what minerals form depend strongly on the chemistry of the brine and the minerals and the cements present in the porous rock. Dissolved CO_2 in brine reduces pH and forms carbonate and bicarbonate ions that can react to dissolve calcium carbonate or silicate minerals [**113**].

Technological options for reducing anthropogenic emissions of CO_2 include:

- Reducing the use of fossil fuels
- Increasing the use of nonfossil fuel sources including renewable and nuclear energy. Renewable energy sources and nuclear energy do not produce CO_2.
- Substituting less carbon-intensive fossil fuels in the place of more carbon-intensive fuels.
- Replacing fossil fuel technologies with near-zero-carbon alternatives.
- Enhancing the absorption of atmospheric CO_2 by natural systems.
- Using highly efficient devices.
- Adaptation to reduce the impacts of the climate change [**84,110,111**].

CO_2 is the main component of the greenhouse gases and its accumulation in the environment is leading to severe global warming issues [**117**]. As a result, recycling of CO_2 has been a topic of intense research, and a subject of discussion not only from a scientific but also from an ecological–political point of view [**118]**. Similarly, the Clean Development Mechanism (CDM) of the Kyoto Protocol allows countries to reduce part of their CO_2 emissions through carbon sequestration.

Natural sequestration of CO_2 occurs through photosynthesis of green plants, calcification of CO_2 by phytoplankton, and mineralization in ground root systems. Tree plantations are most important natural method for carbon sequestration. Plantation

typically combine higher productivity and biomass with greater annual transpiration and rain fall, particularly for ever green species **[119,120].** Forest currently absorb nearly 3 billion tons of CO_2 globally every year (absorbing about 30% of all CO_2 emissions from fossil fuel burning and net deforestation) an economic subsidy worth hundreds of billions of dollars if an equivalent sink had to be created in other ways [**121].**

The available options of current potential technology for CO_2 sequestration may be included: absorption, adsorption, and low-temperature distillation. The selection of these appropriate technologies should be based on process simplicity, environmental impact, and economic considerations. There are some advantages of absorption process over other available process: chemical absorption is the commercial technology, most widely used by various industries. These reactions show pseudo-first-order reactions and they need low regeneration energy. Whereas, during adsorption, CO_2 gases are captured at higher pressure and released at lower pressure. The adsorption technology is requiring a vacuum unit for regeneration. And also desorption needs heat energy. Adsorption processes required very long regeneration cycle, and as a result large quantities of adsorbent are needed. Similarly, distillation process is costly for CO_2 sequestration from low concentration source **[93]**.

2.4.7. Main problems of CO_2 sequestration:

There are lots of research and lots of talking, but little real progress of carbon sequestration.

- Due to high cost of CCS and high energy requirement, because it consume electricity which will also produce CO_2, so power plants need to burn more fuel to produce the same amount of electricity, roughly doubling the cost of that energy. For CCS, power plants must install a bulk capture unit, which uses an amine-based solvent to strip CO_2 from exhaust gases. New power plant can use a more compact strategy in which coal or other fossil fuels are transformed into

CO_2 and hydrogen, and the hydrogen is then burned. A third, relatively new concept involves burning fuel in pure oxygen, creating a waste stream of water and CO_2. The chemical transformations required in all these technologies suck up energy **[110,122].**

- Investors are uncertain about the viability of technologies at large scales CCS [**122**].
- Although CO_2 is a green chemical reagent in many cases, but there are main problem to mitigate greenhouse effect. (1) Chemical fixation of CO_2 does not necessarily the total CO_2 amount, because CO_2 transformation requires energy and produces CO_2. (2) The amount of CO_2 fixed by chemical industries would be much smaller compared to CO_2 emission through fuel combustion. (3) Organic chemicals in which CO_2 is fixed will emit CO_2 at the disposal stage [**3**].
- Lifetime of fossil fuel CO_2 in the atmosphere is 50–200 years, though the oceans suck up huge amounts of the gas each year, the average CO_2 molecule does spend about 5 years in the atmosphere. But the oceans also release much of that CO_2 back to the air, such that man-made emissions keep the atmosphere's CO_2 levels elevated for millennia. Even as CO_2 levels drop, temperatures take longer time to fall. Because of long life time of CO_2 it is very difficult to solve the problem of global warming and climate change **[123].**

Coal is the cheapest source for production of electricity by power plants, as shown in Fig. 2.4. So, it will be used by different countries, until cleaner forms of energy become economically competitive [**122**].

From an environmental point of view, however, the technology is relatively cheap. Studies suggested that, once the technology matures, commercial carbon-capture coal plants would spend US$ 50-80 for every ton of CO_2 to avoid emitting. The costs of electricity produced by mature CCS plants would overlap with those for other low-carbon electricity options, such as solar, wind, and nuclear power.

Actually CCS will raise the energy prices, but if we look at reaching certain targets, such as keeping below 2°C of warming. Then it is cost-effective system. It was reported by Howard Herzog, who worked on carbon sequestration at Massachusetts Institute of Technology in Cambridge **[122]**.

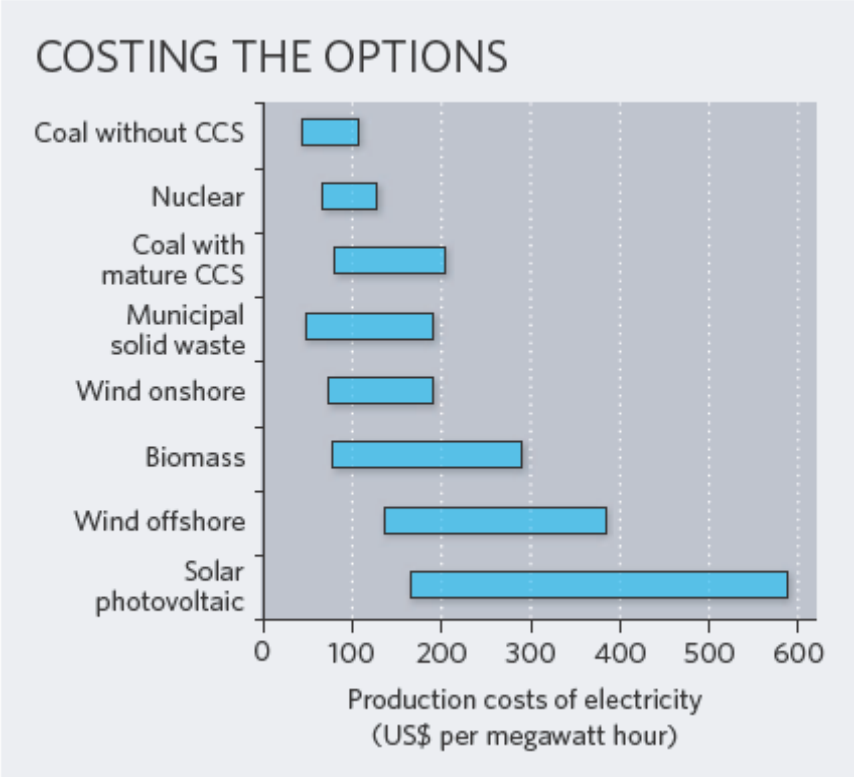

Fig. 2.4: Production costs of electricity **[122]**.

In theory, these technologies would be more competitive if some sort of cost were associated with emitting CO_2, but few countries have taken that step. European Union (UN) has a carbon emissions trading scheme that effectively sets a price on CO_2 pollution from large emitters. But at a current rate of around US$18 per ton of CO_2, the EU price is well below the level that would provide an incentive for coal plants to capture their emissions.

Government's greenish light: governments in developed nations will need to invest US$3.5 billion to $4 billion in demonstration CCS projects in each year from 2010 to 2020. Europe, Canada, the United States, Australia and China have so far publicly allocated just $7.3 billion, although they have promised a total of around $20 billion [**122**].

Capture of CO_2 from air (0.04%) will cost more than capture from power plants when both are operated under the same economic conditions. Two factors make capture of CO_2 from air more difficult than from the exhaust streams: (1) the higher thermodynamics barrier due the lower concentration of CO_2 in air, and (2) the energy and materials cost moving great quantities of air through an absorbing structure. Cost factor is the main problem of CO_2 sequestration. It is not possible to determine the cost through small-scale university research alone. The costs will only become evident with pilot-scale process development. One method of capture of CO_2 is ion exchange membranes with humidity-swing regeneration, whereas other method solid amines on a mesoporous silica substrate are used to capture CO_2 from power plants. Most of other methods start with the absorption of CO_2 by an alkaline aqueous solution, which is a cheaper process but raises the cost of regeneration. Similarly, CO_2 capture with alkaline hydroxide solutions are strongly absorbing, contamination-insensitive, and can have minimal water loss, which lower the cost and technical risk of the absorption step. Some researchers have been using solar energy, natural gas, electrochemical cells as an energy source to regenerate spent caustic solution, and some are using weaker hydroxide with catalysts to overcome slower CO_2 uptake of the weaker absorbent **[124].**

CO_2 Sequestration is a robust technology in the mitigation of climate change. Public acceptance may have a strong impact on the progress of this technology. From the findings of the previous research showed that laypeople hold about storage mechanisms as well as about leakage and socio-economic issues, which all appeared to influence risk perception and benefit perception. Appropriate images about storage

mechanisms and climate change awareness were increasing the perception of benefits [**125**].

2.5. Summary

Currently, most of the pollution control technologies have been adopted to convert one form of pollutant into another usable form. Similarly, a lot of works have been done for successful utilizations of red mud. But till now no economically feasible industrial technology has been developed for large-scale utilization of red mud. Presently some small fractions of this waste are used as building material and road making. The waste minimization through their utilization can reduce the cost of waste management and environmental impact, by giving the product values.

Rapid industrialization for global economic completion is mainly responsible for uncontrolled emission of greenhouses gases to the earth atmosphere. This is highly responsible for burning of earth and rising of temperature of earth. Studies on the utilization of CO_2 by using industrial waste will be an important part of the future research. It is important to increase the number of industrial applications by improving these reactions for commercialization. Such fundamental research will lead to the new seeds for industrialization. Large-scale sequestration of CO_2 is highly needed as soon as possible by applying low-cost material and technology to save the earth from catastrophic global warming and climate change.

But natural CO_2 sequestration by afforestation of degraded forest lands and geological sequestration by soils are the permanent and natural solutions to save the planet earth. The green plants never release any type of pollutants during the consumption of CO_2 from atmosphere for the photosynthesis. Planting trees will provide a proven tool for managing Earth's carbon cycle.

*****

Chapter 3

Materials and Methods

3.1. Neutralization of red mud using CO_2 sequestration cycle

3.1.1. Materials

Fresh red mud used in this study was obtained from R&D Laboratory of NALCO, Damanjodi, Orissa, India, in the form of dried-clay.

Hydrochloric acid (HCl) used in this study was of analytical grade and was purchased from Merck. Nitric acid (HNO_3) was purchased from Rankem. Research grade CO_2 (Concentration of > 99.998 % was used without further purification) gas cylinder was purchased from SKP Corporative Service Rourkela. Rota-meter was purchased from Bombay Instrument Co.

3.1.2. Materials preparation

The red mud samples were air-dried and grounded in a mortar and pestle. Subsequently, sieved to pass through a 1 mm sieve, prior to analysis, and stored in vacuum desiccators until used. Particle size of the red mud was in the range of 0.1–160 µm. The red mud suspension was prepared by mixing 10 g of fresh red mud with 100 mL of distilled water in 150 mL plastic bottle to obtain a sufficient volume of slurry for carbonation reaction. The red mud suspensions were kept 24 h with constant magnetic stirring at 180 rpm for standard solid–liquid contact. All these suspensions were prepared in triplicate to get average value.

All the carbonation experiments and measurements were carried out at ambient conditions. All solutions were prepared with distilled water. All plastic sample bottles and glassware were cleaned in 1N HNO_3 acid baths then rinsed with distilled water and dried at 60 °C in a temperature controlled oven.

3.1.3. Materials characterization

3.1.3.1. XRD

The powder X-ray diffraction (XRD) of sample was determined by using Philips PANanalytical X'Pert X-ray diffractometer with a Cu Kα radiations source generated at 35 kV and 30 mA. Scattering angle 2θ was ranged from 10 to 90º at a scanning rate of 2 º min^{-1} and was analyzed using standard software provided with the instrument. The samples were oven-dried at a temperature of 110 ºC for 2 h before their analyses. The XRD pattern of the material and mineral composition of different phases were determined by using XRD.

3.1.3.2. SEM-EDX

The surface micro-morphology of materials was investigated using a high resolution Scanning Electron Microscope (SEM) and qualitative element composition was analyzed using Energy Dispersive X-ray (EDX) operated at an accelerating voltage of 20 keV, by JOEL model JSM-6480LV (Japan). The chemical compositions of major oxides were measured by EDX. These measurements were done in triplicate to measure the average value.

3.1.3.3. FT-IR

FT-IR spectra of the samples were obtained by using PerkinElmer FT-IR Spectrometer Spectrum RX-I. Samples were homogeneously crushed with anhydrous KBr in a ratio of 1:50. The powder was pressed at 5 tons cm^{-2} to make a translucent tablet pallet for recording FT-IR spectra. The spectrum was scanned from 4000 to 400 cm^{-1}.

3.1.3.4. The pH and electrical conductivity

The pH measurements were made using a calibrated Orion 2 Star Bench top pH meter. The electrical conductivities were measured using CM 138, EC-TDS analyzer. The pH and electrical conductivity were measured after centrifugation of suspensions (prepared as indicated in section 3.1.2.) for 20 min at 3000 rpm and filtration were done using Whatman 40 filter paper. The parameters were measured by adding distilled water to the fresh red mud at a solid to liquid ratio of 1:2.5 standard methods [**126**]. All these suspensions were prepared in triplicate, and the pH was found ~11.8.

3.1.3.5. Auto titrator

The titrations were done using an Auto Titrator SCHOTT Instrument TitroLine easy (Germany). The acid neutralizing capacities (ANC) of RM and NRM were measured by

automatic titration of suspension (mixture of 20.0 g red mud with 50 mL distilled water) with 0.1 M HCl solutions to end point pH 5.5. The titration was repeated after each 24 h until pH becomes stable at 5.5 [**19,127**]. Similarly, the total alkalinity of red mud is defined as the concentration of all the bases that can accept H^+ when a titration is made with HCl to the carbonic acid end point (~4.5) **[81]**.

3.1.3.6. BET

The BET surface areas of the samples were measured at liquid nitrogen temperature (–196°C) using the Brunauer–Emmett–Teller (BET) surface area analyzer (Quantachrome AUTOSORB–1, USA). All samples were degassed at 150 °C in vacuum. Helium was used as carrier gas and surface area was measured by nitrogen adsorption–desorption method. The BET-N_2 surface area of RM and NRM are 31.7 and 28.55 $m^2 g^{-1}$ respectively.

3.1.3.7. Particle size analyzer

Particle size of the red mud was measured using Master Sizer 33370-45 (Malverns, UK).

3.1.3.8. Ultra Sonic

High frequency ultra sonic sound wave of frequency 20 kHz is used. According to the principle of ultra sonic agitation, the electrical energy is converted to mechanical energy by using transducer.

3.1.3.9. CHNS

Carbon content was determined by using varioELcube CHNS Elemental Analyzer, Germany. The O_2 gas was used as fuel, Helium gas was used as carrier gas and to provide inert atmosphere. The operating temperature of combustion tube and reduction tube were 1150 °C and 850 °C, respectively.

3.1.3.10. Thermal analysis (TG-DSC)

The thermogravimetric analysis and differential scanning calorimetry (TGA/DSC) analysis of air dried samples were carried out using NETZSCH STA 409C, Germany. In this analysis, 24–30 mg of sample was used and alumina was used as reference. The sample was heated in an Al_2O_3 crucible at a heating rate of 10.0 ºC min^{-1} from 25 to 910 ºC.

3.1.4. CO_2 sequestration

An attempt was made to neutralize caustic red mud using CO_2 sequestration technique. The CO_2 sequestration reactions were performed at ambient condition at different gas flow rate mL/min for different times. Similarly, different amount of red mud was taken for carrying out the experiment. But the gas flow rate of 5 mL/min and 10 g of red mud was found to be effective. The reactions were performed in gas tight plastic bottles with an inlet for CO_2 gas and an outlet to vent the pressure. The gas was passed through a rotameter and subsequently passed into the red mud solution through a micro bubbles stone for 5, 10, 20, 24, 48, 72 h. The solution was stirred through a magnetic stirrer at effective constant speed 180 rpm to increase their solubility for all the experimental tests reported here. The CO_2-neutralized red mud (CNRM) was collected after a centrifugation for 20 min at 3000 rpm. It was treated as cycle-1 for each carbonation period. The initial and final pH and electrical conductivity were measured according to the technique described in Section 3.1.3.4. The alkalinity was measured by using mass balance method **[22].** Only 5 h carbonation processes were repeated for cycles-2 and 3.

3.1.5. Cost estimation

A rough cost is calculated in the SI per ton of CO_2 sequestered in our basic method. Two main components are considered for the cost calculation: electricity for operating

magnetic stirrer and centrifuge machine by excluding the cost of machine, plastic bottles, pipes, micro-bobble stone, distilled water, CO_2 used, capital cost, etc. For magnetic stirrer and centrifuge machine energy, it is more convenient to use energy per total mass of CO_2 sequestered, E/M, and then absolute energy [**128**]:

$$\frac{E}{M} = Pt_s + Pt_c \tag{3.1}$$

where P is the power, t is the total time of stirring (s) and centrifuge (c). The unit of E/M is kW-h/ton. To estimate the CO_2 sequestration cost, T_c, we assume that electricity is purchased at a price, P_{elec}, of \$ 0.07/kW-h according to the year 2008. Applying Eq. (3.1), we express the sequestration cost by

$$T_c = \frac{P_{elec}E}{M} \tag{3.2}$$

3.2. Utilization of activated CO_2-neutralized red mud for removal of arsenate from aqueous solutions

3.2.1. Materials

All chemicals, including HCl, NaOH, HNO_3, $NaBH_4$, KI, KBr and arsenic standard solution of 1000 mg L^{-1} used in the present study were of analytical grade and obtained from Merck (Germany), sodium arsenate heptahydrate ($Na_2HAsO_4 \cdot 7H_2O$), NaCl from Nice chemicals and L–cysteine from Loba chemicals, $BaSO_4$ from Wako pure chemicals. In all experiments, double distilled water was used for preparation, dilution and analytical purposes of the solutions. As(V) stock solution of 1000 mg L^{-1} was prepared by dissolving 4.164 g $Na_2HAsO_4 \cdot 7H_2O$ in 1 L of double distilled water. Various test solutions of arsenate mainly with concentrations 1–100 mg L^{-1} were prepared from the stock solution.

3.2.2. Adsorbent preparation

The fresh red mud used in this study was obtained from R&D Laboratory of NALCO, Damanjodi, Orissa, India, in the form of dried-clay. The chemical compositions of the RM based on the dry weight are Fe_2O_3 (54%), Al_2O_3 (13%), SiO_2 (7%), Na_2O (8%), and TiO_2 (3.5%). The RM was neutralized using sequestration of CO_2 gas. The pH of RM suspension was decreased from 11.8 to 8.45. This partially neutralized RM sample was dried at 110 °C for 2 h and calcinated at 500 °C for 2 h and referred as activated neutralized red mud (ANRM).

3.2.3. Characterization of adsorbent

3.2.3.1. XRD

The powder X-ray diffraction (XRD) of sample was determined by using Philips X'Pert X-ray diffractometer with a Cu Kα radiations generated at 35 kV and 30 mA.

Scattering angle 2θ was ranged from 10 to 80º at a scanning rate of 2 º min^{-1} and was analyzed using standard software provided with the instrument.

3.2.3.2. SEM-EDX

The surface micro-morphology of materials was investigated using a scanning electron microscope (SEM) and qualitative element composition was analyzed using energy dispersive X-ray (EDX) operated at an accelerating voltage of 20 keV, by JOEL model JSM-6480LV (Japan).

3.2.3.3. BET

The BET surface area was measured at liquid nitrogen temperature (–196°C) using the Brunauer–Emmett–Teller (BET) surface area analyzer (Quantachrome AUTOSORB–1, USA). BET surface area was analyzed by using nitrogen adsorption–desorption multi-molecular principle. All samples were degassed at 150 °C in vacuum. Helium was used as carrier gas.

3.2.3.4. Particle size analyzer

Particle size of the red mud was measured using Master Sizer 33370-45 (Malverns, UK).

3.2.3.5. FT-IR

FT-IR spectra of the samples were obtained by using PerkinElmer FT-IR Spectrometer Spectrum RX-I. The spectrum was scanned from 4000 to 400 cm^{-1}. Samples were homogeneously crushed with anhydrous KBr in a ratio of 1:50. The powder was pressed at 10 tons cm^{-2} to make a translucent tablet for recording FT-IR spectra.

3.2.3.6. Solid UV-vis

The diffuse reflectance spectra of powder samples were carried out on a UV–vis spectrophotometer (UV–2450; Shimadzu, Japan) at room temperature and $BaSO_4$ was used as a reflectance standard.

The diffuse reflectance spectra of powder samples were converted into the absorption spectra by the Kubelka–Munk relationship, $K/S = (1 – R)^2/2R$, where R, K, and S are the value of reflectance measurements (relative value to the reflectance of $BaSO_4$), and the absorption, and scattering coefficients of the sample, respectively.

3.2.3.7. The pH meter

The pH measurements of arsenate aqueous solutions were made using a calibrated Orion 2 Star Bench top pH meter. According to the principle the glass electrode (Ag/AgCl) is used to measure the hydrogen ion activity of the solution by measuring the potential deference.

3.2.3.8. Atomic absorption spectrometer (AAS)

Quantitative analysis of the As(V) ion in the filtrate, after adsorption was determined by using hydride generated atomic absorption spectrometer (MHS 15, AAS, PerkinElmer, AAnalyst 200, USA) using standard method. Calibration was achieved using dilutions prepared from a commercially available 1000 mg L^{-1} standard arsenic solution [**129,130**]. For hydride generation, 3% $NaBH_4$ (prepared in 1% NaOH) and 1.5% HCl solutions were reacted with the samples for total arsenate determination. Specific hollow cathode lamp of 193.7 nm wavelength was used. According to the principle of AAS, as the quantity of input energy is known and output energy is calculated from the number of electronic transitions of elements present in the solution by detector using Beer-Lambert Law.

3.2.3.9. Batch experiments

Batch experiments were carried out at room temperature (25 ± 2 ºC) using 100 mL stoppered polylab plastic bottles. 0.2 g of ANRM adsorbent was weighted and put into the different plastic bottles, into which 50 mL of As(V) solutions at different initial concentration were added separately. The bottles were capped tightly for all tests to avoid change in concentration, due to evaporation. The pH was adjusted to the desired level with 0.1 M NaOH or 0.1 M HCl solutions. A number of experimental parameters such as adsorbent dose, contact time, initial arsenate concentration, pH which affect the adsorption of arsenate have been studied to optimize the removal process. The solutions were stirred using magnetic stirrer at about 300 rpm for 24 h until the adsorption equilibrium time was reached. All adsorption studies were carried out at a constant ionic strength of 0.01 M maintained with NaCl. After stirring, the solutions were allowed to settle for 10 min and the samples were centrifuged 3000 rpm for 20 min and filtered through Whatman 42 filter paper. The filtrate was used for the analysis of remaining arsenate concentration in the solution. The amount of arsenate adsorbed (removal) was calculated as follows:

$$\%adsorbed = \frac{[C]_i - [C]_f}{[C]_i} \times 100 \qquad (3.3)$$

where $[C]_i$ and $[C]_f$ are the initial and final concentrations of the arsenate in the aqueous solutions (mg L^{-1}), respectively. All experiments were conducted in duplicate and the mean values were considered.

3.2.3.10. Desorption and regeneration studies

The recovery of the adsorbed As(V) ions as well as reusability of activated red mud mainly depends on the ease with which arsenate (V) ions get desorbed from loaded ANRM sample. For this 50 mL of 10 mg L^{-1} arsenate solution was treated with 0.2 g of ANRM and was kept under stirring for 24 h. The content of the flask was filtered and

separated. The filtered adsorbent was retreated with 50 mL neutral distilled water and they were adjusted to different pH with the help of 1.0 M NaOH. The samples were stirred at 300 rpm at room temperature (25 ± 2 °C) for 24 h.

3.3. Extraction of fine iron oxide from CO_2-neutralized red mud

3.3.1. Experimental section

The caustic red mud was neutralized using CO_2 sequestration cycle [**143**]. The method of "extraction of fine iron from red mud" has been filed for a patent [**160**], and for commercialization of this environment-friendly technique; Vedanta Alumina Limited has signed MoU (Memorandum of Understanding) with NIT Rourkela **[161,162].**

*****

Chapter 4

Results and Discussion

4.1. Neutralization of red mud using CO_2 sequestration

4.1.1. Mineralogical characterization by X-ray diffraction

The X-ray diffraction patterns of red mud (RM) and CO_2–neutralized red mud (NRM) are represented in Fig. 4.1a and Fig. 4.1b, respectively. From the XRD peaks of RM the following mineral phases were identified: hematite (α-Fe_2O_3), goethite (α-FeO(OH)), gibbsite (γ-$Al(OH)_3$), calcite ($CaCO_3$), rutile/anatase (TiO_2), sodalite: zeolite (I) ($1.08Na_2OAl_2O_31.68SiO_21.8H_2O$), quartz ($SiO_2$), sodium aluminum silicate ($Na(AlSiO_4)$), and magnetite (Fe_3O_4) as referred from JCPDS (Joint Committee of Powder Diffraction Standards) file of X'Pert High Score software. XRD pattern of NRM was revealed that the intensity of gibbsite was increased prominently whereas other mineral phases were decreased. Also, confirmed the formation of new mineral ilmenite ($FeTiO_3$). This may be due to dissolution of mineral phases during long period

of carbonation. The dissolution of $Na(AlSiO_4)$ is also responsible for increase of intensity of the gibbsite in NRM.

It is important to observe that the availability of Na_2O (5.79%, w/w) exceeds the SiO_2 total content (8.45%, w/w). Because, it mainly engaged in $Na(AlSiO_4)$ formation, thus revealing the presence of additional sodium oxide species which is not detected by XRD analysis [**131**].

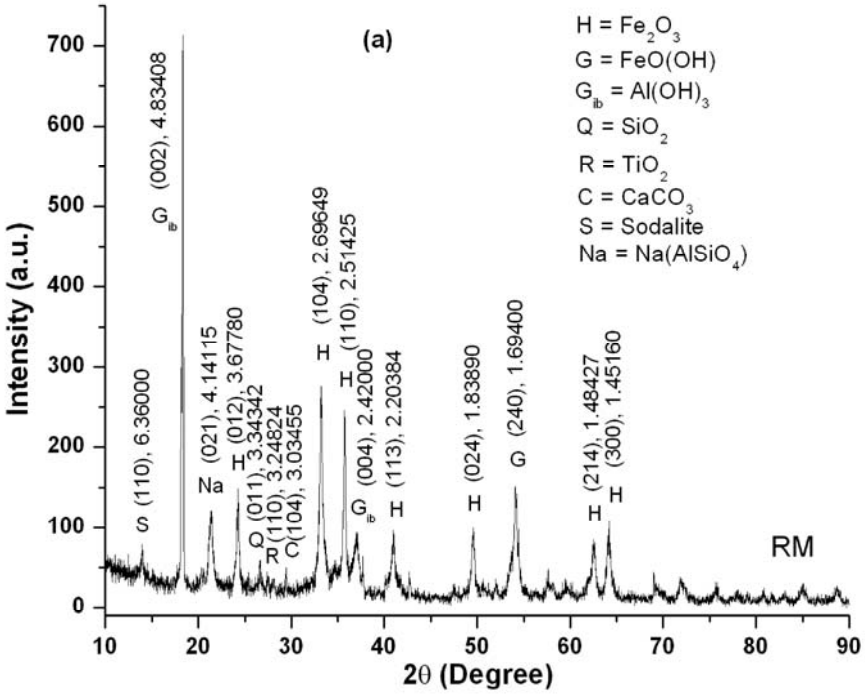

Fig. 4.1. (a) Variation of powder XRD patterns of red mud.

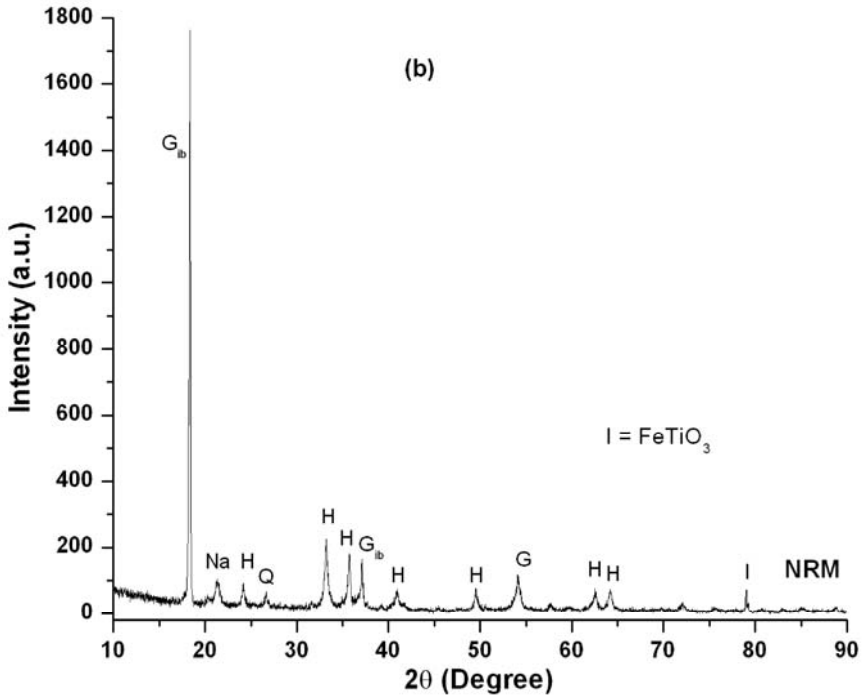

Fig. 4.1. (b) Variation of powder XRD patterns of CO_2–neutralized red mud.

4.1.2. Thermal analysis using TG-DSC

The thermal decomposition behaviors of RM (Fig. 4.2) show five steps for the weight loss. The first step occurs at 30–180 ºC (weight loss was about 3.34% of the total weight), due to evaporation of water; the second one occur in the range of 180–390 ºC (6.75%), due to loss of H_2O and also removal of H_2O from $Al(OH)_3$; third one occurred in the range of 390–635 ºC (1.13%), corresponding to release of CO_2 during calcinations of $CaCO_3$ to CaO. The fourth and fifth steps occurred at 635–700 ºC and 700–910 ºC, corresponding to weight loss 0.35% and 0.38%, respectively. The DSC curve shows two broad peaks centered at around 65 ºC and 291.5 ºC, corresponding to physically adsorbed water and chemically adsorbed water, respectively [**127,132,133**].

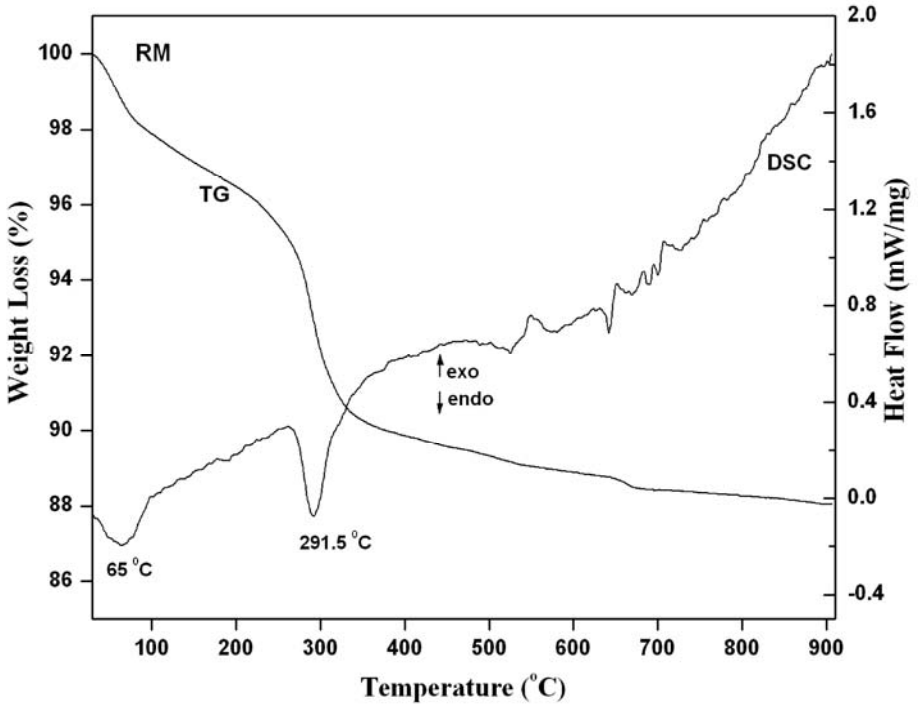

Fig.4.2. TG-DSC diagrams showing weight loss of red mud in the temperature range of 30–910ºC.

TG and DSC analyses of neutralized red mud were carried out and results are presented in Fig. 4.3. First weight loss from TG analysis was found to be 1.41%. This weight loss was probably due to the physically adsorbed water on the neutralized red mud. The DSC graph showed the endothermic process peak at 283 °C and the corresponding weight loss from TG analysis was found to be 8.55%. This may be due to loss of loosely bound water, and strongly bound water. The third weight loss was 2.00% which may be due to the remaining evolution of H_2O and CO_2.

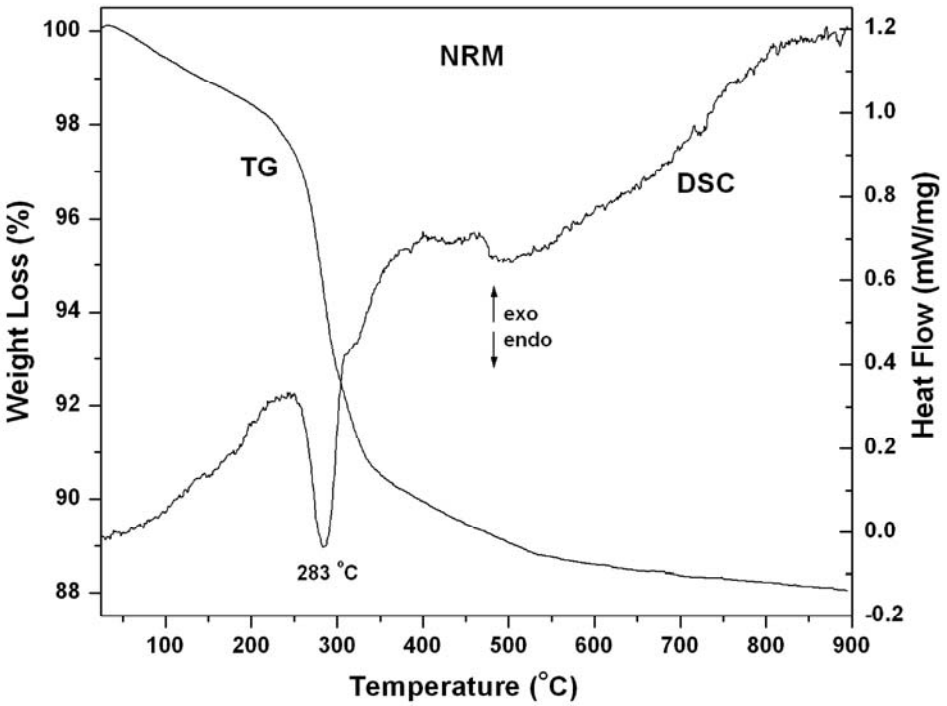

Fig.4.3. TG-DSC diagrams showing weight loss of CO_2-neutralized red mud (CNRM) in the temperature range of 30–910ºC.

4.1.3. Particle size and surface area of RM and NRM.

The BET-N_2 surface area, pore volume, pore diameter of RM were found to be 31.7 $m^2\ g^{-1}$, 0.01514 $cm^3\ g^{-1}$, 18.20 A°, respectively, (Table 4.1). Fig. 4.4 shows the particle size distribution of red mud particles. The horizontal axis denotes the diameter of the particles distributed over the range of 0.1–160 μm, with volume-based peaks at about 0.31μm and 48.27 μm.

Table – 4.1. The BET-N_2 surface area, pore volume, pore diameter of RM.

S_{BET}	31.7 $m^2 g^{-1}$
Particle size	0.1–160 μm
Pore volume	0.01514 $cm^3 g^{-1}$
Pore diameter	18.20 A°

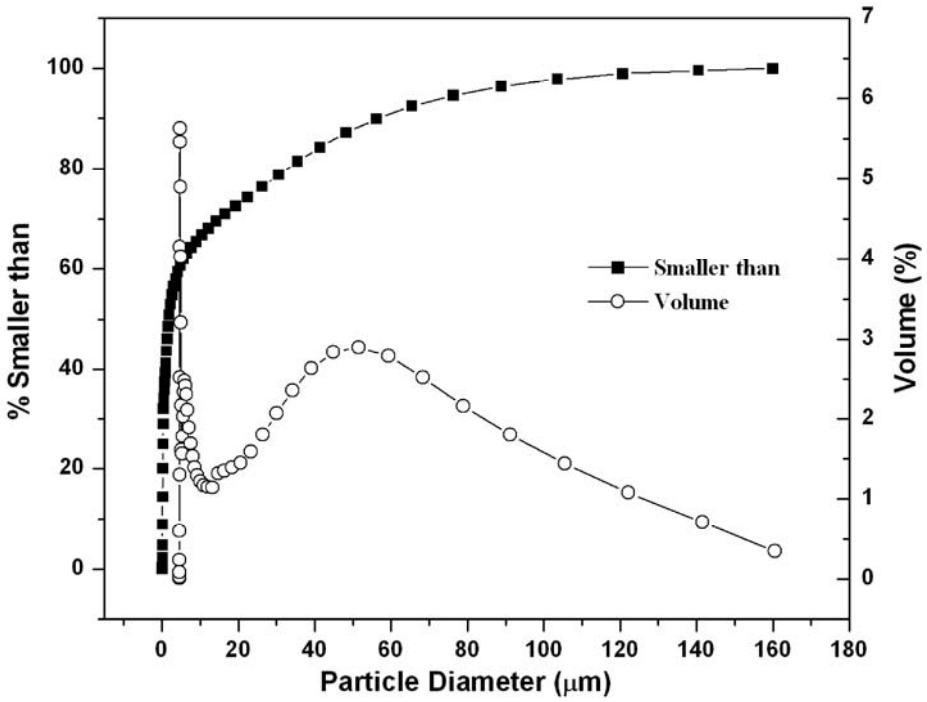

Fig. 4.4. Particle size distributions of red mud.

Red mud is a mixture of fine and coarse particles. The particle size was decreased after the neutralization experiment from 0.1–160 to 0.1–90 μm. Fig. 4.5 shows the particle size distribution of red mud and neutralized red mud. Since, CO_2 is a weak acid, and it helps in dissolution of larger particles.

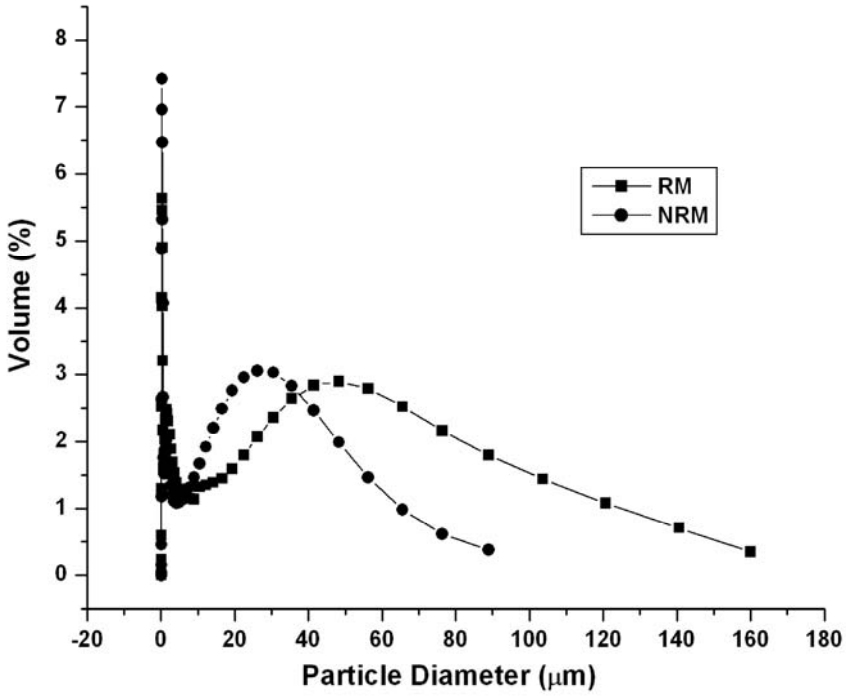

Fig. 4.5. Particle size distribution of RM and NRM.

4.1.4. Micro-morphological characterization by SEM & change of chemical composition by EDX

However, CO_2 sequestration decreases with respect to decrease of particle size because CO_2 sequestration is mainly depends on concentration of NaOH in the red mud. SEM images (Fig. 4.6.a and b) showed that the rounded shape aggregate particles (poorly-crystallized/amorphous forms) present in RM were decreased in the NRM [**12**]. This indicates that some mineral phases mainly calcite, sodalite contained in the RM are more soluble in acidic environment. However, some silicates often react with sodium aluminate in alkaline solution to form silicate mineral such as hydroxysodalite [**12**]. SEM images (Fig. 4.6.c-e) revealed the presence of needle morphology in the dried carbonated filtrate this may be due to presence of Na_2CO_3 [**134**].

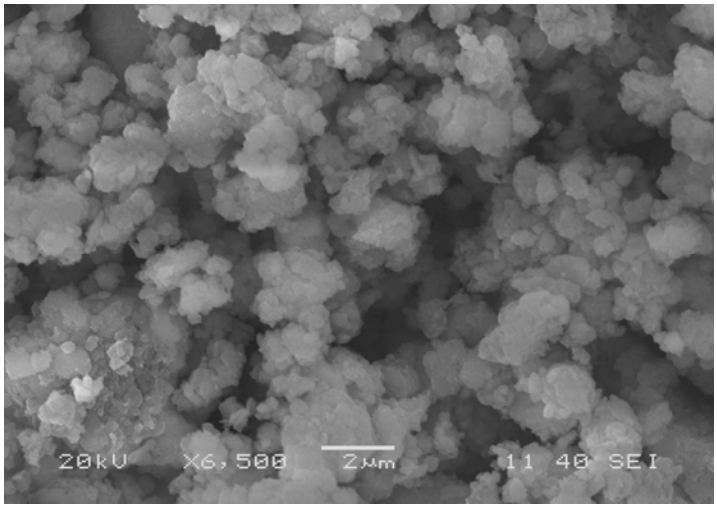

Fig. 4.6. (a) SEM micrograph of RM.

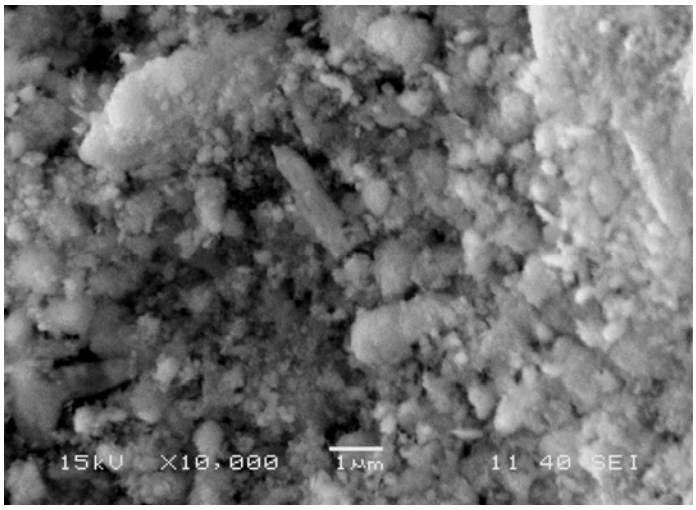

Fig. 4.6. (b) SEM micrograph of NRM.

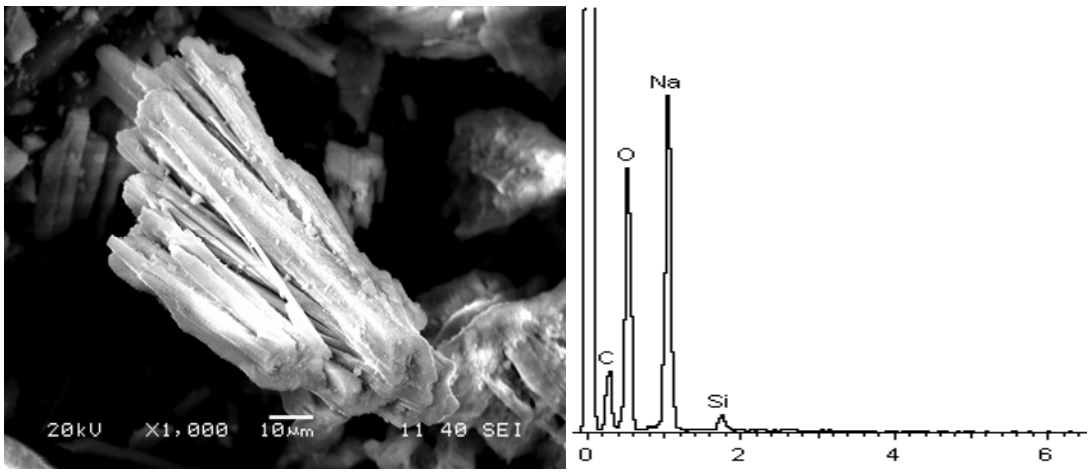

Fig. 4.6. (c) SEM micrograph of 5 h carbonation filtrate with EDX microanalysis spectrum of cycle-1.

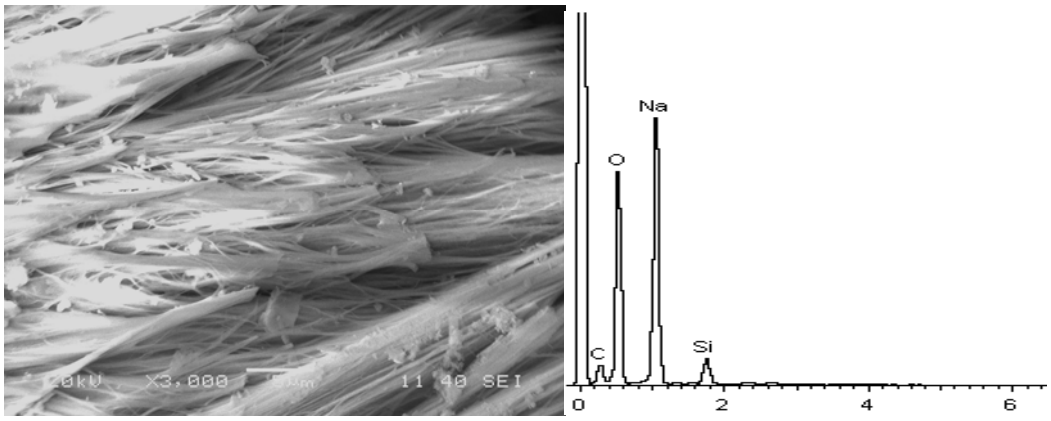

Fig. 4.6. (d) SEM micrograph of 5 h carbonation filtrate with EDX microanalysis spectrum of cycle-2.

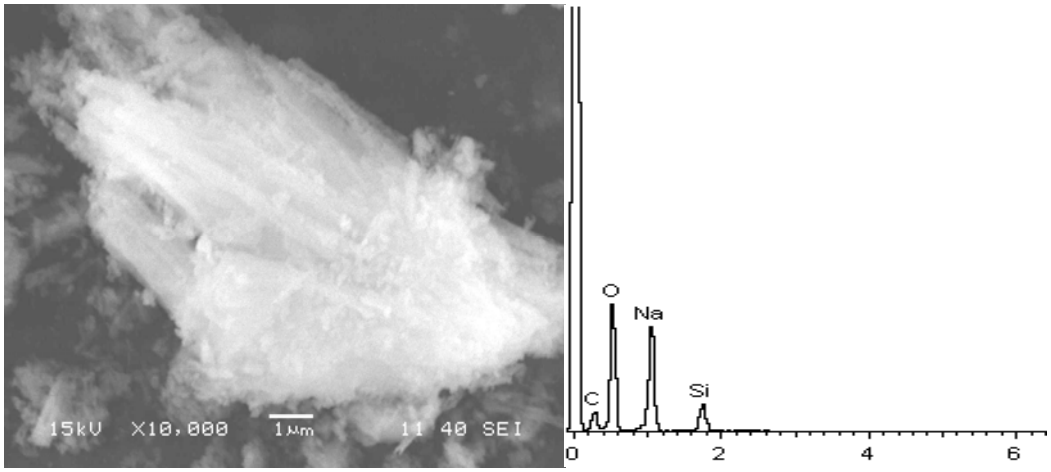

Fig. 4.6. (e) SEM micrograph of 5 h carbonation filtrate with EDX microanalysis spectrum of cycle-3.

The element composition and chemical composition of major oxides were measured by using EDX as in Tables 4.2 and 4.3. The samples of carbonated filtrate were dried in water bath at 50 °C to know the permanent capture of CO_2 and C per 10 g of red mud. The compositions were determined from spot analysis and pallet of the samples. EDX analyses spectra (Fig. 4.6.c-e) revealed that the carbonated filtrate were rich in C (~17.93%), O (~49.12%) and Na (~32.75%) with lower amount of Si (0.56%) in cycle-1. Subsequently, the amount of CO_2 sequestration and leaching of Na^+ ions were decreased, whereas the amounts of Si were increased (Tables 4.2 and 4.3). Amount of CO_2 %(w/w) sequestered permanently in the cycle-1, 2, and 3 were ~58.01, ~55.37, and ~54.42 whereas the amount of C content in each cycle were ~17.93, ~13.59, and ~11.27, respectively. From this it was confirmed that the amount of CO_2 sequestration decreased in each subsequent cycles. The leaching of sodium ions in the cycles 1, 2, and 3 were ~32.75, ~29.87, and ~26.51% (w/w) whereas the compound Na_2O (Na_2CO_3 and $NaHCO_3$) was ~40.82, ~43.52, and ~33.31, respectively.

Table – 4.2.

Major compound composition (%w/w) of RM, NRM and carbonated filtrate of cycles-1, 2, 3 in average as determined by energy dispersive X-ray.

Major oxide	RM	NRM	Carbonated filtrate		
			Cycle-1	Cycle-2	Cycle-3
Fe_2O_3	54.26	47.64	0.00	0.00	0.00
Al_2O_3	12.20	14.37	0.00	0.00	0.00
TiO_2	3.04	3.57	0.00	0.00	0.00
SiO_2	8.45	7.80	1.17	10.11	12.27
Na_2O	5.79	0.29	40.82	34.52	33.31
CaO	0.23	0.00	0.00	0.00	0.00
MgO	0.18	0.00	0.00	0.00	0.00
CO_2	7.23	26.33	58.01	55.37	54.42

Table – 4.3.

Major element composition (%w/w) of RM, NRM and carbonated filtrate in average as determined by energy dispersive X-ray.

Major element	RM	NRM	Carbonated filtrate		
			Cycle 1	Cycle 2	Cycle 3
C	1.97	7.19	17.93	13.59	11.27
O	31.86	42.40	49.12	53.18	55.08
Na	4.30	0.95	32.75	29.87	26.51
Al	5.86	7.76	0.00	0.00	0.00
Si	3.83	2.18	0.56	3.36	7.14
Ca	0.74	0.00	0.00	0.00	0.00
Ti	1.82	1.60	0.00	0.00	0.00
Fe	47.95	37.92	0.00	0.00	0.00
Zr	1.67	0.00	0.00	0.00	0.00
Total	100.00	100.00	100.00	100.00	100.00

4.1.5. FT-IR spectroscopy

Fig. 4.7 shows the FT-IR spectra of RM and NRM. In both the spectra, the positions of the absorption bands are nearly similar. The relative intensities are more intense in the case of RM. The FT-IR absorption by RM was showed a broad band at ~3140 and a weak peak at ~1640 cm^{-1} due to the stretching vibrations of O–H bonds and H–O–H bending vibrations of interlayer adsorbed H_2O molecule, respectively. Water hydroxyl-stretching vibrations are intense in an infrared spectrum, because of large change in

dipole moment. The OH-stretching vibrations of carbonated NRM were showed at higher wavenumber at ~3463 cm^{-1}. This shift is associated with the shorter O–H bonds existing in NRM than RM, causing an increase in electrostatic attraction within the RM layer. The shifting of peaks in NRM is due to weaker intermolecular hydrogen bonding, which is due to weaker dipole moment. This may be due to change of chemical composition w/w% after neutralization of red mud. The absorption bands at ~1476 and ~1489 cm^{-1} are due to stretching vibrations of C=O, confirmed the presence of carbonate groups [**135**]. This may be due to chemisorbed CO_2 in fresh RM and NRM respectively. It confirmed that the fresh red mud was absorbed CO_2 from the atmosphere. Characteristic bands correspond to Si–O vibration were detected at ~993 and ~1008 cm^{-1}, and for O–Si–O at ~803, ~807 cm^{-1} proved the presence of silicate groups. Peaks at ~544 and ~466 cm^{-1} are due to bending vibration of Si–O–Al and stretching vibrations of Fe–O bonds respectively [**38,136,137**]. Intensities of these peaks were decreased in NRM which confirmed the dissolution of minerals like silicate, $Na(AlSiO_4)$ during cyclic carbonation.

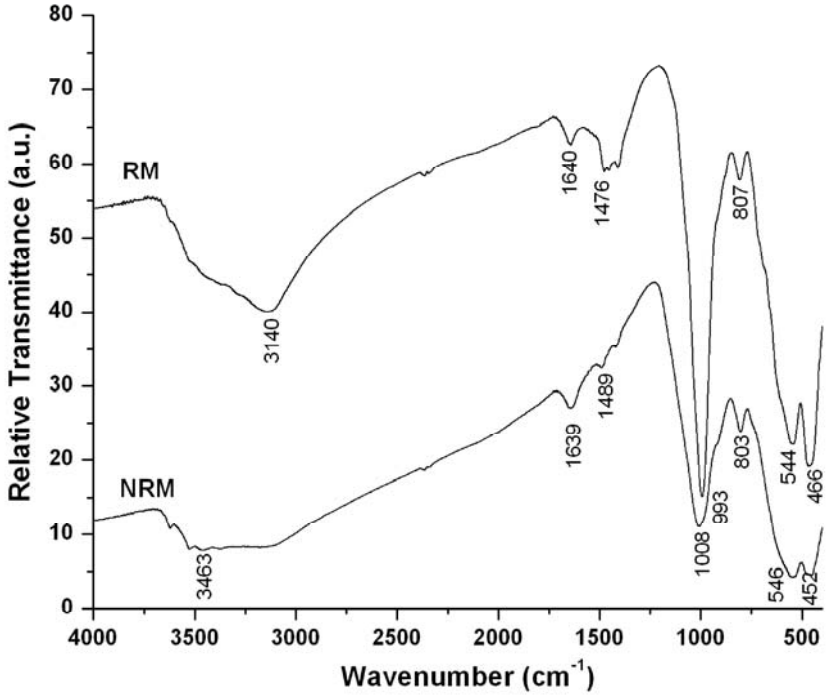

Fig. 4.7. Variation of FT-IR spectra of RM and NRM.

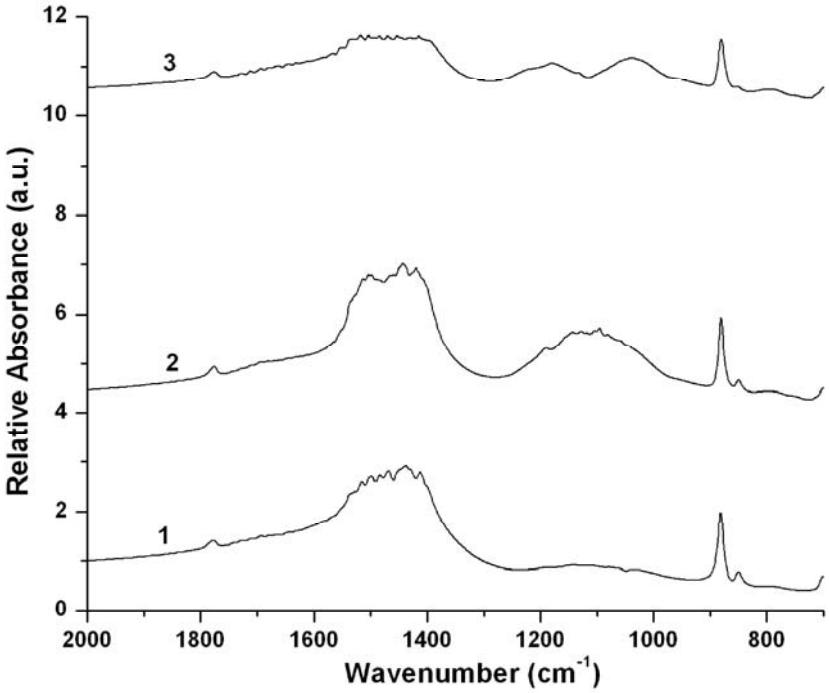

Fig. 4.8. Variation of FT-IR spectra of cycles-1, 2, and 3, each of them treated for 5 h sequestration.

Fig. 4.8 shows FT-IR absorption spectrum of carbonated filtrate in the region ~1600–800 cm^{-1}. The vibrational bands at about ~1540 cm^{-1}, ~1460 cm^{-1} and ~875 cm^{-1} are due to CO_3^{2-} [**138,139**] which confirmed CO_2 sequestration. The broad peaks in between ~1600–1200 cm^{-1} are also due to CO_3^{2-} and HCO_3^- [**140,141**]. Most intense peaks of filtrate at ~1600–1200 and ~875 cm^{-1} indicates sequestration of CO_2 more in filtrate as compared to the suspension. These peaks were more intense in cycles 1 and 2; subsequently decreased in cycle 3, as the amount of CO_2 sequestration decreased. Thus, these ions were formed into stable compounds as Na_2CO_3 and $NaHCO_3$.

4.1.6. Determination of pH, alkalinity, electrical conductivity and sequestration cycle

The variations of pH, electrical conductivity and alkalinity of RM, carbonated RM are indicated in Fig. 4.9 and Table 4.4. The equilibrium pH was achieved in between ~6.8– ~7.1, mainly due to HCO_3^- ions. Fig. 4.9a–c showed the rapid decrease of pH, electrical conductivity and alkalinity of RM within 5 h of carbonation, after that rebound slowly. The pH of carbonated slurry rebound again and again, without sequestration cycles. Because, the carbonates were dissolved during equilibrium with the gas phase buffers the water. Also, due to dissolution of alkaline minerals, and as the partial pressure of CO_2 *in situ* is more than atmosphere, so CO_2 moves toward the atmosphere. The pH was decreased from ~11.80 to ~6.81 at the end of cycle 1. The alkalinity was decreased from ~10,789 to ~2,583 mg/L. The pH and alkalinity was decreased maximum during 5 h carbonation process. Therefore, neutralization of red mud was done using 5 h carbonation process for subsequent cycles 2 and 3. Ionic solution can sequester CO_2 in a more efficient way. Utilization and sequestration of CO_2 using ionic solution needs less amount of activation energy to form immobilized stable product. Similarly, low viscous solution can dissolve more amounts of alkaline minerals during the long period of carbonation.

Table – 4.4.

The average pH, electrical conductivity, and alkalinity of cycles 1, 2 and 3, each of them treated for 5 h sequestration.

	Cycle-1	Cycle-2	Cycle-3
pH of sequestration	6.81	6.49	6.33
Electrical conductivity (mS/cm)	4.91	2.36	1.41
Alkalinity (mg/L)	2583	834	178

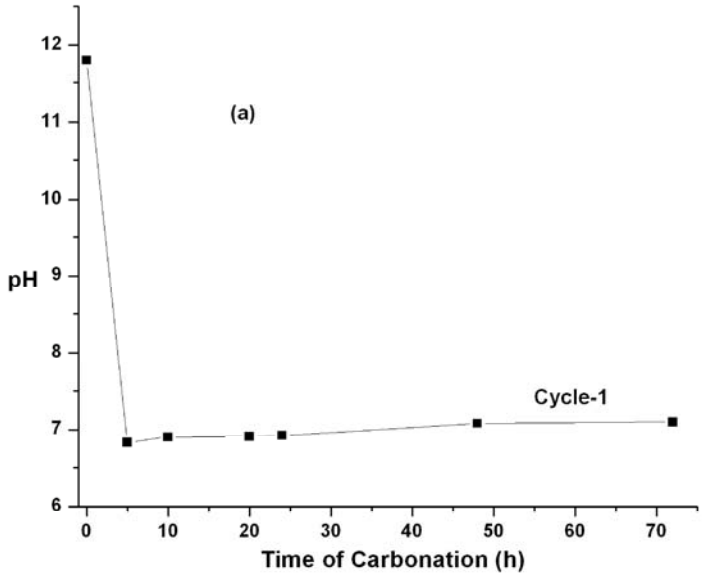

Fig. 4.9. (a) The average pH of carbonated red mud of cycle 1.

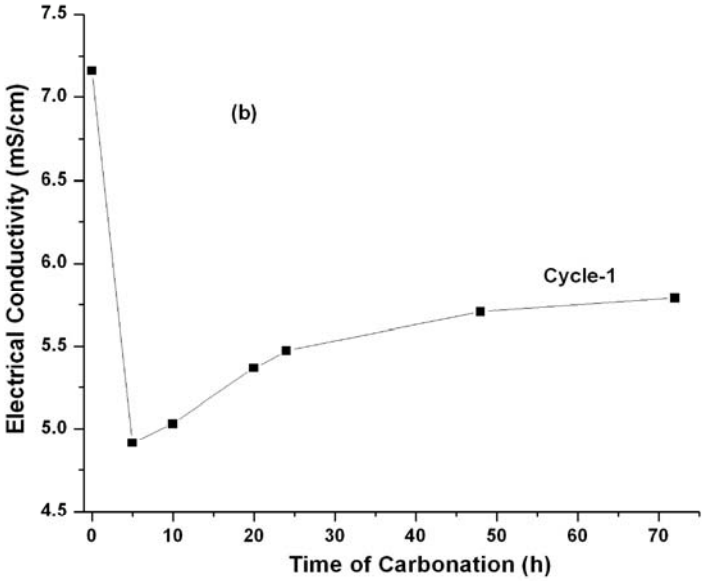

Fig. 4.9. (b) The average electrical conductivity of carbonated red mud of cycle 1.

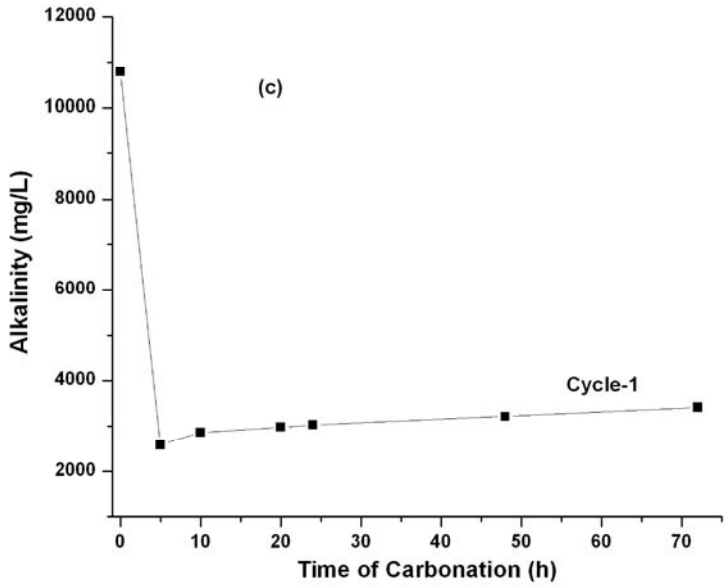

Fig. 4.9. (c) The average alkalinity of carbonated red mud of cycle 1.

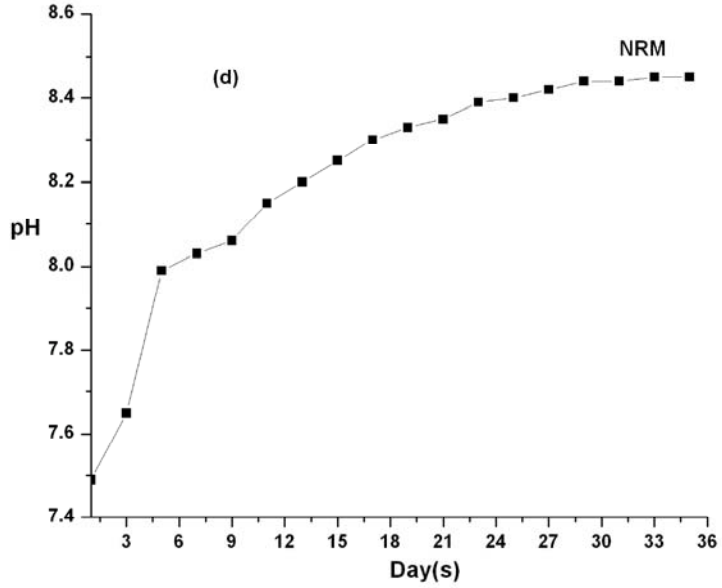

Fig. 4.9. (d) The average rebound pH of the NRM after cycle 3.

The dissociation of Na^+ ions increases the electrical conductivity of the filtrate (Fig. 4.9b). Complete exchange of Na^+ ions requires longer time of carbonation to reduce the reversible pH. The pH of red mud solution was decreased due to dissolve acidic CO_2, H_2CO_3, CO_3^{2-} and much more in the form of HCO_3^- [**142**]. The red mud solution rapidly absorbs CO_2 in the form of carbonic acid and neutralizes the excess base in the form of NaOH, Na_2CO_3, $Al(OH)_4^-$. The pH, electrical conductivity and alkalinity of RM after cycle 3 were ~6.33, ~1.41, and ~178 mg/L respectively. Fig. 4.9d showed that the pH of NRM after cycle 3 was rebound slowly for few days after that it remain constant at 8.45. It is due to presence of some undissolved alkaline minerals like sodalite, $Na(AlSiO_4)$.

4.1.7. Amount of CO_2 captured as determined by CHNS elemental analysis

Amount of CO_2 removed for cycles 1, 2, 3 and NRM were 3.54, 2.28, 0.63, 0.57 g CO_2/100 g of red mud, respectively, as determined by CHNS analyzer at 1150°C. So, total calculated CO_2 removal was 7.02 g/100 g of red mud.

Comparison of CO_2 sequestration capacity of this method with previously used materials by researchers shows the calculated results as: 24.7 g of CO_2/100 g of steel slag [**5**], 2.3 g of CO_2/100 g red mud [**16,18**], 81 g CO_2/L of MOFs [**7**], whereas this study shows 7.02 g CO_2 /100 g of red mud [**143**]. The direct comparison among MOFs, steel slag and red mud is difficult because the mechanism of absorption differs completely from adsorption. The sequestration of CO_2 depends on composition of material used. It is expected that CO_2 sequestration using caustic red mud will solve the environmental problem of red mud storage.

4.1.8. Acid neutralizing capacity (ANC) and cost estimation

Fig. 4.10 showed that the ANC of RM and NRM were ~1.3 and ~0.23 mol H^+/ kg of red mud, respectively. The ANC of NRM was lower due to leaching of strong basic cations Na^+ from carbonated red mud and formation of Na_2CO_3 and $NaHCO_3$.

Cost per unit mass of the CO_2 sequestered (Eq. (3.2)) highly depend on the amount of electricity. However, the cost of distilled water can be lowered by using normal water. According to the different assumptions about the energy price the cost will varies. Therefore, the roughly calculated cost of CO_2 sequestration is at \$147/ton-CO_2**.**

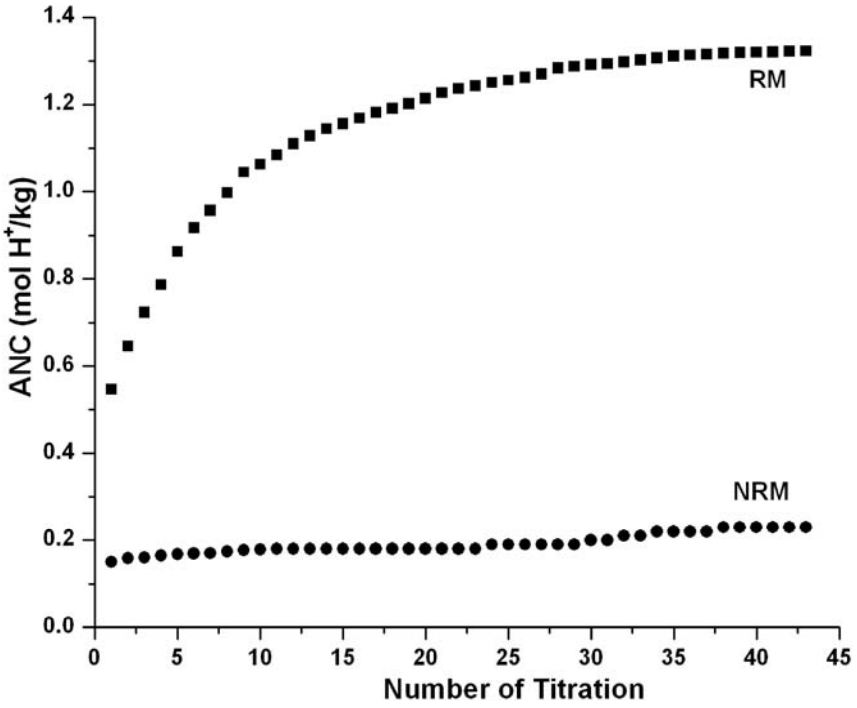

Fig. 4.10. Variation of acid neutralizing capacity of RM and NRM as obtained by auto titration with 0.1 M HCl solution.

4.1.9. Mechanism of immobilization of CO_2

Dissolution of CO_2 begins immediately when it comes in contact with caustic solution. The CO_2 is immobilized while it continues to dissolve slowly. These immobilization mechanisms act in parallel over the life of storage to increase storage security with time. Dissolved CO_2 in caustic solution reduces pH and forms carbonate and bicarbonate ions **[113].** Reduction/oxidation of CO_2 changes the electronic arrangement on the atom due to loss or gain of the electron. Linear shape changes to angular shape, which can able to decrease heat (IR radiation) absorption capacity.

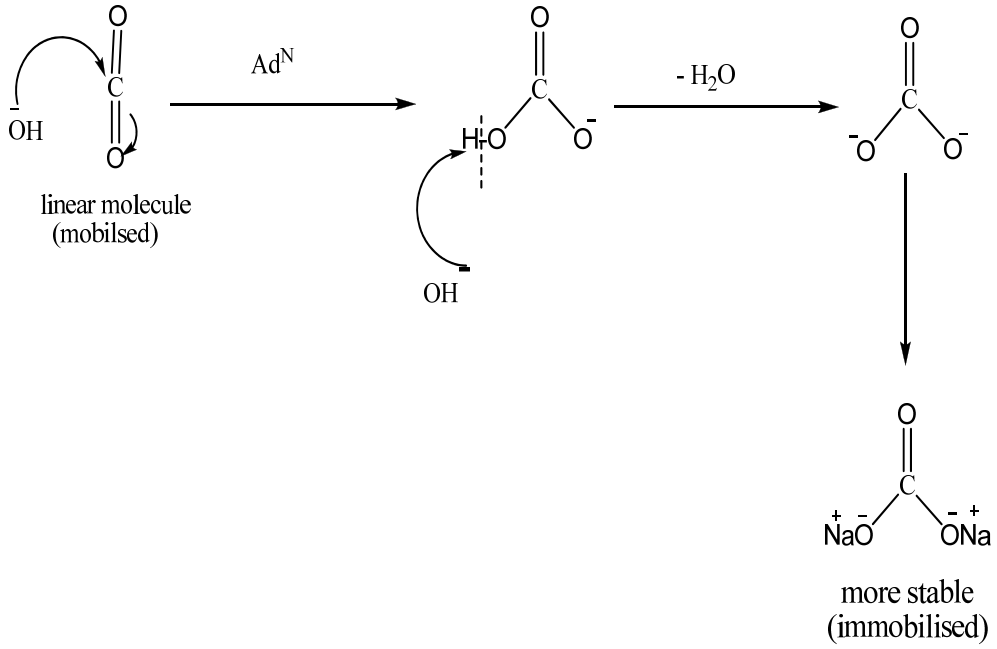

Fig. 4.11. Mechanism of immobilization of CO_2.

- CO_2 is a linear molecule which can absorb IR radiation from earth.

- It can store and reradiate heat radiation in the atmosphere by its bending, vibration & rotation.

- When it reacts with NaOH to form $NaHCO_3$ & Na_2CO_3 its bond angle decreases from 180° to 120°.

- Kinetically feasible and thermodynamically stable compound Na_2CO_3 was formed.

4.1.10. Reaction mechanism of neutralization

CO_2 sequestration through neutralization of carbonic acid to form carbonates or bicarbonates is a safer and permanent method. Neutralization based sequestration accelerates natural weathering processes that are exothermic and thermodynamically favored, and results in stable products that are common in nature. In fact, mineral deposits larger than fossil resources ensure essentially unlimited supplies of base ions (mainly Mg^{2+}, Ca^{2+}, Na^{+}, and K^{+}) **[144]**.

In pure water (pH = 7 before CO_2 dissolution), aqueous salvation of CO_2 is accompanied by hydration, resulting in carbonic acid (H_2CO_3) (Eq. 4.1), and subsequent acid-base chemistry leading to bicarbonate ions (HCO_3^-) and carbonate ions (CO_3^{2-}) (Eq. 4.2). Furthermore, some other reactions are represented in Eqs. 1.1 to 1.5 and 2.8 to 2.11. Due to the widespread importance of aqueous bicarbonate chemistry and its conjugate acid is carbonic acid (H_2CO_3). H_2CO_3/HCO_3^- buffer system has been known to play in regulating the pH of fluids **[145]**. Similar process takes place in nature and living organisms. Therefore, neutralization of red mud using CO_2 sequestration is a nature-bio-inspired absorption method.

$$CO_2\,(g) + 3H_2O \leftrightarrow CO_2\,(aq) + 3H_2O \leftrightarrow H_2CO_3 + 2H_2O \quad (4.1)$$

$$H_2CO_3 + 2H_2O \leftrightarrow HCO_3^- + H_3O^+ + H_2O \leftrightarrow CO_3^{2-} + 2H_3O^+ \quad (4.2)$$

The net result is a decrease in pH. Bicarbonate acts as a moderately weak base in solutions below neutral pH. The determination of H_2CO_3 in time-resolved experiments by rapid mixing of CO_2 (aq) and a basic solution is difficult to achieve, because the

kinetics of the forward reactions Eq. 4.1 are dominated by the slowest step, namely hydration of CO_2 (aq) resulting in H_2CO_3. The ensuring dissociation of H_2CO_3 into H_3O^+ and HCO_3^- (Eq. 4.2) then leads to rapid depletion of H_2CO_3, precluding a substantial transient population build-up. The reverse reaction, involving transient protonation of HCO_3^-, could potentially lead to substantial generation of H_2CO_3 **[145]**.

The $[HCO_3^-]$ is more in aqueous media **[79]**. At pH ~6.0, bicarbonate ions (anions) concentration is highest $[HCO_3^-] >> [CO_3^{2-}]$ and $[HCO_3^-] >> [OH^-]$. Therefore, electroneutrality was maintained by bicarbonate ions **[146]**.

4.1.11. Advantages of neutralization of red mud using CO_2 sequestration cycle

A widely accepted idea is that CO_2 is thermodynamically and kinetically stable, due to which it is rarely used to its fullest potential. However, due to the electron deficiency of the carbonyl carbons, CO_2 has a strong affinity toward nucleophiles and electron-donating reagents. In other words, CO_2 is an "anhydrous carbonic acid", which rapidly reacts with basic compounds. Water, amines also add to CO_2 in similar manners to produce compounds with a carboxyl or carboxylate group. However, few industrial processes utilize CO_2 as a raw material. Because CO_2 is the most oxidized state of carbon, the biggest obstacle for establishing industrial processes based on CO_2 as a raw material due to its low energy level. In other words, a large energy input is required to transform CO_2 **[3].** Then also, neutralization of red mud using CO_2 sequestration has some advantages over other neutralization methods:

- It is an environment-friendly, nontoxic process.
- Cost-effective.
- Sequester large amount of CO_2 and simultaneously neutralizes the RM.
- Minimizes global warming.
- Recovery of caustic liquor by addition of lime water can be done.

- By this sequestration mechanism mobilized CO_2 of atmosphere can be converted to immobilize (stable compound). So that it does not reach the atmosphere. As a result it does not reradiate heat radiation in the atmosphere.

Because CO_2 is a highly oxidized, thermodynamically stable compound. Its utilization requires reaction with specific high energy substances **[118]**. Waste caustic of red mud is a resource to sequester CO_2. NaOH is a good choice; energy cost can be brought down by using waste NaOH **[82]**. Absorption of CO_2 by an alkaline aqueous solution is a cheaper process but raises the cost of regeneration **[124]**.

Similarly, by comparing with other CO_2 sequestration methods, the least expensive way to neutralize CO_2 may be its injection into alkaline mineral strata. CO_2 would gradually dissolve into the pore water, because CO_2 is acidic. Fortunately ocean water accept far large amount of bicarbonates than carbonic acid. Most sequestration methods require concentrated CO_2, which is best captured at larger plants that generate clean, carbon-free energy carriers such as electricity and hydrogen. CO_2 is three times as heavy as fuel and therefore cannot be stored in cars or airplanes. CO_2 from these sources will have to be released into the atmosphere and recaptured later **[144]**.

Currently, photosynthesis is the only practical form of the CO_2 sequestration by absorption method. Sequestration from air flowing over chemical sorbents– such as strong alkali solutions or activated substrates–appears feasible but needs to be demonstrated. The additional cost of sorbent recycling should also be affordable. Today's most urgent need for CO_2 emission reductions can be possible by using low-cost CO_2 sequestration technology.

4.2. Utilization of activated CO_2-neutralized red mud for removal of arsenate

4.2.1. Characterization of activated CO_2-neutralized red mud (adsorbent)

Particle size of red mud was in the range of 0.1–160 μm. The BET-N_2 surface area of RM, NRM and ANRM were found to be 31.7, 59.33 and 63 $m^2 g^{-1}$, respectively. The surface areas of NRM and ANRM were increased, due to acidic CO_2 and thermal treatment, respectively.

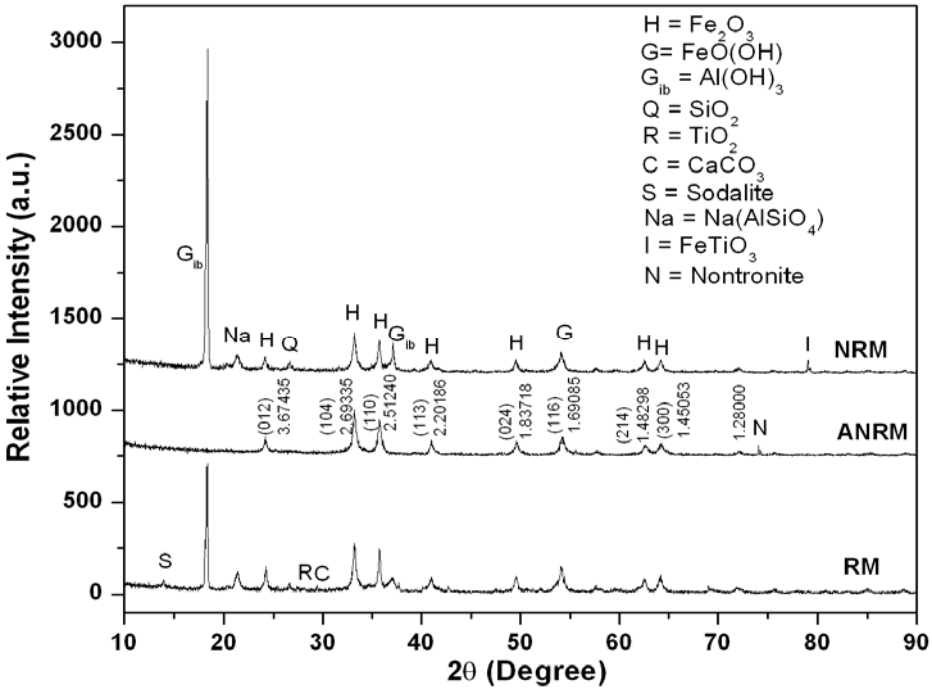

Fig.4.12. XRD patterns of RM, NRM, and ANRM.

The crystalline phases of RM, NRM and ANRM were obtained by powder XRD and the graph is presented in Fig. 4.12. The following mineral phases were analyzed with Philips X'Pert High Score software: hematite (α-Fe_2O_3), goethite (α-FeO(OH)),

gibbsite (γ-$Al(OH)_3$), calcite ($CaCO_3$), rutile/anatase (TiO_2), sodalite: zeolite (I) ($1.08Na_2OAl_2O_31.68SiO_21.8H_2O$), quartz ($SiO_2$), sodium aluminum silicate ($Na(AlSiO_4)$), and magnetite (Fe_3O_4) as referred from JCPDS (Joint Committee of Powder Diffraction Standards) file of X'Pert High Score software. The results obtained from the analysis indicated that there were remarkable differences among RM, NRM, and ANRM, which suggests that phase transformation has taken place. It revealed that the peaks of gibbsite in NRM were increased prominently and a new mineral ilmenite ($FeTiO_3$) was formed, due to CO_2 treatment. But, after thermal treatment of NRM, the intensity of hematite containing small amount of FeO was increased significantly, whereas the peaks of gibbsite disappeared, due to decomposition. As a result, hematites are dominant phases in ANRM.

Fig. 4.13 shows the FT-IR spectra of RM, NRM and ANRM. The positions of the absorption bands are nearly similar in all spectra. But, the relative intensities of RM are more intense. RM showed a broad band at ~3142 and a weak peak at ~1644 cm^{-1}, due to the stretching vibrations of O–H bonds and H–O–H bending vibrations of interlayer adsorbed H_2O molecule respectively. Water hydroxyl-stretching vibrations are intense in an infrared spectrum, because of large change in dipole moment. The OH-stretching vibrations of NRM and ANRM show at higher wave number of ~3461, 3396 cm^{-1}, respectively. This shift is associated with the shorter O–H bonds existing in RM than NRM and ANRM, causing an increase in electrostatic attraction within the RM layer. The absorption bands at ~1473, ~1410 and ~807 of RM and ~1486, ~1410 and ~803 cm^{-1} of NRM are due to stretching vibrations of C=O, confirmed the presence of CO_3^{2-} groups [**135,138,139**]. This may be due to chemisorbed CO_2 in RM and NRM, respectively. These peaks were disappeared in ANRM, due to decomposition of carbonate group by heat treatment.

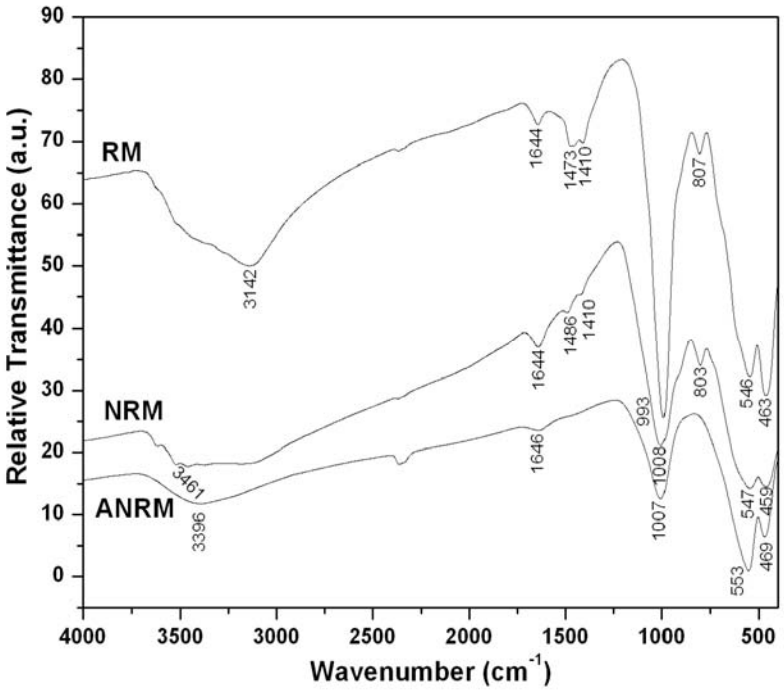

Fig.4.13. FT-IR patterns of RM, NRM, and ANRM.

Characteristic bands correspond to Si–O vibration were detected at ~993 – ~1007 cm^{-1} proved the presence of silicate groups. Peaks at ~553 – ~546 and ~469 – ~459 cm^{-1} are due to bending vibration of Si–O–Al and stretching vibrations of Fe–O bonds, respectively [**38,136**]. Intensities of these peaks were decreased in NRM, ANRM which confirmed the dissolution of minerals like silicate, $Na(AlSiO_4)$. Hence, FT-IR results support the evidence of phase change data of XRD.

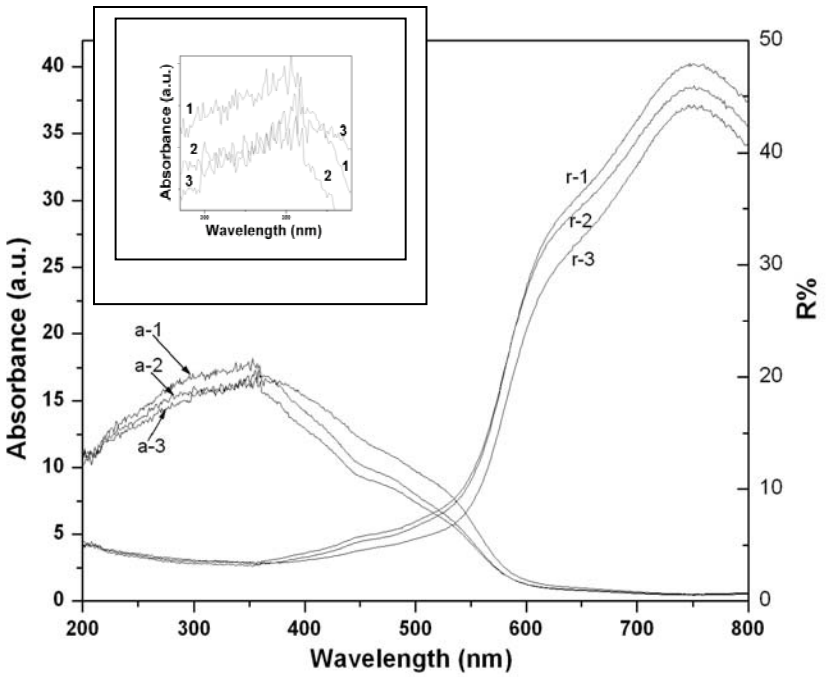

Fig.4.14. UV–vis diffuse reflectance spectra of (1) RM, (2) NRM, and (3) ANRM. The inset is the enlarged view of the spectra between 285–390 nm. In this figure, r-1, r-2, r-3 are the reflectance and a-1, a-2, and a-3 are the absorbance of RM, NRM, and ANRM, respectively.

The diffuse reflectance spectra of powder samples were converted into the absorption spectra by the Kubelka–Munk relationship,

$$K/S = (1 - R)^2/2R \qquad (4.3)$$

where *R*, *K*, and *S* are the value of reflectance measurements (relative value to the reflectance of $BaSO_4$) and the absorption and scattering coefficients of the sample, respectively.

Fig. 4.14 shows the UV–vis diffuse reflectance and absorption spectra of RM, NRM and ANRM. It shows that the peak maxima are observed at slightly different positions for the three samples and the spectral patterns are very similar. However, the

absorbance peak broadening of ANRM was observed, as shown in Figure 4.14 (inset). This study of spectra suggests that there is no effect of CO_2-neutralization and further heat treatment on the structure of Fe^{3+} ions of Fe_2O_3. In the region from 600 to 800 nm UV-vis light was not absorbed, which determines the red color from Fe^{3+} of RM, NRM and ANRM. As a result, in this region maximum reflection of light radiation was observed. Furthermore, reflectance % and peaks broadening of solid powder samples gradually decreased depending upon the decrease of concentration of alkaline oxides.

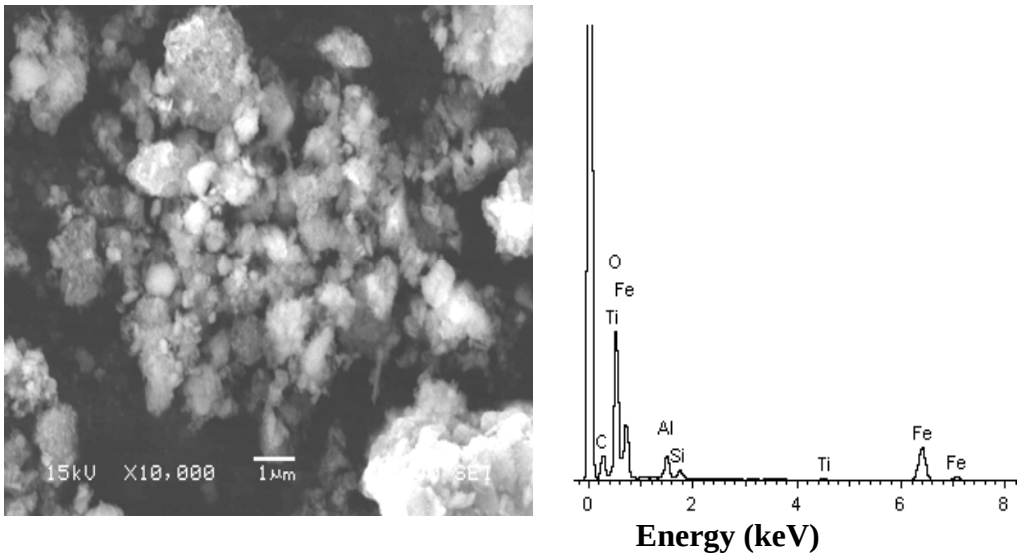

Fig.4.15. SEM micrographs/EDX spectrum of ANRM.

SEM micrograph (Fig. 4.15) provides the surface micro-morphology of the ANRM. Some mineral phase mainly calcite, sodalite, quartz were soluble in acidic environment. As a result their rounded shapes of aggregate disappeared. On thermal treatment porosity of the material was developed. The EDX spectrum of ANRM shows the presence of Fe, O, Al, Ti, Si and C.

4.2.2. Effect of adsorbent dose and pH

It is evident from the Fig. 4.16 that the % removal of As(V) was increased from ~73 to ~98% with increase of the adsorbent concentration (1–4 g L^{-1}) with initial arsenate concentration of 10 mg L^{-1}. Because number of active sites increases with respect to increase of adsorbent dose. However, it was observed that after dose of 4 g L^{-1}, there was no significant change in % removal of As(V). This may be due to overlapping of active sites at higher dose. So, there was not any appreciable increase in the effective surface area due to the agglomeration of exchanger particles **[147]**. So, 0.2 g/50 mL was considered as optimum dose and was used for further study.

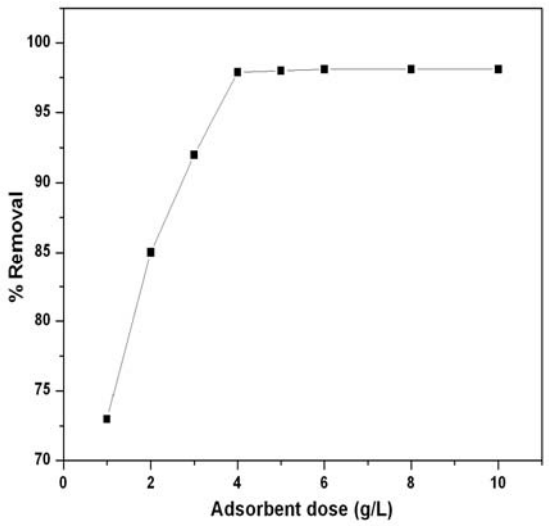

Fig.4.16. Adsorbent dose versus percentage removal of As(V) by ANRM.

Some experiments were carried out to examine the effect of initial pH on the adsorption. The arsenate removal was favored at acidic pH (3–6), whereas adsorption gradually decreased with the increase of pH. Furthermore, the adsorption of As(V) was very low at pH 10.0, as shown in Fig. 4.17.

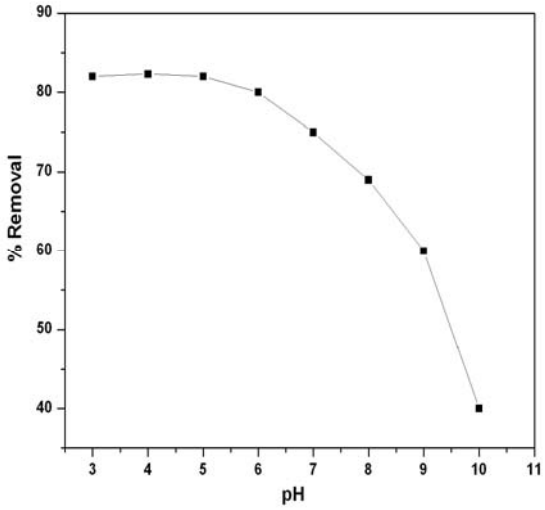

Fig.4.17. Effect of initial pH on As(V) adsorption on ANRM.

Solution pH not only affects the surface charge property of the ANRM through the protonation, but also influences arsenate speciation in the solution. Arsenate exists as H_3AsO_4, $H_2AsO_4^-$, $HAsO_4^{2-}$, and AsO_4^{3-} species in aqueous solution. $H_2AsO_4^-$ is the main species in solution at pH from 3–6, while $HAsO_4^{2-}$, and AsO_4^{3-} become major species at pH above 8. Therefore, arsenate species are anionic in this pH range. With increase of solution pH, the number of protonated groups (positive charges) on ANRM decreased, while the number of negative charge of arsenic species increased. As a consequence, the adsorption amount of ANRM for arsenate decreased. In acidic environment, OH^- ions concentration in the solution is lower, so less competition with As(V) anions for the available active sites. The above data suggest that the optimum pH for removal of arsenate was ~4. In the pH range 3–7, $H_2AsO_4^-$ and $HAsO_4^{2-}$ are the predominant species of As. Solutes interact with mineral surfaces due to their electrical surface charge, because of reactions involving functional groups (H^+, OH^-) on the mineral surface and ions in the solution **[34].**

4.2.3. Mechanism of arsenate removal

The acid–base titration of the sorbent is interpreted as the reactions of protonation and deprotonation of the surface sites (Eqs. 4.4 and 4.5). Arsenate is adsorbed to a monodentate site ≡Fe–OH to form monodentate surface complexes $\equiv FeOAsO_3^{2-}$ (Eq. 4.6). Whereas, arsenate adsorption to a bidentate site $\equiv(Fe–OH)_2$ forms binuclear bidentate surface complex $\equiv(FeO)_2AsO_2^-$ (Eq. 4.7) [**34**].

Surface acidity reaction

$$\equiv Fe–OH_2^+ = \equiv Fe–OH + H^+ \quad (4.4)$$

$$\equiv Fe–OH = \equiv Fe–O^- + H^+ \quad (4.5)$$

Adsorption reaction

$$\equiv Fe–OH + AsO_4^{3-} + H^+ = \equiv FeOAsO_3^{2-} + H_2O \quad (4.6)$$

$$\equiv(Fe–OH)_2 + AsO_4^{3-} + 2H^+ = \equiv(FeO)_2AsO_2^- + 2H_2O \quad (4.7)$$

Hydroxylated surface of the oxides of red mud develops charge on the surface in the water. The adsorption between surface hydrohyl group and As(V) ion follows ligand exchange reaction mechanism and exists as inner sphere surface complexes [**13**]. The binuclear bidentate surface complex $\equiv(FeO)_2AsO_2^-$ is predominated and the dominant form of arsenate in the range of pH 4–6.8, whereas the monodentate complex $\equiv FeOAsO_3^{2-}$ is dominate above pH 6.8 [**34**]. This involves columbic interaction and is referred as surface coordination:

$$\equiv S–OH + L^- + H^+ \leftrightarrow \equiv S–L + H_2O \quad (4.8)$$

where ≡S–OH is a surface hydroxyl group and ≡S–L is the ligand-adsorbed species. Red mud is a heterogeneous mixture of several minerals. The hydroxyl surfaces of

mixture of Fe, Al, Ti oxides of ANRM provide strong adsorption affinity for arsenate adsorption by forming inner-sphere complexes.

The surface of a solid is inherently different than the rest of the solid (the bulk). The bonding at the surface is different than that in the bulk. Surface atoms always want to react in some way, either with each other or with foreign atoms, to satisfy their bonding requirements. These bonding are different from the bonding requirements in bulk atoms. Chemisorption is highly directional due to all chemical bonds formation. Therefore, adsorbates that are chemisorbed stick at specific sites and they exhibit a binding interaction that depends strongly on their exact position and orientation with respect to the adsorbent. On metals, chemisorbed atoms tend to sit in sites of the highest coordination. Oxygen atom forms strong bonds with a number of elements, for instance, iron, aluminum and silicon are highly susceptible to oxidation. When adsorbate reacts and forms strong bond with adsorbent, it forms new compound. Whereas, physisorption undergo van der Waals attractions and do not experience such strong directional interactions **[148]**.

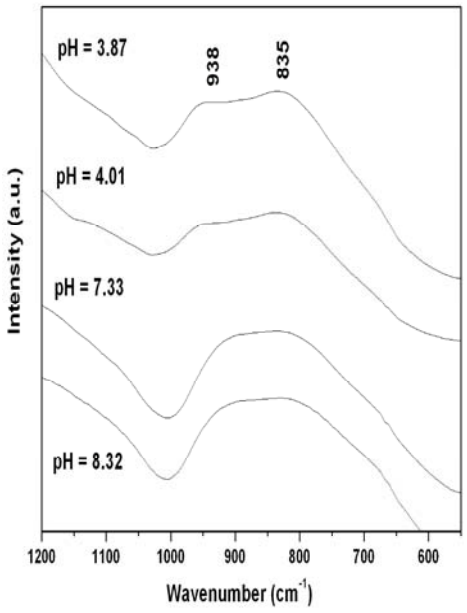

Fig.4.18. FT-IR patterns of As(V) adsorbed on ANRM at different pH.

The adsorbed As(V) on ferric hydroxide shows two peaks at 835 and 938 cm^{-1} in acidic medium as shown in Fig. 4.18. This is due to symmetric stretching (ν_s) of As–O bond and asymmetric stretching (ν_{as}) of As–O bond in As–O–Fe species, respectively. The peak position is strongly affected by changes in pH. Therefore, they show prominent peaks at optimum acidic pH. From FT-IR data there is a clear evidence for surface precipitation of poorly crystalline ferric arsenate in acidic pH ~4, whereas at alkaline pH arsenate is adsorbed via surface complexation. The observed As(V) FT-IR bands at various pH are in agreement with previous reports [**149–153**].

4.2.4. Effect of contact time and adsorption kinetics

Adsorption of As(V) at different contact time was studied for determination of equilibrium time of reaction. These experiments were carried out at equilibrium pH ~4, with initial arsenate concentration 10 mg L^{-1} at room temperature. The percentage removal was 85% for first 0.5 h of contact time. The results of the Fig. 4.19 showed that the maximum removal was 99% and attained equilibrium at 24 h. After that there was no significant change in the percentage removal. This indicates the possible monolayer formation of As(V) ions on the outer surface.

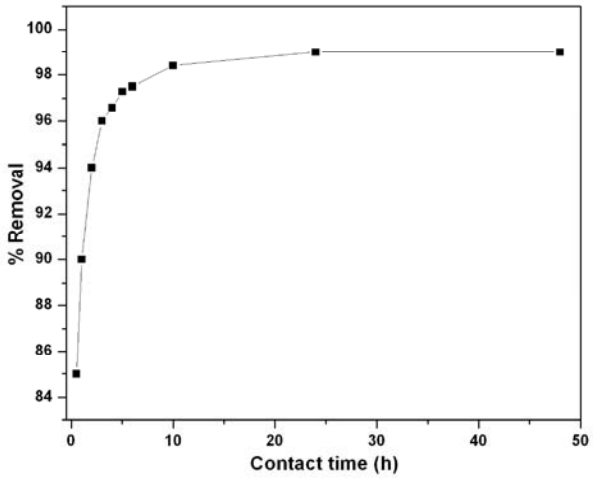

Fig.4.19. Time versus percentage removal of As(V).

The rate constant K_1 for adsorption of As(V) was studied by Lagergren rate equation [**36**] for initial arsenate concentration of 10 mg L^{-1}. Pseudo-first-order rate expression of Lagergren equation:

$$\log(q_e - q_t) = \log q_e - \frac{K_1 t}{2.303} \tag{4.9}$$

where q_e and q_t are the amount of arsenate adsorbed (mg g^{-1}) at equilibrium and at time t (min), respectively. K_1 is the pseudo-first-order rate constant (min^{-1}). The K_1 and R^2 were found to be 0.0076 and 0.939 respectively, which are extremely low, indicating that the adsorption of As(V) onto ANRM did not follow pseudo-first-order rate model. The pseudo-second-order rate expression:

$$\frac{t}{q_t} = \frac{1}{K_2 q_e^2} + \frac{t}{q_e} \tag{4.10}$$

where K_2 is the pseudo-second-order rate constant (g mg^{-1} min^{-1}). The values of K_2, and R^2 were given in Table 4.5.

Table – 4.5

Pseudo-second-order kinetics constants and related regression coefficients.

Initial solution pH	q_e (mg g^{-1})	K_2 (g mg^{-1} min^{-1})	R^2
5	52.604	6.234 x 10^{-3}	0.998
7	46.620	0.420 x 10^{-3}	0.999
9	34.106	1.395 x 10^{-3}	0.994

The low value of K_2 and high value of R^2 indicates that the adsorptions followed pseudo-second-order kinetics.

4.2.5. Adsorption equilibrium isotherms

Commonly adsorption isotherm has been used to evaluate the adsorption capacity of an adsorbent for an adsorbate. The linearized Langmuir adsorption isotherm equation is as follows [**154**]:

$$\frac{1}{q_e} = \frac{1}{q_m b C_e} + \frac{1}{q_m} \tag{4.11}$$

where C_e is the equilibrium concentration of adsorbate in solution (mg L^{-1}), q_e is the amount adsorbate adsorbed at equilibrium (mg g^{-1}), q_m is the theoretical maximum adsorption capacity (mg g^{-1}), and b is the Langmuir constant (L mg^{-1}). Arsenate adsorption is well fitted by Langmuir adsorption isotherm with correlation coefficient $R^2 = 0.996$, as shown in Fig. 4.20. This indicates a monolayer sorption of arsenate onto the adsorbent surface. The maximum adsorption capacity (q_m) of ANRM for arsenate was 55.55 mg g^{-1} according to the Langmuir model **[155]**, which is better than that of the previous research on most of adsorbents [**13,17,35,36**], single component materials [**156**] used to remove arsenate in the literature.

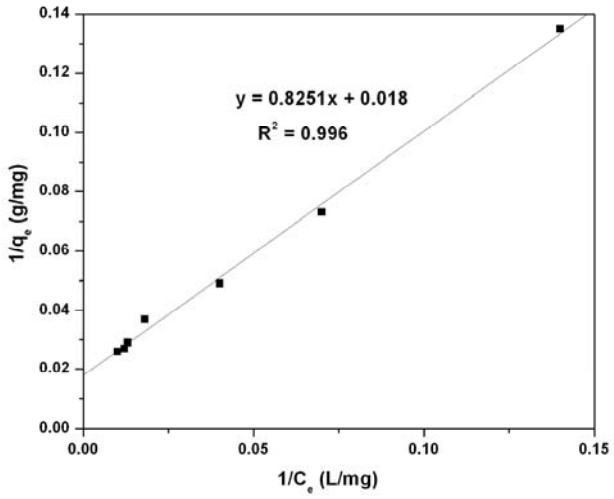

Fig. 4.20. Langmuir adsorption isotherm plot of $1/C_e$ versus $1/q_e$.

Freundlich adsorption isotherm assumes multilayer adsorption on heterogeneous surfaces. Linearized form of the Freundlich equation is given by the following equation [**36**]:

$$\ln q_e = \ln K_f + 1/n \ln C_e \quad (4.12)$$

where q_e is the amount of arsenate ions adsorbed at equilibrium time (mg g^{-1}), C_e is the equilibrium concentration of arsenate ions in the solution (mg L^{-1}), K_f is the adsorption capacity (mg g^{-1}), and n is an empirical parameter. The value of K_f, n, *and* R^2 are 10.86 mg g^{-1}, 2.0411, 0.977, respectively. This indicates that the highest correlation coefficient of Langmuir isotherm fits the adsorption data better than the Freundlich isotherm.

4.2.6. Desorption and regeneration studies

Regeneration studies were carried out in order to know the reusability of ANRM, when the adsorption capacity of the adsorbent is exhausted. Initially, desorption of arsenate was difficult in the pH range 4–8.

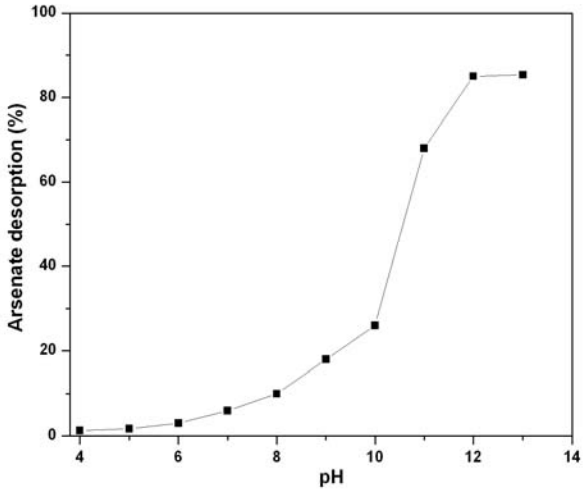

Fig.4.21. Desorption of arsenate with respect to solution pH.

Because, in the pH range of 4–9, Lewis bases ligands arsenates get selectively adsorbed through the formation of inner-sphere complexes [**157**]. But, as the pH increases from 9 to12, desorption of arsenate increases and maximum desorption (92%) occurred at pH 12, as shown in Fig. 4.21. Because, at pH > 11.0, negatively charged FeO^- is the predominant surface functional group, thus rejects all ions including arsenates [**158**]. Therefore, desorption of arsenate with NaOH solution is very efficient. The surface of adsorbent (ANRM) becomes fresh and active sites are regenerated. But, adsorption capacity of regenerated ANRM decreases gradually, chemisorptions exhibits poor desorption, adsorbate species are bound tightly to the adsorbent with comparatively stronger bonds [**36**].

4.3. Extraction of fine iron oxide from CO_2-neutralized red mud

4.3.1. Characterization by XRD, SEM

The XRD peaks of RM (Fig. 4.1. (a)) showed the presence of α-Fe_2O_3, α-FeO(OH), γ-$Al(OH)_3$, $CaCO_3$, TiO_2, $1.08Na_2OAl_2O_31.68SiO_21.8H_2O$, SiO_2, $Na(AlSiO_4)$, and Fe_3O_4.

SEM images (Fig. 4.6.a and b) showed that the rounded shape aggregate particles (poorly-crystallized/amorphous forms) present in RM were decreased in the NRM. This indicates that some mineral phases mainly calcite, sodalite contained in the RM are more soluble in acidic environment [**12**]. SEM image (Fig. 4.22) of recovered fine iron oxide showed different micromorphology as compared to RM and NRM.

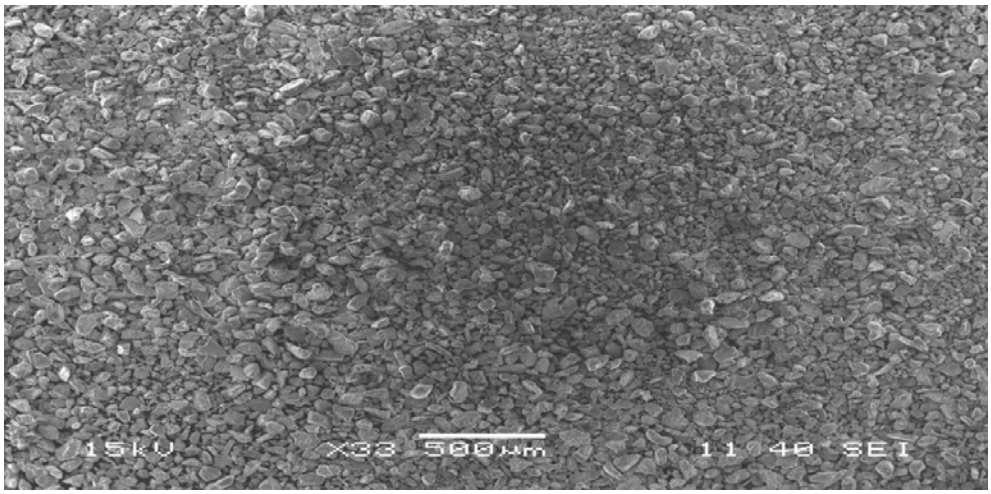

Fig. 4.22. SEM image of recovered fine iron oxide.

4.3.2. Element composition by EDX

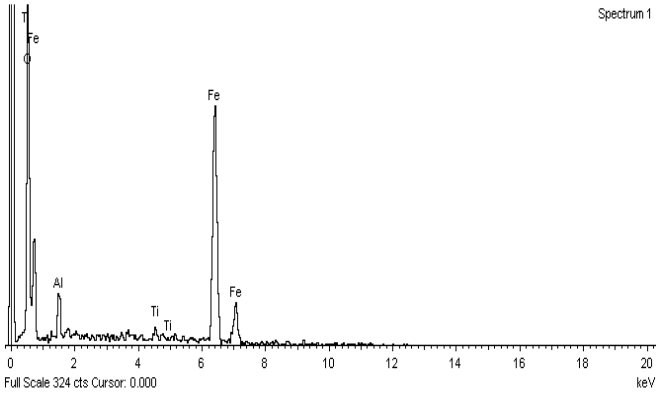

Fig. 4.23. EDX analysis spectrum of recovered fine iron oxide.

Major compound compositions of RM are represented in Table 4.2. EDX spectrum (Fig. 4.23) showed the presence of Fe, Al, Ti, O in the recovered fine iron oxide. Similarly, the element composition NRM and recovered fine iron oxide were represented in Tables 4.3 and 4.6, respectively. From this, it was confirmed that the recovered fine iron oxide contain Fe (71.71%) [**160**]. This Fe (w/w) % in fine iron oxide is higher as compared to RM and NRM. The increase of concentration of Fe in extracted fine iron oxide can help for the economical extraction of metallic iron.

Table. 4.6. Element composition (wt%) of recovered fine iron oxide.

Element	**Wt%**
Al	3.01
Ti	1.24
Fe	71.71
O	24.05

- Micro morphological studies of recovered fine iron oxide showed 71.71% of Fe [**160**].

- Direct use of RM as a secondary ore for Steel plant is not possible due to its caustic nature.
- By this ore beneficiation process large amount of RM can be used directly in the steel plant as high grade iron ore.

Extraction of fine iron oxide using CO_2

- Due to formation of CO_2–in–water microemulsions.
- Dispersion of CO_2 in water solubilizes hydrophilic materials.
- During hot condition only fine iron settled down faster as compared to other oxides.

However, CO_2 is nonpolar, which results in relatively low reaction rates for reaction that have polar transition states. This low reaction rates increases by heating. These CO_2-expanded liquid are inducing separations, precipitation of fine particles. Since CO_2 is used as a viscosity-reducing agent. The viscosity reduction due to expansion of liquid on addition of CO_2 helps in separation **[87]**.

Furthermore, CO_2 was utilized along with the biodegradable surfactant for extraction of fine iron ore from CO_2–neutralized red mud. Surfactant molecules can group together as micelles, colloid-sized clusters of molecules, for their hydrophobic tails tend to congregate, and their hydrophobic heads provide protection. Micelles form only above the critical micelle concentration (CMC) and above the Krafft temperature. Micelles are important in industry due to their solubilizing function **[159].**

4.3.3. Advantages

- Environment-friendly technology.
- Control caustic pollution at alumina industry area.
- Help to mitigate global warming.
- Cyclic process removes ~90% of Na from RM.
- Large-scale utilization red mud by extraction of fine iron oxide [**160**].

*****

Chapter 5

Conclusions

CO_2 sequestration is a competitive, fast-paced, interdisciplinary research field involving geology, chemistry, and engineering with contributions from social science, law, and policy. Moreover, afforestation of degraded forest lands and use of nature-friendly and environment-friendly technologies can prevent the most challenging problem of today's global warming and climate change; though there is a global economic competition.

Neutralization and utilization of waste red mud as a resource is a core business objective for alumina industry. Poor environmental performance damages a company's efficiency, sustainability and prosperity. However, chemical composition and properties of red mud varies depending upon the origin of bauxite ore in the earth crust and also due to chemical and thermal processing of bauxite ore during extraction of alumina.

In this thesis three main problems: neutralization of red mud, sequestration of CO_2 and their utilizations has been investigated. The novelty of the present work is the

utilizations of waste red mud and sequestration of CO_2 to solve the environmental pollution and also for their utilizations as a resource to solve another environmental problem.

In this work caustic red mud was neutralized using CO_2 sequestration cycle. The red mud was treated with CO_2 at 5 mL/min for 5 h in each of the cyclic process. The pH and alkalinity of red mud was decreased from ~11.8 to ~8.45 and ~10,789 to ~178 mg/L at the end of the cycle 3, respectively. The permanently captured CO_2 %(w/w) per 10 g of red mud were ~26.33, ~58.01, ~55.37, and ~54.42 in NRM and first, second, third cycles of carbonated filtrate, respectively. The cyclic carbonation was captured more amount of carbon as compared to without cycle. This indicates that caustic filtrate of red mud is more efficient for CO_2 sequestration.

The CO_2 gas was sequestered in the form of Na_2CO_3, $NaHCO_3$, and H_2CO_3 as stable or solid compounds as revealed from FT-IR. The pH rebound of NRM was within the permissible limit of environment at the end of the cycles. Furthermore, mobilized CO_2 gas is converted into immobilize stable compounds using waste caustic red mud.

Hence, utilization of hazardous caustic red mud minerals for sequestration of CO_2 and its neutralization will reduce the environmental problem of red mud storage area.

Furthermore, adsorption is one of the most commonly used cost-effective techniques to remove arsenate from contaminated water. In this study, red mud was neutralized using CO_2 and thermally activated neutralized red mud was used as adsorbent. FT-IR analysis revealed that the adsorption of As(V) on the surface of ANRM through the electrostatic interaction between the positively protonated hydroxyl groups and negatively charged arsenate. The percentage removal was increased with decrease of pH and attained maximum adsorption at pH ~4. The adsorption kinetics was found to follow pseudo-second-order rate law and equilibrates within 24 h. The

ANRM can be used as a low cost adsorbent for the removal of arsenate to meet its acceptable limit in water. This process can be employed as a preliminary investigation for utilization of ANRM for removal of arsenate from aqueous solutions.

Furthermore, CO_2 was used for extraction of fine iron ore from RM. In fact, it is an enrichment process of Fe in red mud. So that larger amount of fine iron oxide can be utilized in the iron industry.

From the above studies it is concluded that, both the red mud and CO_2 are waste materials, but their utilizations produce environment-friendly NRM. It can solve some problems of global warming, and utilization of NRM can enhance the economical benefit of alumina industry. Therefore, it is a low-cost environment-friendly technique. Transfer of low-cost environment-friendly technique of neutralization and sequestration of CO_2 through academic-industry relationship is highly needed for sustainable development, mitigation of global warming and climate change.

Therefore, neutralization of red mud using CO_2 sequestration is a nature-bio-inspired absorption method. Today's most urgent need for CO_2 emission reductions can be possible by using low-cost CO_2 sequestration technology.

*****

Chapter 6

Scope for Future Work

Based on the findings of the present invention, the following suggestions may be made for the future scope of studies.

1. Pilot plant study of large-scale neutralization of RM using CO_2 sequestration technique is highly needed for sustainable development of alumina industry. Full-scale industrial experiments can be done for CO_2 sequestration.
2. CNRM can be used in metallurgical industry as a resource. Pilot plant study can be done for extraction of fine iron oxide from RM. For this environment-friendly technology, Vedanta Alumina Limited has already signed MoU with NIT Rourkela **[161,162]**.
3. CNRM can be used as a low-cost adsorbent for removal of hazardous heavy metal ions from water.
4. CNRM can be used for synthesis of nano-adsorbent.
5. Neutralization of red mud using CO_2 sequestration is a cost-effective environment-friendly technique. It can be favored for the creation of job opportunities in industry.
6. Neutralization of caustic red mud can be done by sequestering CO_2 from chimney of coal-fired power plant.

*****

References

[**1**] T.M.L. Wigley, A combined mitigation/geoengineering approach to climate stabilization, *Science* 314 (**2006**) 452–454.

[**2**] D.J. Darensbourg, Making plastic from carbon dioxide: salen metal complexes as catalysts for the production of polycarbonates from epoxides and CO_2, *Chem. Rev.* 107 (**2007**) 2388–2410.

[**3**] T. Sakakura, J-C Choi, H Yasuda, Transformation of carbon dioxide, *Chem. Rev.* 107 (**2007**) 2365–2387.

[**4**] R. Lal, Soil carbon sequestration impacts on global climate change and food security, *Science* 304 (**2004**) 1623–1627.

[**5**] D. Bonenfant, L. Kharoune, S. Sauve, R. Hausler, P. Niquette, M. Mimeault, M. Kharoune, CO_2 sequestration potential of steel slags at ambient pressure and temperature, *Ind. Eng. Chem. Res.* 47 (**2008**) 7610–7616.

[**6**] G. Montes-Hernandez, R. Perez-Lopez, F. Renard, J.M. Nieto, L. Charlet, Mineral sequestration of CO_2 by aqueous carbonation of coal combustion fly-ash, *J. Hazard. Mater*. 161 (**2009**) 1347–1354.

[**7**] D. Britt, H. Furukawa, B. Wang, T.G. Glover, O.M. Yaghi, Highly efficient separation of carbon dioxide by a metal-organic framework replete with open metal sites, *Proc. Natl. Acad. Sci. U.S.A.* 106 (**2009**) 20637–20640.

[**8**] S.M.V. Gilfillan, B.S. Lollar, G. Holland, D. Blagburn, S. Stevens, M. Schoell, M. Cassidy, Z. Ding, Z. Zhou, G. Lacrampe-Couloume, C.J. Ballentine, Solubility trapping in formation water as dominant CO_2 sink in natural gas fields, *Nature* 458 (**2009**) 614–618.

[**9**] R.T. Wilkin, D.C. Digiulio, Geological impacts to groundwater from geologic carbon sequestration: controls on pH and inorganic carbon concentrations from reaction path and kinetic modeling, *Environ. Sci. Technol.* 44 (**2010**) 4821–4827.

[**10**] C.L. Quere, C. Rodenbeck, E.T. Buitenhuis, T.J. Conway, R. Langenfelds, A. Gomez, C. Labuschagne, M. Ramonet, T. Nakazawa, N. Metzl, N. Gillett, M. Heimann, Saturation of the southern ocean CO_2 sink due to recent climate change, *Science* 316 (**2007**) 1735–1738.

[**11**] A.C. Mitchell, K. Dideriksen, L.H. Spangler, A.B. Cunningham, R. Gerlach, Microbially enhanced carbon capture and storage by mineral-trapping and solubility-trapping, *Environ. Sci. Technol.* 44 (**2010**) 5270–5276.

[**12**] T. Newson, T. Dyer, C. Adam, S. Sharp, Effect of structure on the geotechnical properties of bauxite residue, *J. Geotech. Eng.* 132(2) (**2006**) 143–151.

[**13**] H. Genc-Fuhrman, J.C. Tjell, D. McConchie, Increasing the arsenate adsorption capacity of neutralized red mud (bauxsol), *J. Colloid Interface Sci.* 271 (**2004**) 313–320.

[**14**] E. Fois, A. Lallai, G. Mura, Sulfur dioxide absorption in a bubbling reactor with suspensions of Bayer red mud, *Ind. Eng. Chem. Res.* 46 (**2007**) 6770–6776.

[**15**] A. Collazo, M.J. Cristobal, X.R. Novoa, G. Pena, M.C. Perez, Electrochemical impedance spectroscopy as a tool for studying steel corrosion inhibition in simulated concrete environments-red mud used as rebar corrosion, *J. ASTM Int.* 3(2) (**2006**) 1–10.

[**16**] R.M. Enick, E.J. Beckman, C. Shi, J. Xu, Remediation of metal-bearing aqueous waste streams via direct carbonation, *Energy Fuels* 15 (**2001**) 256–262.

[**17**] C. Brunori, C. Crmisini, P. Massanisso, V. Pinto, L. Torricelli, Reuse of treated red bauxite waste: studies on environmental compatibility, *J. Hazard. Mater.* B117 (**2005**) 55–63.

[**18**] C. Shi, J. Xu, E. Beckman, R. Enick, Carbon dioxide sequestration via pH reduction of red mud using liquid CO_2, *ACS Div. Fuel Chem.* 45(4) (**2000**) 703–705.

[**19**] C. Hanahan, D. McConchie, P. John, R. Creeiman, M. Clark, C. Stocksiek, Chemistry of sea water neutralization of bauxite refinery residues (red mud), *Environ. Eng. Sci.* 21 (**2004**) 125–138.

[**20**] D. Bonenfant, L. Kharoune, S. Sauve, R. Hausler, P. Niquette, M. Mimeault, M. K.haroune, CO_2 sequestration by aqueous red mud carbonation at ambient pressure and temperature, *Ind. Eng. Chem. Res.* 47 (**2008**) 7617–7622.

[**21**] S. Khaitan, D.A. Dzombak, G.V. Lowry, Mechanisms of neutralization of bauxite residue by carbon dioxide, *J. Environ. Eng.* 135 (**2009**) 433–438.

[**22**] G. Jones, G. Joshi, M. Clark, D. McConichie, Carbon capture and the aluminium industry: preliminary studies, *Environ. Chem.* 3 (**2006**) 297–303.

[**23**] D.K. Nordstrom, Worldwide occurrences of arsenic in ground water, *Science* 296 (21) (**2002**) 2143–2145.

[**24**] A.H. Smith, P.A. Lopipero, M.N. Bates, C.M. Steinmaus, Arsenic epidemiology and drinking water standards, *Science* 296 (21) (**2002**) 2145–2146.

[**25**] M. Zaw, M.T. Emett, Arsenic removal from water using advanced oxidation process, *Toxicol. Lett.* 133 (**2002**) 113–118.

[**26**] Y. Masue, R.H. Loeppert, T.A. Kramer, Arsenate and arsenite adsorption and desorption behavior on coprecipitated aluminum: iron hydroxides, *Environ. Sci. Technol.* 41 (**2007**) 837–842.

[**27**] X. Meng, S. Bang, G.P. Korfiatis, Effect of silicate, sulfate, and carbonate on arsenic removal by ferric chloride, *Water Res.* 34 **(**4**)** (**2000**) 1255–1261.

[**28**] J.A. Munoz, A. Gonzalo, M. Valiente, Arsenic adsorption by Fe(III)-loaded poen-celled cellulose sponge. Thermodynamic and selectivity aspects, *Environ. Sci. Technol.* 36 (**2002**) 3405-3411.

[**29**] J.S. Zhang, R. Stanforth, S.O. Pehkonen, Irreversible adsorption of methyl arsenic, arsenate, and phosphate onto goethite in arsenic and phosphate binary systems, *J. Colloid Interface Sci.* 317 (**2008**) 35–43.

[**30**] S. Dixit and J.G. Hering, Comparison of arsenic (V) and arsenic (III) sorption onto iron oxide minerals: implications for arsenic mobility, *Environ. Sci. Technol.* 37 (**2003**) 4142–4189.

[**31**] C. Su, R.W. Puls, Significance of iron(II, III) hydroxycarbonate green rust in arsenic remediation using zerovalent iron in laboratory column tests, *Environ. Sci. Technol.* 38 (**2004**) 5224–5231.

[**32**] H. Zhang, H.M. Selim, Kinetic of arsenate adsorption-desorption in soil, *Environ. Sci. Technol.* 39 (**2005**) 6101–6108.

[**33**] Z. Chen, Y. Cai, H.S. Gabriele, G.H. Snyder, J.L. Cisar, Interactions of arsenic and the dissolved substances derived from turf soils, *Environ. Sci. Technol.* 40 (**2006**) 4659–4665.

[**34**] H. Zeng, B. Fisher, D.E. Giammar, Individual competitive adsorption of arsenate and phosphate to a high-surface-area iron oxide-based sorbent, *Environ. Sci. Technol.* 42 (**2008**) 147–152.

[**35**] H.S. Altundogan, S. Altundogan, F. Tumen, M. Bildik, Arsenic adsorption from aqueous solutions by activated red mud, *Waste Management.* 22 (**2002**) 357–363.

[**36**] H. Genc-Fuhrman, J.C. Tjell, D. McConchie, Adsorption of arsenic from water using activated neutralized red mud, *Environ. Sci. Technol.* 38 **(2004**) 2428–2434.

[**37**] W. Huang, S. Wang, Z. Zhu, L. Li, X. Yao, V. Rudolph, F. Haghseresht, Phosphate removal from water using red mud, *J. Hazard. Mater.* 158 (**2008**) 35–42.

[**38**] S.J. Palmer, R.L. Frost, T. Nguyen, Hydrotalcites and their role in coordination of anions in Bayer liquors: anion binding in layered double hydroxides, *Coordi. Chem. Rev*. 253 (**2009**) 250–267.

[**39**] W.R. Richmond, M. Loan, J. Morton, G.M. Parkinson, Arsenic removal from aqueous solution via ferrihydrite crystallization control, *Environ. Sci. Technol.* 38 **(2004**) 2368–2372.

[**40**] Azom.com, the A to Z of Materials, Dealing with red mud by-product of the Bayer process for refining aluminum, *Materials World,* 11(**2003**) 22–24.

[**41**] http://www.qal.com.au, The Process.

[**42**] L.D. Hart, Alumina Science and Technology Handbook Chemicals, The American Ceramic Society, Inc., Westerville, Ohio, USA, **1990**.

[**43**] The International Aluminium Institute, **2010**, www.world-aluminium.org.

[**44**] www.redmud.org/home.html

[**45**] R.K. Paramguru, P.C. Rath, V.N. Misra, Trends in red mud utilization – a review, *Mineral Processing & Extractive Metall. Rev.* 26 (**2005**) 1–29.

[**46**] A. Satapathy, Thermal spray coating of red mud on metals, *PhD Thesis*, NIT Rourkela, India, **2005**.

[**47**] M.J. Chaddha, Asia pacific partnership of clean development & climate on industry perspectives-an overview, Jawaharlal Nehru Aluminum Research Development and Design Centre, **2009**.

[48] A. Agrawal, K.K. Sahu, B.D. Pandey, Solid waste management in non-ferrous industries in India, *Resources, Cosenvation and Recycling* 42 (**2004**) 99–120.

[**49**] R. Kumar, J.P. Srivastava, Premchand, Utilization of iron values of red mud for metallurgical application, Environmental waste management in non-ferrous metallurgical industries. NML, Jamsedpur, 29–30 January (**1998**) 19–108.

[**50**] H.S. Patra, A. Murthy, Fact finding report of NALCO, 14.6.**2006**.

[51] P.K. Pattajoshi, Assessment of airborne dust associated with chemical plant: A case study, *Indian J. of Occup. Env. Medi.* 10 (**2006**) 32–34.

[**52**] D. McConchie, M. Clark, F. McConchie, New strategies for the management of bauxite refinery residues (red mud), 6^{th} international alumina quality workshop, Brisbane, Australia, Sept. **2003**.

[**53**] P.J. Baldwin, N.K. Murray, C.R. Lee, M.W. Farrall, Double replacement cation neutralization of high alkalinity waste materials, *US Patent 20060051286* (**2006**).

[**54**] L. Kotai, I.E. Sajo, I. Gacs, K. Papp, A. Bartha, G. Banvolgyi, An environmentally friendly method for removing sodium in red mud, *Chemistry Letters* 35 (**2006**) 1278–1279.

[**55**] G.A. Graham, R. Fawkes, Red mud disposal management at QAL, Proc. International bauxite tailing workshop (**1992**) 188–195.

[**56**] H. Genc-Fuhrman, Arsenic removal from water using seawater-neutralized red mud (Bauxsol), *PhD Thesis*, Environment & Resources DTU, Technical University of Denmark, **2004**.

[**57**] A. Tor, N. Danaoglu, G. Arslan, Y. Cengeloglu, Removal of fluoride from water by using granular red mud: batch and column studies, *J. Hazard. Mater.* 164 (**2009**) 271–278.

[**58**] R.C.C. Costa, F.C.C. Moura, P.E.F. Oliveira, F. Magalhaes, J.D. Ardisson, R.M. Lago, Controlled reduction of red mud waste to produce active systems for environmental applications: heterogeneous Fenton reaction and reduction of Cr(VI), *Chemosphere* 78 (**2010**) 1116–1120.

[**59**] S.J. Palmer, M. Nothling, K.H. Bakon, R.L. Frost, Thermally activated seawater neutralized red mud used for the removal of arsenate**,** vanadate and molybdate from aqueous solutions, *J. Colloid Interface Sci.* 342 (**2010**) 147–154.

[**60**] H. Nadaroglu, E. Kalkan, N. Demir, Removal of copper from aqueous solution using red mud, *Desalination* 251 (**2010**) 90–95.

[**61**] Q. Yue, Y. Zhao, Q. Li, W. Li, B. Gao, S. Han, Y. Qi, H. Yu, Research on the characteristics of red mud granular adsorbents (RMGA) for phosphate removal, *J. Hazard. Mater.* 176 (**2010**) 741–748.

[**62**] Y. Zhao, J. Wang, Z. Luan, X. Peng, Z. Liang, L. Shi, Removal of phosphate from aqueous solution by red mud using a factorial design, *J. Hazard. Mater.* 165 (**2009**) 1193–1199.

[**63**] S. Smiljanic, I. Smiciklas, A. Peric-Grujic, B. Loncar, M. Mitric, Rinsed and thermally treated red mud sorbents for aqueous Ni^{2+} ions, *Chem. Eng. J.* 162 (**2010**) 75–83.

[**64**] W. Liu, J. Yang, B. Xiao, Review on treatment and utilization of bauxite residues in China, *Int. J. Miner. Process.* 93 (**2009**) 220–231.

[**65**] S. Wang, H.M. Ang, M.O. Tade, Novel applications of red mud as coagulant, adsorbent and catalyst for environmentally benign processes, *Chemosphere* 72 (**2008**) 1621–1635.

[**66**] E. Karimi, A. Gomez, S.W. Kycia, M. Schlaf, The thermal decomposition of acetic and formic acid catalyzed by red mud–implications for the potential use of red mud as a pyrolysis bio-oil upgrading catalyst, *Energy Fuels* 24 (**2010**) 2747–2757.

[**67**] I. Vangelatos, G.N. Angelopoulos, D. Boufounos, Utilization of ferroalumina as raw material in the production of ordinary Portland cement, *J. Hazard. Mater.* 168 (**2009**) 473–478.

[**68**] N. Zhang, H. Sun, X. Liu, J. Zhang, Early-age characteristics of red mud–coal granule cementitious material, *J. Hazard. Mater.* 167 (**2009**) 927–932.

[**69**] L.M. Despland, M.W. Clark, M. Aragno, T. Vancov, Minimising alkalinity and pH spikes from Portland cement-bound Bauxsol (seawater-neutralized red mud) pellets for pH circum-neutral waters, *Environ. Sci. Technol.* 44 (**2010**) 2119–2125.

[**70**] J.B. Wehr, I. Fulton, N.W. Menzies, Revegetation strategies for bauxite refinery residue: A case study of Alcan in Northern Territory, Australia. *Envir. Manag.* 37 (**2006**) 297–306.

[**71**] H. Yang, C. Chen, L. Pan, H. Lu, H. Sun, X. Hu, Preparation of double-layer glass-ceramic/ceramic tile from bauxite tailing and red mud, *J. Eur. Ceram. Soc.* 29 (**2009**) 1887–1894.

[**72**] J. Yang, B. Xiao, Development of unsintered construction materials from red mud wastes produced in the sintering alumina process, *Const. Build. Mater.* 22 (**2008**) 2299–2307.

[**73**] D.D. Dimas, I.P. Giannopoulou, D. Panias, Utilization of alumina red mud for synthesis of inorganic polymeric materials, *Mineral Processing & Extractive Metall. Rev.* 30 (**2009**) 211–239.

[**74**] A.R. Hind, S.K. Bhargava, S.C. Grocott, The surface chemistry of Bayer process solids: a review, *Colloids Surf.* 146 (**1999**) 359–374.

[**75**] S. Zhang, C. Liu, Z. Luan, X. Peng, H. Ren, J. Wang, Arsenate removal from aqueous solutions using modified red mud, *J. Hazard. Mater.* 152 (**2008**) 486–492.

[**76**] V. Mymrin, H-A. Ponte, O.F. Lopes, A.V. Vaamonde, Environment–friendly method of high alkaline bauxite,s red mud and ferrous slag utilization as an example of green chemistry, *Green Chemistry* 5 (**2003**) 357–360.

[**77**] D.P. Schrag, Storage of carbon dioxide in offshore sediments, *Science* 325 (**2009**) 1658–1659.

[**78**] H.Y. Kim, H. M. Lee, J-N. Park, Bifunctional mechanism of CO_2 methanation on Pd-MgO/SiO_2 catalyst: independent roles of MgO and Pd on CO_2 methanation, *J. Phys. Chem. C* 114 (**2010**) 7128–7131.

[**79**] L. Zhao, L. Sang, J. Chen, J. Ji, H.H. Teng, Aqueous carbonation of natural brucite: relevance to CO_2 sequestration, *Environ. Sci. Technol.* 44 (**2010**) 406–411.

[**80**] C.L. Quere, M.R. Raupach, J.G. Canadell, G. Marland et al., Trends in the sources and sinks of carbon dioxide, *Nature Geosci.* 2 (**2009**) 831–836.

[**81**] F.J. Millero, The marine inorganic carbon cycle, *Chem. Rev.* 107 (**2007**) 308–341.

[**82**] W.S. Broecker, CO_2 arithmetic, Science 315 (**2007**) 1371.

[**83**] E. Kintisch, Carbon Emissions, Report backs more projects to sequester CO_2 from coal, *Science* 315 (**2007**) 1481.

[**84**] IPCC Special Report on Carbon dioxide Capture and Storage (IPCC, **200**1c).

[**85**] Carbon dioxide (CO_2) properties, uses, applications, CO_2 gas and liquid carbon dioxide, *Universal Industrial Gases, Inc., USA*, **2008**.

[**86**] D.B. Dell'Amico, F. Calderazzo, L. Labella, F. Marchetti, G. Pampaloni, Converting carbon dioxide into carbamato derivatives, *Chem. Rev.* 103 (**2003**) 3857–3897.

[**87**] P.G. Jessop, B. Subramaniam, Gas-expanded liquids, *Chem. Rev.* 107 (**2007**) 2666–2694.

[88] H. Arakawa, M. Aresta, J.N. Armor, M.A. Barteau, E.J. Beckman, A.T. Bell, J.E. Bercaw, C. Creutz, E. Dinjus, D.A. Dixon, K. Domen, D.L. DuBois, J. Eckert, E. Fujita, D.H. Gibson, W.A. Goddard, D.W. Goodman, J. Keller, G.J. Kubas, H.H. Kung, J.E. Lyons, L.E. Manzer, T.J. Marks, K. Morokuma, K.M. Nicholas, R. Periana, L. Que, J. Rostrup-Nielson, W.M.H. Sachtler, L.D. Schmidt, A. Sen, G.A. Somorjai, P.C. Stair, B.R. Stults, , Catalysis research of relevance to carbon management: progress, challenges, and opportunities, *Chem. Rev.* 101 (**2001**) 953–996.

[**89**] P. Jaramillo, W.M. Griffin, S.T. Mccoy, Life cycle inventory of CO_2 in an enhanced oil recovery system, *Environ. Sci. Technol.* 43 (**2009**) 8027–8032.

[**90**] R. Angamuthu, P. Byers, M. Lutz, A.L. Spek, E. Bouwman, Elecrocatalytic CO_2 conversion to oxalate by a copper complex, *Science* 327 (**2010**) 313–315.

[**91**] S. Atsumi, W. Higashide, J.C. Liao, Direct photosynthetic recycling of carbon dioxide to isobutyraldehyde, *Nature Biotechnol.* 27 (**2009**) 1177–1180.

[**92**] S.A. Mathias, P.E. Hardisty, M.R. Trudell, R.W. Zimmerman, Screening and selection of sites for CO_2 sequestration based on pressure buildup, *Int. J. Greenhouse Gas Control* 3 (**2009**) 577–585.

[**93**] K.S. Jung, CO_2 sequestration and regeneration study from power plant flue gases with reclaimed $Mg(OH)_2$, *PhD Thesis*, University of Cincinnati, **2005**.

[94] D.N. Huntzinger, Carbon dioxide sequestration in cement kiln dust through mineral carbonation, *PhD Thesis*, Michigan Technological University, **2006**.

[95] R. Pierantozzi, Carbon dioxide, Kirk Othmer Encyclopaedia of Chemical Technology, John Wiley and Sons, **2003**.

[**96**] L. Cao, G. Bala, K. Caldeira, R. Nemani, G. Ban-Weiss, Importance of the carbon dioxide physiological forcing to future climate change, *PNAS Early Edition* (**2010**) 1–6, doi/10.1073/pnas.0913000107.

[**97**] S. Khatiwala, F. Primeau, T. Hall, Reconstruction of the history of anthropogenic CO_2 concentrations in the ocean, *Nature* 462 (**2009**) 346–349.

[**98**] G. Shaffer, Long-term effectiveness and consequences of carbon dioxide sequestration, *Nature Geoscience* 3 (**2010**) 464–467.

[**99**] D.M. Sigman, M.P. Hain, G.H. Haug, The polar ocean and geological cycles in atmospheric CO_2 concentration, *Nature* 466 (**2010**) 47–55.

[**100**] M.D. Iglesias-Rodriguez, P.R. Halloran, R.E.M. Rickaby, I.R. Hall, E. Colmenero-Hidalgo, J.R. Gittins, D.R.H. Green, T. Tyrrell, S.J. Gibbs, P.V. Dassow, E. Rehm, E.V. Armbrust, K.P. Boessenkool, Phytoplankton calcification in a high-CO_2 world, *Science* 320 (**2008**) 336–340.

[**101**] C.L. Sabine, R.A. Feely, N. Gruber, R.M. Key, K. Lee, J.L. Bullister, R. Wanninkhof, C.S. Wong, D.W.R. Wallace, B. Tilbrook, F.J. Millero, T-H Peng, A. Kozyr, T. Ono, A.F. Rios, The oceanic sink for anthropogenic CO_2, *Science* 305 (**2004**) 367–371.

[102] R.A. Feely, C.L. Sabine, K. Lee, W. Berelson, J. Kleypas, V.J. Fabry, F.J. Millero, Impact of anthropogenic CO_2 on the $CaCO_3$ system in the oceans, *Science* 305 (**2004**) 362–366.

[103] B.A. Seibel, P.J. Walsh, Potential impacts of CO_2 injection on deep-sea biota, *Science* 294 (**2001**) 319–320.

[**104**] D.G. Boyce, M.R. Lewis, B. Worm, Global phytoplankton decline over the past century, *Nature* 466 (**2010**) 591–596.

[**105**] H. Hu, A. Boisson-Dernier, M. Israelsson-Nordstrom, M. Bohmer, S. Xue, A. Ries, J. Godoski, J.M. Kuhn, J.I. Schroeder, Carbonic anhydrases are upstream regulators of CO_2–controlled stomatal movements in guard cells, *Nature Cell Biol.* 12 (**2010**) 87–93.

[**106**] F. Wagner, B. Aaby, H. Visscher, Rapid atmospheric CO_2 changes associated with the 8,200-years-B.P. cooling event, *Proc. Natl. Acad. Sci. USA* 99 (**2002**) 12011–12014.

[**107**] J.A. Langley, J.P. Megonigal, Ecosystem response to elevated CO_2 levels limited by nitrogen-induced plant species shift, *Nature* 466 (**2010**) 96–99.

[108] S.P. Long, E.A. Ainsworth, A.D.B. Leakey, J. Nosberger, D.R. Ort, Food for thought: Lower-than-expected crop yield stimulation with rising CO_2 concentrations, *Science* 312 (**2006**) 1918–1921.

[**109**] http://geography.about.com

[**110**] D.P. Schrag, Preparing to capture carbon, *Science* 315 (**2007**) 812–813.

[111] G.T. Rochelle, Amine scrubbing for CO_2 capture, *Science* 325 (**2009**) 1652–1654.

[**112**] J. Tollefson, For climate relief, US will turn to gas, *Nature News* 26 June **2010**.

[113] F.M. Orr Jr., Onshore geologic storage of CO_2, *Science* 325 (**2009**) 1656–1658.

[**114**] W. Liu, B. Feng, Y. Wu, G. Wang, J. Barry, J.C.D.D. Costa, Synthesis of sintering-resistant sorbents for CO_2 capture, *Environ. Sci. Technol.* 44 (**2010**) 3093–3097.

[**115**] R.L. Gresham, S.T. Mccoy, J. Apt, M.G. Mogan, Implication of compensating property owners for geologic sequestration of CO_2, *Environ. Sci. Technol.* 44 (**2010**) 2897–2903.

[116] D.S. Goldberg, T. Takahashi, A.L. Slagle, Carbon dioxide sequestration in deep-sea basalt, *Proc. Natl. Acad. Sci. USA* 105 (**2008**) 9920–9925.

[**117**] S.R. Venna, M.A. Carreon, Highly permeable zeolite imidazolate framework-8 membranes for CO_2/CH_4 separation, *J. Am. Chem. Soc.* 132 (**2009**) 76–78.

[**118**] B. Chan, L. Radom, Zeolite-catalyzed hydrogenation of carbon dioxide and ethane, *J. Am. Chem. Soc.* 130 (**2008**) 9790–9799.

[119] R.B. Jackson, E.G. Jobbagy, R. Avissar, S.B. Roy, D.J. Barrett, C.W. Cook, K.A. Farley, D.C. le Maitre, B.A. McCarl, B.C. Murray, Trading water for carbon with biological carbon sequestration, *Science* 310 (**2005**) 1944–1947.

[120] S. Chu, Carbon capture and sequestration, *Science* 325 (**2009**) 1599.

[121] J.G. Canadell, M.R. Raupach, Managing forests for climate change mitigation, *Science* 320 (**2008**) 1456–1457.

[**122**] R.V. Noorden, Carbon sequestration: Buried trouble, *Nature* 463 (**2010**) 871–873.

[123] M. Inman, Carbon is forever, *Nature Reports Climate Change*, 2 (**2008**) 156–158.

[124] D.W. Keith, Why capture CO_2 from the atmosphere? *Science* 325 (**2009**) 1654–1655.

[**125**] L. Wallquist, V.H.M. Visschers, M. Siegrist, Impact of knowledge and misconceptions on benefit and risk perception of CCS, *Environ. Sci. Technol.* 44 (**2010**) 6557–6562.

[**126**] A.F. Bertocchi, M. Ghiani, R. Peretti, A. Zucca, Red mud and fly ash for remediation of mine sites contaminated with As, Cd, Cu, Pb and Zn, *J. Hazard. Mater. B* 134 (**2006**) 112–119.

[127] Y. Liu, C. Lin, Y. Wu, Characterization of red mud derived from a combined Bayer Process and bauxite calcinations method, *J. Hazard. Mater.* 146 (**2007**) 225–261.

[**128**] J.K. Stolaroff, D.W. Keith, G.V. Lowry, Carbon dioxide capture from atmosphere air using sodium hydroxide spray, *Environ. Sci. Technol.* 42 (**2008**) 2728–2735.

[**129**] ASTM D 2972–03, Standard Test Methods for Arsenic in Water, Test Method B, **2007**.

[**130**] A.E. Greenberg, R.R. Trussell, L.S. Clesceri, Standard Methods for the Examination of Water and Wastewater, 16th ed., APHA, AWWA, WPCF, Washington, DC, **2005**.

[**131**] V.M. Sglavo, R.C. Ampostrini, S. Maurina, G. Carturan, M. Monagheddu, G. Budroni, G. Cocco, Bauxite red mud in the ceramic industry. Part 1. Themal behavior, *J. Eur. Ceram. Soc.* 20 (**2000**) 235–244.

[**132**] Y.N. Zhang, Z.H. Pan, Characterization of red mud thermally treated at different temperature, *J. Jinan University (Sci & Tech.)* 19 (4) (**2005**) 293-297.

[133] S. Sushil, A.M. Alabdulrahmn, M. Balakrishnan, V.S. Batra, R.A. Blackley, J. Clapp, J.S.J. Hargreaves, A. Monaghan, I.D. Pulford, J.L. Rico, W. Zhou, Carbon deposition and phase transformations in red mud on exposure to methane, *J. Hazard. Mater.* 180 (**2010**) 409–418.

[**134**] K.E. Moretto, A process for crystallizing out impurities from Bayer process liquors, *European Patent* EP0662451, (**1999**).

[**135**] C. Cardell, I. Guerra, J. Romero-Pastor, G. Cultrone, A. Rodriguez-Navarro, Innovative analytical methodology combining micro-X-ray diffraction, scanning electron microscopy-based mineral maps, and diffuse reflectance infrared Fourier transform spectroscopy to characterize archeological artifacts, *Anal. Chem.* 81(2) (**2009**) 604-611.

[**136**] A. Gok, M. Omastova, J. Prokes, Synthesis and characterization of red mud/polyaniline composites: electrical properties and thermal stability, *Eur. Polym. J.* 43 (**2007**) 2471–2480.

[137] C. Navarro, M. Diaz, M.A. Villa-Garcia, Physico-chemical characterization of steel slag. Study of its behaviour under simulated environmental conditions, *Environ. Sci. Technol.* 44 (**2010**) 5383–5388.

[**138**] P. Regnier, A.C. Lasaga, R.A. Berner, Mechanism of CO_3^{2-} substitution in carbonate-fluorapatite: evidence from FTIR spectroscopy, ^{13}C NMR, and quantum mechanical calculations, *Am. Miner.* 79 (**1994**), 809–818.

[**139**] R.V. Siriwardane, C. Robinson, M. Shen, T. Simonyi, Novel regenerable sodium-based sorbents for CO_2 capture at warm gas temperatures, *Energy Fuels* 21 (**2007**) 2088–2097.

[**140**] L. Meng, S. Burris, H. Bui, W. Pan, Development of an analytical method for distinguishing ammonium bicarbonate from the products of an aqueous ammonia CO_2 scrubber, *Anal. Chem.* 77 (**2005**) 5947–5952.

[**141**] J.A. Tossell, H_2CO_3(s): a new candidate for CO_2 capture and sequestration, *Environ. Sci. Technol.* 43 (**2009**) 2575–2580.

[**142**] G.A. Hill, Measurement of overall volumetric mass transfer coefficients for carbon dioxide in a well-mixed reactor using a pH probe, *Ind. Eng. Chem. Res.* 45 (**2006**) 5796–5800.

[143] R.C. Sahu, R.K. Patel, B.C. Ray, Neutralization of red mud using CO_2 sequestration cycle, *J. Hazard. Mater*. 179 (**2010**) 28–34.

[144] K.S. Lackner, A guide to CO_2 sequestration, *Science* 300 (**2003**) 1677–1678.

[145] K. Adamczyk, M. Premont-Schwrz, D. Pines, E. Pines, E.T.J. Nibbering, Real-time observation of carbonic acid formation in aqueous solution, *Science* 326 (**2009**) 1690–1694.

[146] J.J. Fornero, M. Rosenbaum, M.A. Cotta, L.T. Angenent, Carbon dioxide addition to microbial fuel cell cathodes maintains sustainable catholyte pH and improves anolyte pH, alkalinity, and conductivity, *Environ. Sci. Technol.* 44 (**2010**) 2728–2734.

[147] H. Tahir, Comparative trace metal contents in sediments and the removal of the chromium using Zeolite-5A, *EJEAF Chem.* 4(4) (**2005**) 1021–1032.

[148] K. W. Kolasinski, Surface science: foundations of catalysis and nanoscience, Queen Mary, University of London, UK, John Wiley & Sons Ltd., **2002**, 85-86.

[**149**] C. Jing, G.P. Korfiatis, X. Meng, Immobilization mechanisms of arsenate in iron hydroxide sludge stabilized with cement, *Environ. Sci. Technol.* 37 (**2003**) 5050–5056.

[**150**] Y. Jia, L. Xu, Z. Fang, G.P. Emopoulos, Observation of surface precipitation of arsenate on ferrihydrite, *Environ. Sci. Technol.* 40 (**2006**) 3248–3253.

[**151**] A. Voegelin, S.J. Hug, Catalyzed oxidation of arsenic(III) by hydrogen peroxide on the surface of ferrihydrite: an in situ ATR-FTIR study, *Environ. Sci. Technol.* 37 (**2003**) 972–978.

[**152**] X.H. Guan, T. Su, J. Wang, Quantifying effects of pH and surface loading on arsenic adsorption on nanoactive alumina using a speciation-based model, *J. Hazard. Mater.* 166 (**2009**) 39–45.

[**153**] M. Pena, X. Meng, G.P. Korfiatis, C. Jing, Adsorption mechanism of arsenic on nanocrystalline titanium dioxide, *Environ. Sci. Technol.* 40 (**2006**) 1257–1262.

[**154**] L. Yang, S. Wu, J.P. Chen, Modification of activated carbon by polyaniline for enhanced adsorption of aqueous arsenate, *Ind. Eng. Chem. Res.* 46 (**2007**) 2133–2140.

[155] R.C. Sahu, R.K. Patel, B.C. Ray, Utilization of activated CO_2–neutralized red mud for removal of arsenate from aqueous solutions, *J. Hazard. Mater.* 179 (**2010**) 1007–1013.

[**156**] X.H. Guan, J. Wang, C.C. Chusuei, Removal of arsenic from water using granular ferric hydroxide: macroscopic and microscopic studies, *J. Hazard. Mater.* 156 (**2008**) 178–185.

[**157**] S.R. Kanel, J.M. Greneche, H. Choi, Arsenic (V) removal from ground water using nano scale zero-valent iron as a colloidal reactive barrier material, *Environ. Sci. Technol.* 40 (**2006**) 2045–2050.

[**158**] L. Cumbal, A.K. Sengupta, Arsenic removal using polymer-supported hydrated iron (III) oxide nanoparticles: role of Donnan membrane effect, *Environ. Sci. Technol.* 39 (**2005**) 6508–6515.

[**159**] P. Atkins, The Element of Physical Chemistry, Oxford University Press, Third Edition **2001**.

[160] R.C. Sahu, R.K. Patel, B.C. Ray, Extraction of fine iron from red mud, *Indian Patent Filed*, 884/KOL/2009A (19.6.**2009**), page: 1466.

[**161**] MoU inked between NIT Rourkela and Vedanta Aluminum to develop environment-friendly technology, *News*, Rourkela City, 12th August, **2010**.

[162] NIT-Rourkela inks MoU with Vedanta, *News, Times of India, Bhubaneswar,* August 13, **2010**, page: 6.

*****

Biography

Ramesh Chandra Sahu was born at Talita, Bonaigarh, Sundargarh (Orissa), India. He completed his schooling from Jawahar Navodaya Vidyalaya, Zinc Nagar, Sundargarh. He obtained his BSc (Chemistry Honours) from Sambalpur University. He obtained his MSc degree with Physical Chemistry Specialization from P.G. Department of Chemistry, Sambalpur University, India, in 2006. He has been awarded CSIR Fellowship for PhD studies, 2007-2010. He worked in the field of "Neutralization of red mud using CO_2 sequestration and their utilizations" and received financial support from CSIR and MHRD, Government of India, New Delhi, during his PhD studies at National Institute of Technology, Rourkela. He has published research papers in the peer-reviewed international scientific journals and one patent has been filed (No. 884/KOL/2009). His research interests focus on CO_2 sequestration and utilizations, red mud utilizations, surface chemistry.

Peer-reviewed International Publications:

[1] **Ramesh Chandra Sahu**, Rajkishore Patel, Bankim Chandra Ray, Neutralization of red mud using CO_2 sequestration cycle, *J. Hazard. Mater.* 179 (**2010**) 28–34.

[2] **Ramesh Chandra Sahu**, Rajkishore Patel, Bankim Chandra Ray, Utilization of activated CO_2–neutralized red mud for removal of arsenate from aqueous solutions, *J. Hazard. Mater.* 179 (**2010**) 1007–1013.

Patent:

[1] **Ramesh Chandra Sahu**, Rajkishore Patel, Bankim Chandra Ray, Extraction of fine iron from red mud, *Indian Patent Filed*, 884/KOL/2009A (19.6.**2009**), page: 1466.

*****